

**COMPUTATIONAL MODELING OF RUNNING
BIOMECHANICS IN AMATEUR RUNNERS**

TEH YEW WEI

UNIVERSITI TUNKU ABDUL RAHMAN

**COMPUTATIONAL MODELING OF RUNNING BIOMECHANICS IN
AMATEUR RUNNERS**

TEH YEW WEI

**A project report submitted in partial fulfilment of the
requirements for the award of Bachelor of Biomedical
Engineering with Honours**

**Lee Kong Chian Faculty of Engineering and Science
Universiti Tunku Abdul Rahman**

October 2024

DECLARATION

I hereby declare that this project report is based on my original work except for citations and quotations which have been duly acknowledged. I also declare that it has not been previously and concurrently submitted for any other degree or award at UTAR or other institutions.

Signature :  _____

Name : Teh Yew Wei _____

ID No. : 2005970 _____

Date : 11 Oct. 24 _____

APPROVAL FOR SUBMISSION

I certify that this project report entitled “**COMPUTATIONAL MODELING OF RUNNING BIOMECHANICS IN AMATEUR RUNNERS**” was prepared by **TEH YEW WEI** has met the required standard for submission in partial fulfilment of the requirements for the award of Bachelor of Biomedical Engineering with Honours at Universiti Tunku Abdul Rahman.

Approved by,

Signature : 

Supervisor : Dr. Chan Siow Cheng

Date : 11 Oct. 24

Signature : 

Co-Supervisor : Ms. Tan Yin Qing

Date : 11 Oct. 24

The copyright of this report belongs to the author under the terms of the copyright Act 1987 as qualified by Intellectual Property Policy of Universiti Tunku Abdul Rahman. Due acknowledgement shall always be made of the use of any material contained in, or derived from, this report.

© 2024, Teh Yew Wei. All right reserved.

ACKNOWLEDGEMENTS

This study was supported by Universiti Tunku Abdul Rahman under grant number IPSR/ UTARRF RMC/ /2020-C2/C01 and Centre of Healthcare Science and Technology (CHST) fund.

I would like to thank everyone who had contributed to the successful completion of this project. I would like to express my gratitude to my research supervisor, Dr. Chan Siow Cheng and Ms. Tan Yin Qing, my co-supervisor, for their invaluable advice, guidance and his enormous patience throughout the development of the research.

ABSTRACT

This study was motivated by the need to understand the biomechanics of running, especially among amateur athletes, to enhance performance and prevent injuries. The research involved the development of a musculoskeletal model using OpenSim, focusing on the deep muscles of the lower limb. Experimental data were collected from ten amateur runners, and muscle-driven simulations were performed using techniques like Computed Muscle Control (CMC) and Static Optimization (SO). These simulations were compared to experimental data for validation, where Reduce Residual Algorithm (RRA) was found to be most effective in the determination of ankle moment. Statistically, the Root Mean Square Error (RMSE), correlation (r), in knee and ankle moments, under different types of shoe cushioning, no significant differences were found, with 0.3 kg/Nm of RMSE and approximately 95% of correlation in comparison with the experimental data. Thus, in this case, the computational time does become the key factor in evaluating them, where Inverse Kinematics (IK) was the best performed in simulating the knee and ankle joint moments in running motion under different types of hardness shoe cushioning, then followed by RRA and MocoTrack, which had the longest computational time respectively. On the other hand, focusing on muscle activations and joint moments during different running distances and with varying shoe cushioning, the results demonstrated that CMC provided the most accurate muscle force estimations, exhibiting the lowest root mean square error (RMSE) and highest correlation, though at the cost of increased computational time. Analysis revealed significant changes in muscle force generation at 80 km, indicating the body's adaptation to accumulated running distance. Muscles like the sartorius and semitendinosus exhibited compensatory force generation, while the adductor magnus ischial showed adaptive shifts between stance and swing phases. In conclusion, CMC provided the most accurate muscle force predictions. Based on the findings, running biomechanics can be better understood, aiding in improved training routines for amateur runners.

TABLE OF CONTENTS

DECLARATION	i
APPROVAL FOR SUBMISSION	ii
ACKNOWLEDGEMENTS	iv
ABSTRACT	v
TABLE OF CONTENTS	vi
LIST OF TABLES	ix
LIST OF FIGURES	x
LIST OF APPENDICES	xiii

CHAPTER

1	INTRODUCTION	1
	1.1 General Introduction	1
	1.2 Importance of the Study	2
	1.3 Problem Statement	3
	1.4 Aim and Objectives	4
	1.5 Scope and Limitation of the Study	5
2	LITERATURE REVIEW	6
	2.1 Introduction	6
	2.2 Runing Biomechanics Simulation via OpenSim	7
	2.3 Simulation-Experimental Results Validation Process	8
	2.4 OpenSim Virtual Marker Trajectory Tracking Inverse Kinematics Systems	8
	2.5 OpenSim Muscle-driven Simulation	9
	2.6 Superficial Muscle Groups' Function in Running	10
	2.7 The Effect of Shoe Cushioning and Running Distance on Running Performance	13
	2.8 The Role of Lower Limb Deep Muscle on Running	13

3	METHODOLOGY	14
3.1	Introduction	14
3.2	Experimental Data Collection	15
3.3	OpenSim Musculoskeletal Model	18
3.3.1	Scaling	20
3.4	Experimental-Simulation Moment Validation	21
3.4.1	Inverse Kinematics	21
3.4.2	Inverse Dynamics	23
3.4.3	Residual Reduction Algorithm	25
3.5	Muscle-Driven Simulation	26
3.5.1	Mechanical Parameters and Muscle Study Selection	26
3.5.2	Computed Muscle Control & Static Optimization	29
3.6	OpenSim Moco	31
3.6.1	MocoTrack	32
3.6.2	MocoInverse	33
3.7	Data Analysis with MATLAB	34
4	RESULTS AND DISCUSSION	36
4.1	Introduction	36
4.2	Scaling for Musculoskeletal Models	37
4.3	OpenSim's Knee and Ankle Moments Kinetics Validation	37
4.3.1	Gait Analysis	37
4.3.2	RMSE, Correlation and Computational Time	42
4.3.3	Performance Evaluation	47
4.4	Assessing Muscle Driven Optimization Techniques	47
4.4.1	EMG Validation	47
4.4.2	CMC Muscular Force Estimation	50
4.5	Muscle Length and Muscle Velocity Relationship	55

5	CONCLUSIONS AND RECOMMENDATIONS	65
5.1	Conclusions	65
5.2	Recommendations for Future Work	66
	REFERENCES	68
	APPENDICES	73

LIST OF TABLES

Table 2.1:	The Function of The Superficial Muscle Groups in the Aspect of Anatomically and Biomechanically	10
Table 3.1:	The Physical and Physiological Data of the Participants (Boon, 2023)	15
Table 3.2:	The Condition of Shoe Cushioning and the Different Accumulation Running Distance that were acted as the Parameters for Studying the Running Biomechanics of the Amateur Runners	18
Table 3.3:	The Study Parameters and Their Respective Definition in the Simulation Environment	26
Table 3.4:	Deep Muscles Selection for Muscular Force Prediction Analysis	27
Table 4.1:	The RMS of the Scaling Results for Randomly Picked Subjects	37
Table 4.2:	Average Residuals Forces After RRA for Two Randomly Picked Subjects Wearing Hard Cushioning and Soft Cushioning Respectively	38
Table 4.3:	Quantitative View of RMSE, r, and the Computational Time for IK, RRA and MocoTrack in Hard Running Shoe Cushioning	43
Table 4.4:	Quantitative View of RMSE, r, and the Computational Time for IK, RRA and Mocotrack in Soft Running Shoe Cushioning	46
Table 4.5:	The rmse, R-Value and the Computational Time for CMC, SO and MocoInverse Gaslat Validation	50

LIST OF FIGURES

Figure 2.1:	The Workflow of Muscle-Driven Simulation in OpenSim (Uchida and Delp, 2021), Reprinted with Permission from Copyright 2024 The MIT Press.	9
Figure 3.1:	The General Workflow of the Modelling Study	14
Figure 3.2:	The Cameras Setup of the Motion Capture System (Boon, 2023)	16
Figure 3.3:	The Qualisys Optical Markers Position of Placements (Boon et al., 2022)	16
Figure 3.4:	EMG Electrodes Placement on i) Rectus Femoris - RF, ii) Tibialis Anterior – TA, iii) Lateral Gastrocnemius – LG and iv) Biceps Femoris – BF (Boon, 2023)	17
Figure 3.5:	Shoes of Hard Cushioning (Left) and Soft Cushioning (Right) (Boon, 2023)	18
Figure 3.6:	The Full Body Generic Musculoskeletal Model that is also Known as Rajagopal Model (Rajagopal et al., 2016)	19
Figure 3.7:	The Simple Schematic Diagram for Running the Scaling Process	20
Figure 3.8:	The Key Steps to Perform Scaling in OpenSim	21
Figure 3.9:	The Simple Workflow of the Scaling Reiterative Process	21
Figure 3.10:	The Key Steps to Perform IK in OpenSim	23
Figure 3.11:	The Overall Workflow of the IK and ID and the Files Requirements to Run the Tools	24
Figure 3.12:	The Key Steps to Perform ID in OpenSim	24
Figure 3.13:	The Files Requirement of Running the RRA in OpenSim	26
Figure 3.14:	The Files Requirements of Running the CMC and SO	31
Figure 3.15:	The Schematic Diagram for Mocotrack File Requirements	33
Figure 3.16:	OpenSim MocoTrack Result Visualization	33
Figure 3.17:	The Schematic Diagram for MocoInverse File Requirements	34

Figure 4.1:	The Simulation Files for 5 Hard Shoe Cushioning and 5 Soft Cushioning	36
Figure 4.2:	The Simulation Files That Contain the Static and Running Trajectory Marker Files and VGRF File That are Acquired from the Subject Experimentally	36
Figure 4.3:	Knee Moment Gait for Hard Running Shoe Cushioning	38
Figure 4.4:	Knee Moment Gait for Soft Running Shoe Cushioning	39
Figure 4.5:	Ankle Moment Gait for Hard Running Shoe Cushioning	40
Figure 4.6:	Ankle Moment Gait for Soft Running Shoe Cushioning	41
Figure 4.7:	Comparison Of IK, RRA, and Mocotrack for Knee Moment Running Gait under Hard Shoe Cushioning	42
Figure 4.8:	Comparison of IK, RRA, and Mocotrack for Ankle Moment Running Gait under Hard Shoe Cushioning	43
Figure 4.9:	Comparison of IK, RRA, and Mocotrack for Knee Moment Running Gait under Soft Shoe Cushioning	44
Figure 4.10:	Comparison of IK, RRA, and Mocotrack for Ankle Moment Running Gait under Soft Shoe Cushioning	45
Figure 4.11:	The EMG Validation Graph for 40 km Accumulated Running Distance	49
Figure 4.12:	The EMG Validation Graph for 80 km Accumulated Running Distance	49
Figure 4.13:	The Muscular Force Estimation for the Adductor Magnus Ischial across Different Accumulated Running Distance	51
Figure 4.14:	The Muscular Force Estimation for the Sartorius across Different Accumulated Running Distance	52
Figure 4.15:	The Muscular Force Estimation for the Semitendinosus across Different Accumulated Running Distance	53
Figure 4.16:	The Muscular Force Estimation for the Vastus Intermedius across Different Accumulated Running Distance	54
Figure 4.17:	The Muscular Force Estimation for the EDL across Different Accumulated Running Distance	55

Figure 4.18:	Semiten Muscle Length Graph Reported by Arnold et al. (2013) vs the Simulation Result	56
Figure 4.19:	The Muscle Length-Force-Gait 3D Curve for Adductor Magnus Ischial	57
Figure 4.20:	The Muscle Velocity-Force-Gait 3D Curve for Adductor Magnus Ischial	57
Figure 4.21:	The Muscle Length-Force-Gait 3D Curve for Sartorius	58
Figure 4.22:	The Muscle Velocity-Force-Gait 3D Curve for Sartorius	59
Figure 4.23:	The Muscle Length-Force-Gait 3D Curve for Semitendinosus	60
Figure 4.24:	The Muscle Velocity-Force-Gait 3D Curve for Semitendinosus	61
Figure 4.25:	The Muscle Length-Force-Gait 3D Curve for Vastus Intermedius	61
Figure 4.26:	The Muscle Velocity-Force-Gait 3D Curve for Vastus Intermedius	62
Figure 4.27:	The Muscle Length-Force-Gait 3D Curve for Extensor Digitorum Longus	63
Figure 4.28:	The Muscle Velocity-Force-Gait 3D Curve for Extensor Digitorum Longus	64
Figure 5.1:	SCONE's Interface (Left) and osim-rl Training Interface (Right)	66
Figure 5.2:	osim-rl Python Package Stops Without Prompting Any Coding Error	67

LIST OF APPENDICES

Appendix A: Simulation Result with MocoInverse Mesh Interval 0.08	73
Appendix B: IECBES 2024 Conference Paper Submission	74
Appendix C: IECBES 2024 1 st Paper Submission Content: Performance Evaluation on OpenSim's Virtual Markers Trajectory System for Running Simulation	75
Appendix D: IECBES 2024 2 nd Paper Submission Content: Assessing Muscle Driven Optimization Techniques in OpenSim for Long Distance Running and Deep Muscle Adaptations	81
Appendix E: Open Access to Image Rights	87

CHAPTER 1

INTRODUCTION

1.1 General Introduction

Running is a locomotion ability that human equipped to move from one place to another in faster pace than walking. It plays a pivotal role in maintaining overall health and fitness, where studies show that moderate and spontaneous running is able to promote a healthier life free from cardiovascular diseases and psychological diseases (Oswald et al., 2020; McCully, 2004). Among amateur athletes and recreational runners, understanding the mechanics of running can provide valuable insights into performance enhancement and injury prevention. Thus, in-depth study of biomechanics running is necessary, which can be established by utilizing computational modelling to analyse deep muscle dynamics and other physiological factors on their effect towards running. Capability of simulating the complex scene of running is helpful in extracting the data that is approximate to the real human running, thus making the further analysis, interpretation and deduction to be valuable and worthy, which is the main motivation to utilize the computational model in studying running biomechanics. It offers a systematic approach to dissect complex interactions between neuro-musculoskeletal geometry structures and their functions during running.

In the specific context, the field of computational biomechanics merges principles from computing, engineering and biology to elucidate how physical forces interact within the fully dynamic biological systems. In the context of running, computational biomechanical analysis focuses on how neural command, muscles, bones, and joints coordinate to produce movement. By applying computational tools, such as finite element analysis and dynamic simulations, enabling prediction to be done towards the effects of various mechanical loads exerted from or applied towards the human body model.

Amateur runners, similar to those recreational runners, but unlike their professional counterparts, often lack systematic and customized training and professional advice on running causing them to have higher chances to get injury due to improper running approaches and gestures (Millard, 2021;

Stenerson et al., 2023). Therefore, by focusing on this group (amateur runners), the study aims to contribute practical and theoretical knowledge that can be directly applied in everyday training routines.

The utilization of computational models in sports biomechanics is an expanding field that offers innovative solutions and detailed insights into athletic performance. This study not only advances the understanding of running mechanics but also ambitious to set a foundation for future studies. By exploring the intricate details of muscle activation and mechanical forces in running, the study provides a basis for developing targeted interventions that enhance performance and mitigate injury risks among amateur runners.

1.2 Importance of the Study

The importance of studying running biomechanics in amateur runners cannot be overstated. Amateur runners often participate in running activities without professional guidance, which can lead to inefficient running techniques and a higher risk of injuries. Stenerson et al. (2023) provided the insight that out of their 616 study participants, up to 84.4% of them were having at least on injury event that are caused due to running. A detailed study that outlining a detailed biomechanical analysis is to generate more effective training and injury prevention strategies tailored to the needs of amateur runners.

One of the key contributions of this study is providing the detailed, comprehensive and in-depth analysis of lower limb muscle functions during running. The lower limb muscles play unreplaceable roles in movement and stability, and proper technique and gesture to run is essential to ensure their optimal functioning and thus making sure that the runners are safe and efficient. For example, the quadriceps and hamstrings are critical for knee extension and flexion, respectively, and their balanced interaction is necessary for maintaining knee stability and propulsion during running.

Technically, a thorough study in exploring the approaches to get the information of the deep muscle data during running is also important. Since the biomechanical study is niche, and deep muscle analysis is much less resource available to public. Specifically speaking, deep muscle in this case is defined as the lower limb muscle groups that are located further away from the surface of the body and are often positioned underneath superficial muscles or

deeper within the body. There are the lower limb muscle groups that are difficult to be traced or measured by biomechanical tools or instrumentations. Exploring the approaches to study these groups of muscle would provide an insight of the public so that if anyone who wishes to study the deep muscle of other human activities, these approaches can give them a spike to idea on how to start their respective study and analysis.

Moreover, this study extends its impact by contributing to the development of better footwear and orthotic designs. This study also explores the relationship between the running performance and the accumulated running distance. The study of this would allow amateur runners to tailored made their running strategies depending on their running distance. Moreover, the relationship between the type of shoe cushioning and the running also would be enclosed in the subsequence section. By understanding the biomechanical needs of amateur runners, manufacturers can create shoes that offer better support and cushioning, potentially reducing the risk of injuries associated with impact forces during running. The relevancy in between the type of shoe cushioning and the accumulated running distance would be enclosed in this study as well.

1.3 Problem Statement

Running is a widely practiced physical activity that offers numerous health benefits, yet it is associated with a notably high incidence of muscle-related and overuse injuries of the lower extremities among amateur runners. Studies indicate that between 27% and 70% of runners experience these injuries annually, which not only affects their health and performance but also discourages continued participation in running (De Araujo et al., 2015; Kakouris et al., 2021).

In the biomechanical aspect, the high rate of injuries can be attributed to a variety of biomechanical factors, including improper force distribution, inadequate shock absorption during foot strike, and inefficient motion patterns. These improper would be compounded by the dynamic and repetitive running, which accumulatively places intense stresses on the musculoskeletal system. Under different running conditions (shoe cushioning) and needs (accumulated running distance), they would become the starting point dive into those injury

or performance related analysis and studies. Current simulation models, such as those developed using OpenSim, aim to replicate and analyse these complex interactions through advanced techniques like multi-body dynamics equation of motion, interior point optimization, cost function minimization, single shooting, direct coloration and so on. The effectiveness of these mathematically solver in capturing true biomechanical behaviours and in predicting injury risks under varied running conditions is worth to be thoroughly validated and verified.

Anatomically, variations in muscle strength, tendon resilience, and joint stability significantly influence the susceptibility to injuries. Differences in individual anatomy can affect how runners respond to physical stresses, impacting the effectiveness of generic training and prevention programs. Computational models that incorporate detailed anatomical data can potentially offer personalized insights into the biomechanical and anatomical interactions that is able to prevent potential risk of amateur runners to injuries. Yet, the challenge lies in accurately simulating these individual differences and understanding their impact on running biomechanics.

1.4 Aim and Objectives

The aim of this study is to utilize state-of-the-art simulation modelling techniques to enhance our understanding of the biomechanical impacts of running duration and the type of footwear on amateur runners. Specifically, the objectives of this study are to:

1. Develop and scale a tailored musculoskeletal model that accurately represents the biomechanics of amateur runners.
2. Validate the simulation data obtained from OpenSim against high-quality experimental data kinematically and kinetically to ensure the simulation results were informative, reliable and accurate.
3. Conduct muscle-driven simulations and estimations to biomechanically analyse muscle activity and its interactions with the skeletal geometry under varying running durations and different footwear types.

1.5 Scope and Limitation of the Study

This study covers the methodology, analysing and interpreting the results regarding to the running biomechanics of amateur running under the hard and soft shoe cushioning, and also under different accumulative running distances.

In the aspect of limitation, the complexity of human musculoskeletal structure may limit the ability to fully replicate every biomechanical interaction in the simulation environment. In terms of generalizability, the study findings derived from simulated models may not be universally applicable to all runner demographics, including variations in age, fitness level, and biomechanical properties, Since the experimental data collection process is carried out on the treadmill but not overground, thus this differences would cause some extent of discrepancies for overground running runners, in short, surface type factor is not fully considered and covered in this study.

CHAPTER 2

LITERATURE REVIEW

2.1 Introduction

Performing computational modelling with biomechanical analysis requires a simulation program that can run the motion simulation in performing various activities. Running is one of them. Nowadays, there are numerous software available in the market that can perform the biomechanical simulation. Indeed, there are strengths and weaknesses for each software. It is worthy to explore that before selecting one as the centre of the study.

To name a few, OpenSim, AnyBody, and Kinovea are the simulation software that are capable of running biomechanical modelling in running. Although Kinovea has the most user-friendly in among of this, and it allows users to analyse video motion recordings in real-time, however the advanced biomechanical modelling is difficult to be performed due to the restriction of the degree of freedom that this software equipped and it is designed to mainly focus on 2D video analysis, which will be less accurate if performing 3D modelling. Lacking physiological modelling is also another strong point on discouraging to use Kinovea in this study.

OpenSim and Anybody have almost similar capabilities of each other. Except in the aspect of cost, Anybody would be a good alternative software to run the computational modelling in this study. Trinler et al. (2019) also had a strong agreement on this statement, describing that both software have good performance in simulation muscle activation modelling, but they have the difference simulation results in sagittal ankle and hip angles as well as sagittal knee moments. Most substantially, the difference in results happened when both simulating the same subject in terms of individual muscle force estimations via performing static optimization analysis, which in turn, Trinler et al. (2019) recommended that study the mathematical theory behind the simulation tools is a crucial step.

Kim et al. (2018) also brought the same conclusion: both OpenSim and Anybody are performed good in terms of advanced biomechanical simulation. Both have consistency in simulating the muscle activation level

and root mean square value when comparing to the experimental data, showing that OpenSim and Anybody both have the same level of competency.

2.2 Running Biomechanics Simulation via OpenSim

In this study, OpenSim is chosen as the main software to perform the biomechanical simulation modelling where to perform the running biomechanics in the study. 10 subjects were recruited to collect their 3D motion trajectory marker data, tri-axis VGRF data, and other experimentally data. Unlike clinical studies, research related to biomechanics typically does not involve large-scale data collection with hundreds of participants. This is primarily because the principles of physics play a significant role, ensuring a high degree of consistency results when data collection is conducted accurately and meticulously. For instance, Zhao et al. (2022) had focused on hip, knee and ankle individual muscle force studies with the data collection from only eight male participants, averaging 29 years old and running on the treadmill with 5 m/s speed. Another example, 16 male recreational runners were collected with their experimental data by Quan et al. (2023) in order to study the relationship in between the lower limb muscle activation and the running performance under the wearing minimalist shoes or normal shoes to run.

In addition to these studies, Jiang et al. (2021) conducted a study on the effects of bionic shoes versus neutral running shoes in 16 male recreational runners before and after a 5 km run by using OpenSim. Their study focused on ground reaction forces (GRFs), which are critical in understanding the etiology of running-related injuries. GRFs have been implicated in various overuse injuries, which are prevalent among runners. In their study, the authors found that bionic shoes significantly reduced vertical impulse, peak propulsive force, and contact time, while increasing braking impulse and the vertical instantaneous loading rate (VILR). These findings suggest that bionic shoes may reduce injury risk by more closely mimicking barefoot running while offering protective benefits. Furthermore, Jiang et al. (2021) observed that prolonged running—such as a 5 km treadmill run—led to increases in peak vertical impact force, loading rates, and braking forces, which are all associated with an elevated injury risk due to fatigue. This observation aligns

with the findings of Quan et al. (2023), where prolonged running in minimalist footwear altered muscle activation patterns, potentially influencing injury susceptibility.

2.3 Simulation-Experimental Results Validation Process

In the validation process, various parameters would be used to do the comparison in between the experimental biomechanics data with the simulation data to ensure that simulation results are trustable and accurate. It also is a process to inform the operator if their simulation results are error-free. In the study done by Tang et al., (2022) intended to examine the performance of their markerless (ML) motion capture systems. They used Cohen's d value as the comparison in similarity of markerless and marker-based motion capture systems. In the gait analysis results, some part of the gait showed high d -values, indicating that the difference between the two conditions in that part of the gait, is substantial. As the desired outcome, lower d -values would be expected, which indicating that the variables have higher extent of similarity.

Apart from that, RMSE is one of the parameters that would be used to do the comparison. Jung et al., (2016) have done a study focused on estimating the ground reaction force (GRF) during gait using a dynamically adjustable foot-ground contact model, which established that knee moment of RMSE with ranged 2.6 to 0.5, while 2.1 to 0.3 in ankle moment.

Stetter et al., (2020) performed the running knee moment comparison by using another parameter, which is called rRMSE, which showed the value was lower than $22.3 \pm 8.3\%$ in the knee adduction moment and $25.5 \pm 7.0\%$ in knee flexion moment, when they were comparing the result in between those generated by artificial neural network and the experimental data to support the development of assistive devices in knee osteoarthritis patients.

2.4 OpenSim Virtual Marker Trajectory Tracking Inverse Kinematics Systems

Based on data from 10 male participants running at three different speeds, Fox (2024) reported that MocoTrack outperformed RRA by producing lower residual forces and moments. Such deduction reflects that MocoTrack is able

to perform motion tracking where the kinematics information is the more dynamically consistent to the running virtual ground reaction forces.

2.5 OpenSim Muscle-driven Simulation

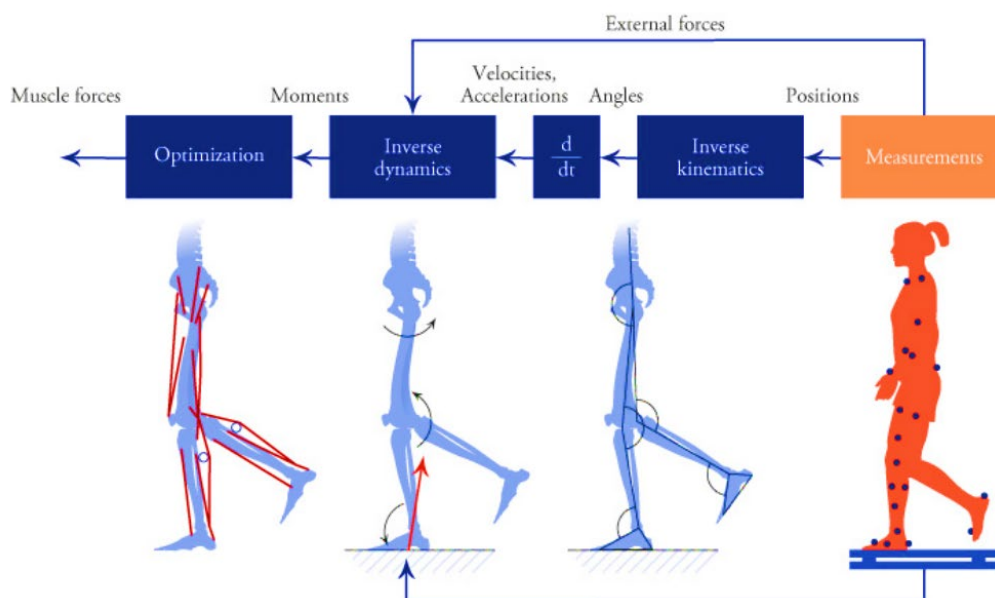


Figure 2.1: The Workflow of Muscle-Driven Simulation in OpenSim (Uchida and Delp, 2021), Reprinted with Permission from Copyright 2024 The MIT Press.

Muscle-driven simulation can be done by three techniques in OpenSim: Static Optimization (SO), Computed Muscle Control (CMC) and MocoInverse. Roelker et al. (2020) conducted a study comparing the performance of SO and CMC. Six subject models were validated using experimental muscle activation and joint torque data. The study found that knee extension torque error was greater with CMC than with SO, and that muscle forces, activations, and co-contraction indices were generally lower with SO. The study concluded that to choose the best optimization technique for muscle-driven simulation in OpenSim, validation with experimental activation data is essential.

Additionally, Lin et al., (2011) have made a study with targeted to compare muscle-force estimated from using three different muscle-driven simulation techniques: SO, CMC, and Neuromusculoskeletal Tracking (NMT). These methods are evaluated using musculoskeletal modeling and

experimental gait data to determine lower-limb muscle forces during walking and running. Specific muscle groups were analyzed include the soleus, gastrocnemius, vastus, rectus femoris, gluteus maximus, gluteus medius, hamstrings, and the combined iliopsoas. The results showed that while all methods are valid, provided similar results in terms of the patterns of muscle forces for both walking and running, However, SO would be more preferable due to its computational efficiency and ability to closely match experimental data with minimal error.

2.6 Superficial Muscle Groups' Function in Running

In this study, deep muscle groups were selected as the focus of analysis for estimating muscle force-length-velocity relationships, as they are typically more difficult to measure accurately using electromyography (EMG) compared to superficial muscles. Additionally, their anatomical and biomechanical roles in running, as well as their contributions to performance enhancement, remain underexplored. In contrast, lower limb superficial muscles have been extensively studied, and substantial knowledge about their anatomical and biomechanical functions in running is widely available.

Table 2.1: The Function of The Superficial Muscle Groups in the Aspect of Anatomically and Biomechanically

Muscle Groups	Anatomical Function in Running	Biomechanical Enhancement in Running Performance
Gastrocnemius Lateral Head	Facilitates plantar flexion at the ankle (Tsuji et al., 2015).	Enhances push-off efficiency, increasing stride power and length (Tsuji et al., 2015).
Gastrocnemius Medial Head	Works with lateral head for effective plantar flexion (Tsuji et al., 2015).	Boosts acceleration and power during sprints and uphill movement (Tsuji et al., 2015).

Table 2.1: (Continue)

Rectus Femoris	Acts to extend the knee and flex the hip.	Increases stride length and speed through powerful knee extension.
Vastus Lateralis	Extends the knee, ensuring stability during movement (Böhm et al., 2018).	Improves lateral knee stability, vital for sustained running pace (Böhm et al., 2018).
Vastus Medialis	Key player in knee extension and patellar stabilization (Tsuji et al., 2015).	Enhances endurance and stability in long runs through knee alignment (Tsuji et al., 2015).
Biceps Femoris Long Head	Extends the hip and flexes the knee.	Facilitates explosive movements and better shock absorption.
Biceps Femoris Short Head	Primarily involved in knee flexion.	Improves quick changes in speed and enhances knee flexion agility.
Gluteus Maximus	Major role in hip extension and trunk stabilization.	Drives forward propulsion and increases overall running power.
Gluteus Medius	Stabilizes the pelvis during the stance phase.	Reduces lateral pelvic tilt, increasing mechanical efficiency.
Gluteus Minimus	Assists in hip stabilization and abduction.	Optimizes energy efficiency by improving pelvic and leg alignment.
Tensor Fasciae Latae	Facilitates hip abduction and stabilizes the pelvis.	Enhances leg swing and stride efficiency, crucial for longer runs.

Table 2.1: (Continue)

Adductor Brevis	Stabilizes pelvis and aids hip adduction.	Improves medial leg stability and control, enhancing stride dynamics.
Adductor Longus	Maintains adduction and medial stabilization of the thigh.	Supports energy conservation and maintains directional stability.
Iliacus	Works with psoas to flex the hip efficiently.	Increases hip flexion strength, aiding in higher and faster leg lifts.
Piriformis	Stabilizes the hip and assists in external rotation.	Prevents excessive internal rotation, optimizing leg alignment.
Psoas	Major hip flexor that lifts the leg during the swing phase.	Enhances stride frequency and length, critical for maintaining pace.
Tibialis Anterior	Responsible for dorsiflexion of the foot (Tsuji et al., 2015).	Prevents foot slap and prepares the foot for smooth ground contact (Tsuji et al., 2015).
Extensor Hallucis Longus	Extends the big toe and aids dorsiflexion.	Strengthens toe-off phase, crucial for effective push-off and balance.

2.7 The Effect of Shoe Cushioning and Running Distance on Running Performance

In most circumstance, running is typically studied with running shoes, and different shoe cushioning affects performance. Lim et al. (2022) and Malisoux et al. (2021) found that shoes increase range of motion, and that hard cushioning creates higher impact forces during the stance phase, while soft cushioning absorbs shock. This cushioning impact can cause inconsistencies in kinematics and dynamics parameters.

Additionally, it is well known that running patterns change with accumulated distance. During ultramarathons (50 km to 100 km), the body adapts by increasing stride frequency, reducing maximum vertical ground reaction forces (GRFs), and decreasing vertical impulse during heel strikes (Thompson, 2017). Beyond these surface-level changes, biomechanically, there is interest in understanding the behavior of individual muscles during long-distance running. Such studies allow for a detailed analysis of how specific muscles contribute to agonist-antagonist interactions, balance, and coordination.

2.8 The Role of Lower Limb Deep Muscle on Running

Deep muscles, located beneath superficial muscles and closer to the bones, play a crucial role in stabilizing joints, maintaining posture, and controlling fine movements. For instance, the adductor magnus muscle, located at the hip, plays a significant role in extending the hip joint and assisting in thigh adduction (Platzer et al., 2003). In contrast, the sartorius muscle flexes and abducts the hip joint (Bablitz-Parker, n.d.). At the knee, the semitendinosus muscle helps with knee flexion and hip extension (Moore et al., 2013; Hislop and Montgomery, 2007). The vastus intermedius, found deep to the rectus femoris in the anterior thigh, contributes to knee extension during running. The extensor digitorum longus, an ankle dorsiflexor muscle, extends the toes by pulling them upwards during running (Jarmey, 2018).

CHAPTER 3

METHODOLOGY

3.1 Introduction

The study can be done by the following key steps of milestone: collecting experimental data such as electromyography data, static and running trajectory marker position data; collecting tri-axis virtual ground reaction force (VGRF) of information; building musculoskeletal model; perform validation process by going through scaling, inverse kinematic and dynamic analysis; and lastly perform muscle-driven simulation and prediction.

To use OpenSim software to conduct the study, the trajectory data of the markers that were pasted on the test subjects needed to be extracted from the C3D (.c3d) format into the Track Row Column (.trc) format. This can be done by either using MATLAB or Python, which the conversion tutorial and the relevant files can be obtained from OpenSim official User's Guide webpage (<https://shorturl.at/deru1>). However, currently OpenSim software itself have the capability of converting these experimental motion capture files. After that, the VGRF information needs to be extracted experimentally as well and organized into left and right; point, vector and torque columns. After this, the simulation can be proceeded seamlessly from the given experimental initial data.

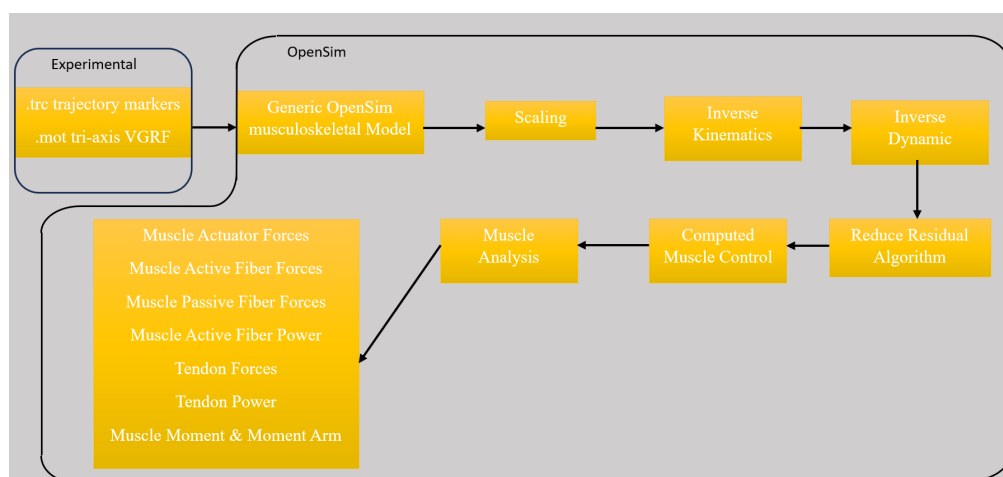


Figure 3.1: The General Workflow of the Modelling Study

The present study builds upon prior research investigating the impact of running shoe cushioning on muscle activation. Boon (2023; 2022) conducted a comprehensive analysis in the effect of running shoe cushioning on muscle activation by using OpenSim, by leveraging the insights and methodologies outlined in Boon's work, this study extends the work towards Computational Modelling of Running Biomechanics in Amateur Runners.

3.2 Experimental Data Collection

Running the computational modelling to study the running biomechanics in amateur running via OpenSim absolutely requires the trajectory marker and the VGRF data that only can be obtained from amateur runners experimentally. Thus, although the experimental data collecting procedure is not under the scope of this study, but the process still is worth to be pointing out roughly.

In this study, 10 Malaysian male non-professional runners were recruited to be the data collection subjects, with each of them enclosed with the thorough description of the experimental data collection protocol and been received their informed consent before conducting the study (Boon, 2023).

Table 3.1: The Physical and Physiological Data of the Participants (Boon, 2023)

Characteristic	Mean \pm Standard Deviation
Age (years)	29.20 \pm 3.52
Height (m)	1.72 \pm 0.05
Weight (kg)	70.05 \pm 6.91
BMI (kg/m²)	23.68 \pm 1.40

They were required to run accumulatively by wearing shoes that were made by either of two types of cushioning: hard or soft. Data collection was based on the accumulated overground running milestones (0km, 40km, 80km, 120km) and the two of shoe cushioning categorization. The running distances were tracked by using the monitoring apps and the smartwatches, and each participant was required to perform data collection session at Sports Performance Laboratory at Malaysia National Sports Institute (Institut Sukan

Negara, ISN) once the specified milestone has been achieved or beyond of that (Boon, 2023).

In the aspect of the setup equipment for the data collection session, it was held in ISN with a comprehensive motion capture system. It was consisted of 11 cameras (Qualisys Track Manager, QTM 2022, 300 Hz), an instrumented treadmill equipped with force plates (Bertec Instrumented Treadmill, 1500 Hz), and 35 Qualisys optical markers (QualisysAB, 2019) placed on the data collection subject's body.



Figure 3.2: The Cameras Setup of the Motion Capture System (Boon, 2023)



Figure 3.3: The Qualisys Optical Markers Position of Placements (Boon et al., 2022)

When the test subjects were came over to the venue for data collection, in order to obtain the data that is as natural or as proximal to reality

running as possible, warming up was performed by test subject running up to his self-paced speed up to 8 minutes, usually would be at 8 km/h of running speed so that they can get to use to the data collection's running speed, which is 12 km/h. Warming up activities were performed to avoid the test subject experienced any discomfort due to the unfamiliarity of the venue, large amount of marker placement on the body, or the speed. This disconformity may cause unnatural running pattern and thus affect the subsequent simulation analysis. Before the data collection phase, maximal voluntary contraction (MVC) exercises were conducted to obtain the necessary electromyography (EMG) data. The placement of the EMG electrodes is illustrated in Figure 3.4.

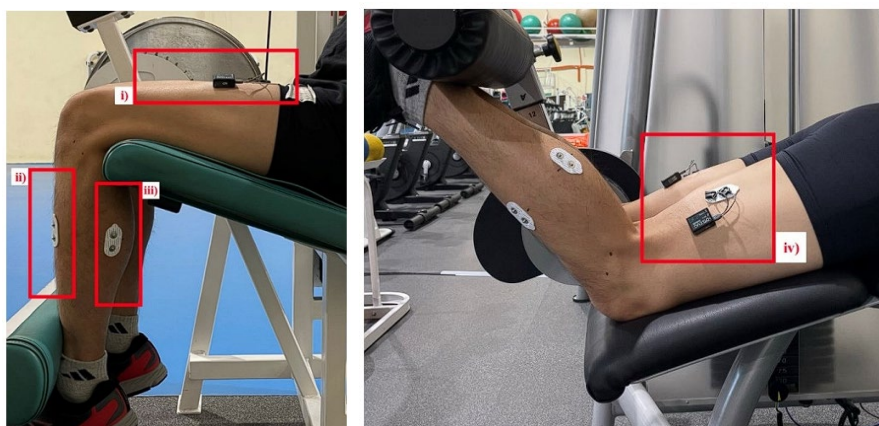


Figure 3.4: EMG Electrodes Placement on i) Rectus Femoris - RF, ii) Tibialis Anterior - TA, iii) Lateral Gastrocnemius - LG and iv) Biceps Femoris - BF (Boon, 2023)

During the data collection session, participants were required to run while wearing EMG electrodes under two shoe cushioning conditions: hard cushioning with a Shore hardness of 42A and soft cushioning with a Shore hardness of 32A, as measured by the Shore 'A' hardness scale and a Digital Shore A durometer. EMG data during running was wirelessly recorded using the Noraxon system (Noraxon MyoMuscle DTS Desktop Receiver System, 1500 Hz, Noraxon, Scottsdale, USA).



Figure 3.5: Shoes of Hard Cushioning (Left) and Soft Cushioning (Right)
(Boon, 2023)

Under different condition of shoe cushioning and the accumulated running distance, the mechanics parameters and the performance amateur runners can be studied by analysing their running biomechanics under computationally modelling.

Table 3.2: The Condition of Shoe Cushioning and the Different Accumulation Running Distance that were acted as the Parameters for Studying the Running Biomechanics of the Amateur Runners

Cushioning Conditions	Hard Shoe Cushioning	Soft Shoe Cushioning
	0km	0km
Accumulated	40km	40km
Running Distance	80km	80km
	120km	120km

3.3 OpenSim Musculoskeletal Model

Once the trajectory marker (.trc) files and the VGRF (.mot) files have been collected, the study can be proceeded to familiar with OpenSim as the open source neuromusculoskeletal simulation and analysis platform. OpenSim offers a variety of generic model to cope with different scene of usage, thus allowing users to develop, analyse, and visualize models of the musculoskeletal system, and to generate various of movement simulation dynamically (Seth et al., 2011).

In this study, the examine parameters and analysis would be more engaged in the lower limbs, lower extremities running parts, as to be proved by Brooks et al (2020), upper extremities mostly acts as the body overall

balancing and has no effect on the running performance. Although the upper extremities movement is still required to be simulated out, however the mechanics study will not be performed in this case. Therefore, in this case, the running and lower extremities focused generic model called “Full Body Model for use in Dynamic Simulations of Human Gait” which can be downloaded from https://simtk.org/projects/full_body would be used as the initiator of the study (Rajagopal et al., 2016). Mentioned by Rajagopal et al. (2016), the generic model was built upon by referencing the previous anatomical measurements of 21 cadaver specimens and magnetic resonance images of 24 young healthy subjects, the full rigid body of the musculoskeletal model has been geometrically built equipped with 37 degrees of freedom to define joint kinematics, Hill-type models of 80 muscle-tendon units actuating the lower limbs, and 17 ideal torque actuators driving the upper body. This generic model is very suited to the focus of study which only scaling is required to be done to adjust the virtual markers against the experimental markers. The model has preset physical data such as the default markers position, height and the marker scale factors, which need to be changed according to the test subjects’ information that been acquired experimentally.

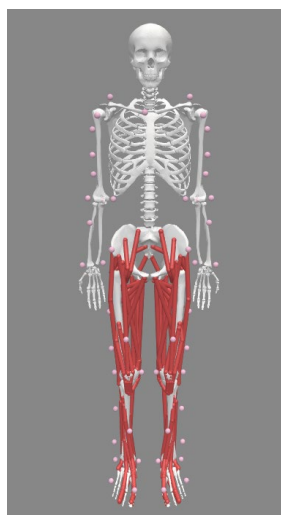


Figure 3.6: The Full Body Generic Musculoskeletal Model that is also Known as Rajagopal Model (Rajagopal et al., 2016)

3.3.1 Scaling

The main purpose of scaling is to adjust the position of the virtual markers position so that it would be as similar to the experimental markers position as possible. This similarity allows the subsequence analysis to be logic, reasonable and accurate to the actual scenario.

Scaling can be conducted by importing the static trajectory maker data onto the interface under the “Scale Model” and the “Adjust Model Markers” sections. Furthermore, in order to setup the generic model so that it is more approximate to the test subject’s body shape, the availability of the markers to be traced; the body part that to be paired by the markers set; the individual marker scale factor; and each markers pose weights, all were needed to do adjustment according to the individual test subject’s markers setup during the data collection session. Lastly, the weight of the model also needs to key in accordance with test subject’s weight. Figure 3.7 illustrates the schematic diagram for running the scaling, where dashed arrow line indicates the file was optional to be provided.

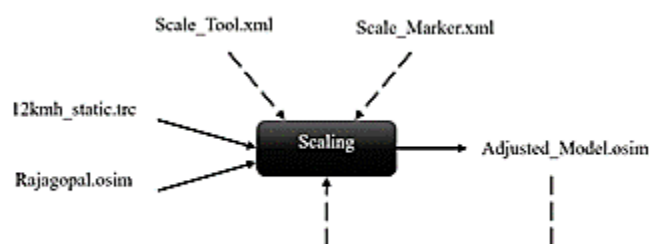


Figure 3.7: The Simple Schematic Diagram for Running the Scaling Process

Once all the marker scale factor and the marker pose weight have been keyed into the interface respectively, hit Run to perform the model scaling. On the terminal, the marker error Root Mean Square (RMS) would be displayed in meter (m) and it is always recommended to be less than 1 cm.

After that, the marker data was saved, and since this scaling mechanism itself contains a certain extent of gradient descent algorithm. The scaling can be run reiteratively, with incorporating with the save marker data, for several times until the result was satisfied.

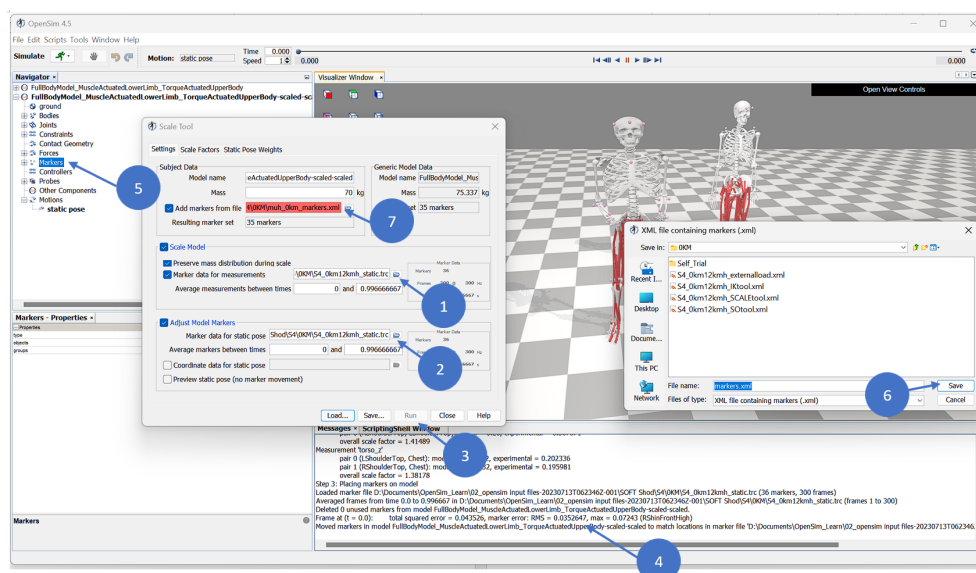


Figure 3.8: The Key Steps to Perform Scaling in OpenSim

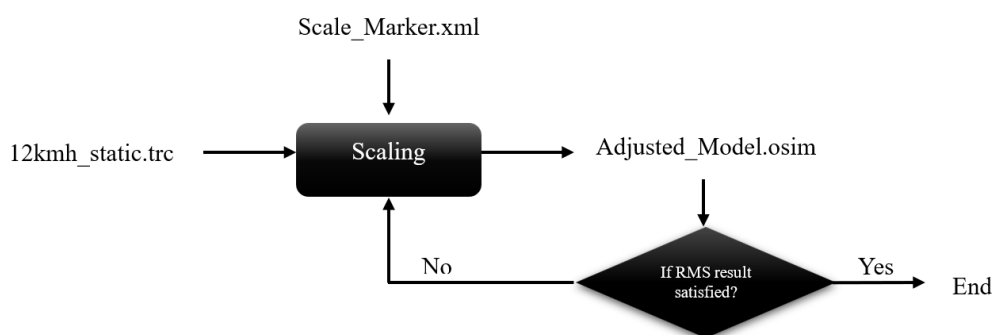


Figure 3.9: The Simple Workflow of the Scaling Reiterative Process

3.4 Experimental-Simulation Moment Validation

After scaling, performing validation involves inverse-based analysis process that includes inverse kinematics and inverse dynamics. Additionally, it also involves extracting the experimental data so that the comparison can be done by examine a few statistics parameter such as root mean square error (RMSE) and Pearson coefficient correlation (R-value).

3.4.1 Inverse Kinematics

This process involves importing the running trajectory markers data of the test subject and also adjusting the weightage of the markers. The weightage involves informing the software which markers are more important and should

be tracked more tightly compared to others (Hicks, 2016). The inverse kinematics solver involves the equation of weighted least squares.

$$\min_q \left[\sum_{i \in \text{markers}} w_i \|x_i^{\text{exp}} - x_i(q)\|^2 + \sum_{j \in \text{unprescribed coords}} w_j (q_j^{\text{exp}} - q_j)^2 \right] \quad (3.1)$$

$q_j = q_j^{\text{exp}}$ for all prescribed coordinated j

where

q is the vector,

i is the marker, while j is coordinate,

w_i is a weight assigned to marker i , while w_j is a weight assigned to coordinate j ,

x_i^{exp} is the experimental position of marker i , while q_j^{exp} is the experimental coordinate j ,

$x_i(q)$ is the position of the marker i , q_j is the model's value for coordinate j .

The goal is to determine the set of joint angles (generalized coordinates) that best match the movement observed in experimental data, subject to constraints like prescribed joint angles. Based on Equation 3.1, the weights w_i and w_j determine the relative importance of each term in the sum. A larger weight means that the term is considered more important during the optimization, and the algorithm will prioritize minimizing that particular error. Therefore, if a body part (or corresponding marker) has a smaller weight w_i assigned to it, the optimization algorithm will consider the error associated with that marker as less significant. As a result, the algorithm might be more willing to accept a larger error for that marker in favor of reducing the error for markers with higher weights. Body parts with the least weighting would be less likely to be accurately represented in the optimized solution because the algorithm doesn't prioritize their accuracy as highly. Thus, in the study, the body part that has involved with the lower extremities would be set up to 1000 compared to other parts which was only 20.

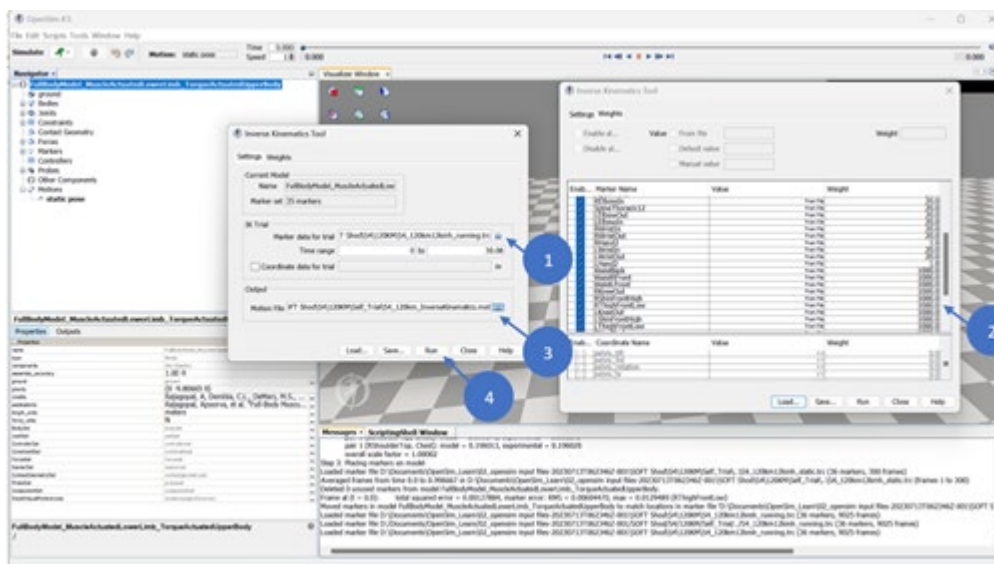


Figure 3.10: The Key Steps to Perform IK in OpenSim

3.4.2 Inverse Dynamics

Since IK only contains the joint angles of the musculoskeletal model, performing moment validation still requires performing ID simulation. The inverse kinematics motion (.mot) file requires to feed into the ID's interface. However, the VGRF of the experimental data was also required to feed into the interface as well. Before feeding the VGRF .mot file into the ID simulation interface, a few settings needed to be done to inform the software on the vector force, point force and the torque of the VGRF labeling and also left and right, which is as illustrated in Figure 3.12(5). Only then, the ID was now right to proceed.

Mathematically, ID solver involves the classical mechanics fundamental of inverse dynamics equation of motion for a multi-body system. Inverse dynamics is a method used to calculate the forces and moments (torques) required at the joints to produce a given motion (Hicks, 2024b). As shown in Equation 2.3, the mathematical result of the torque heavily depends on the kinematics information ($\mathbf{q}, \dot{\mathbf{q}}, \ddot{\mathbf{q}}$) and the VGRF information (\mathbf{C}, \mathbf{G})

$$\boldsymbol{\tau} = \mathbf{M}(\mathbf{q})\ddot{\mathbf{q}} + \mathbf{C}(\mathbf{q}, \dot{\mathbf{q}}) + \mathbf{G}(\mathbf{q}) \quad (3.2)$$

where

$\mathbf{q}, \dot{\mathbf{q}}, \ddot{\mathbf{q}} \in \mathbf{R}^N$ are the vectors of generalized position, velocities and accelerations, respectively,

$M(q)$ is the mass matrix,
 $C(q, \dot{q}) \in R^N$ is the Coriolis and centrifugal force matrix,
 $G(q) \in R^N$ is the gravitational force matrix,
 $\tau = Q$ is the generalized moment or torques for the particular joint.

The position and velocities parameters usually can be deduced through the IK data where the mass distribution, gravity, and the acceleration parameters would be able to obtain via the VGRF motion file. The output file of the ID would be in Storage (.sto) format.

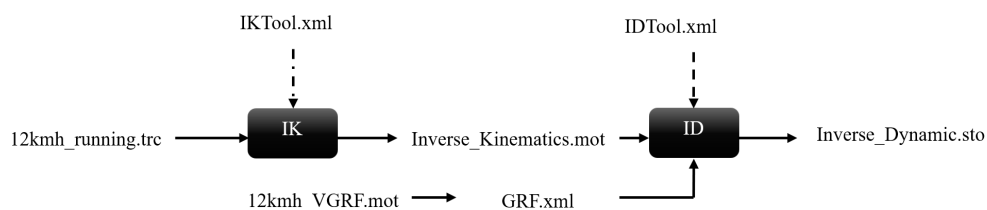


Figure 3.11: The Overall Workflow of the IK and ID and the Files Requirements to Run the Tools

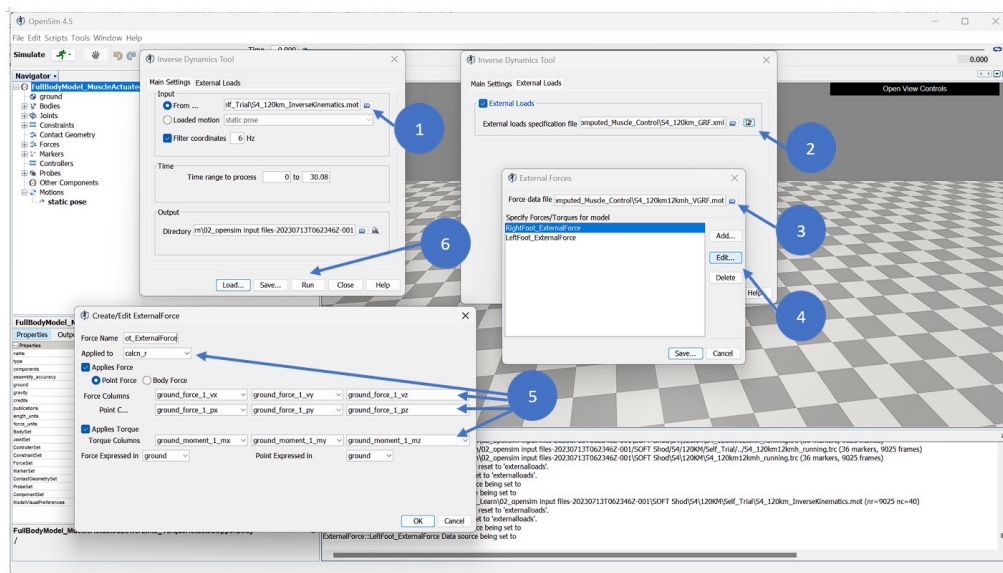


Figure 3.12: The Key Steps to Perform ID in OpenSim

3.4.3 Residual Reduction Algorithm

The main purpose of requiring undergoing RRA before proceeding with the further simulation processes is to ensure that the kinematics and kinetics running information are always dynamically consistence to each other. It plays the role of modifies the mass properties and distribution (like segment masses or inertial properties) of the model to better reflect the actual body dynamics observed in experimental data, and to minimize the unexplained forces (residuals) applied at the joints (Hicks, 2018). RRA serves the kinematics optimization process to ensure that $\mathbf{F} = \mathbf{ma}$ by eliminating and reducing residual force $\mathbf{F}_{residual}$. Figure xx shows the file requirements for running RRA.

Mathematically, the residual force $\mathbf{F}_{residual}$ is considered existing when the kinetic information itself does not fulfill the Newton second's law. In terms of the classical mechanics point of view, the equation of motion only legitis when the residual force added into the system. Thus, the numerical cost function J needs to be reiterated until the residual force has been resolved.

$$\sum \mathbf{F} + \mathbf{F}_{residual} = \mathbf{ma} \quad (3.3)$$

$$\mathbf{M}(\mathbf{q})\ddot{\mathbf{q}} + \mathbf{C}(\mathbf{q}, \dot{\mathbf{q}}) + \mathbf{G}(\mathbf{q}) = \mathbf{F}_{external} + \mathbf{F}_{muscle} + \mathbf{F}_{residual} \quad (3.4)$$

$$\text{Minimize } J = \sum_{i=1}^N \left(\|\mathbf{F}_{residual,i}\|^2 + \|\mathbf{M}_{residual,i}\|^2 \right) \quad (3.5)$$

where

N is the data sample,

J is the cost function,

$\mathbf{q}, \dot{\mathbf{q}}, \ddot{\mathbf{q}}$ are the vectors of generalized position, velocities and accelerations, respectively,

$\mathbf{M}(\mathbf{q})$ is the mass matrix,

$\mathbf{C}(\mathbf{q}, \dot{\mathbf{q}})$ is the Coriolis and centrifugal force matrix,

$\mathbf{G}(\mathbf{q})$ is the gravitational force matrix.

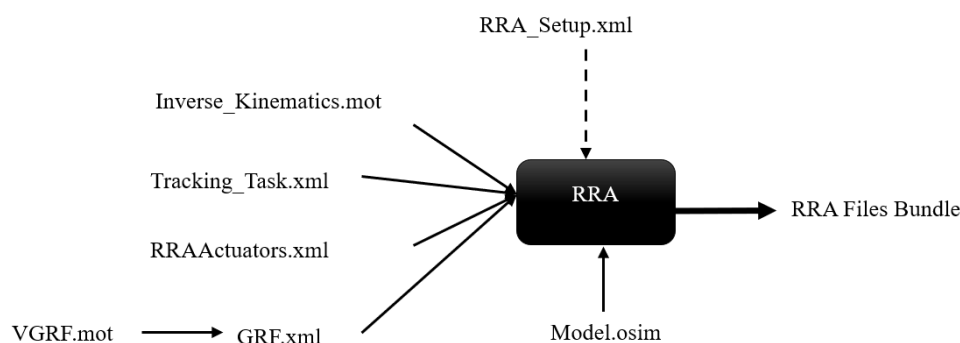


Figure 3.13: The Files Requirement of Running the RRA in OpenSim

3.5 Muscle-Driven Simulation

After the validation, each lower limb muscle activity can be estimated out by using muscle-driven simulation. It is one of the main capabilities of OpenSim: a biomechanical simulation that uses Hill-type muscle models to generate the forces necessary to drive the motion of the body, with that, each muscle activities and properties can be extracted out for further analysis its roles and functions towards the overall running movement.

3.5.1 Mechanical Parameters and Muscle Study Selection

In this study, the interested parameters for this muscle biomechanical study are muscle actuator force, muscle active force and muscle passive force, and their definition in OpenSim is as shown in Table 3.3. While Table 3.4 shows the interested deep muscle to be studied.

Table 3.3: The Study Parameters and Their Respective Definition in the Simulation Environment

Study Parameters	Definition in OpenSim
Muscle actuator force	It refers to the total muscular resultant force generated by that individual muscle group, which directly contributes to drive the particular joint movements in simulation.
Muscle active force	The force produced by the individual muscle group upon contract during the initial spike of the excitation in response to neural activation.

Table 3.3: (Continue)

Muscle passive force	The force produced by the individual muscle group when it is stretched during its resting length, independent of muscle activation.
-----------------------------	---

Table 3.4: Deep Muscles Selection for Muscular Force Prediction Analysis

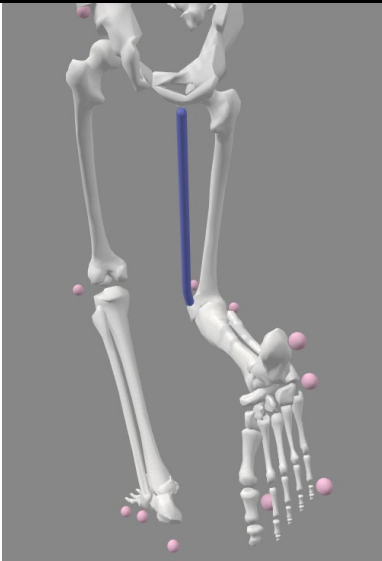
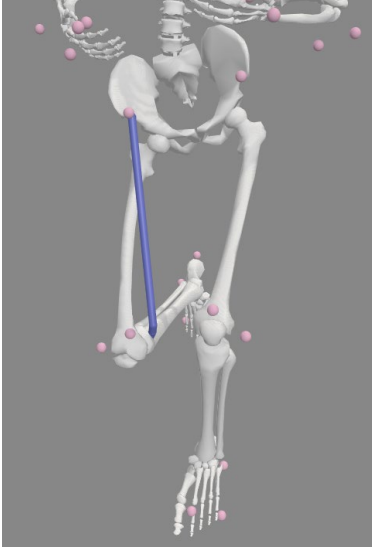
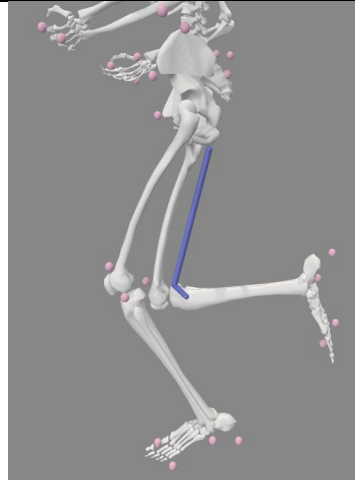
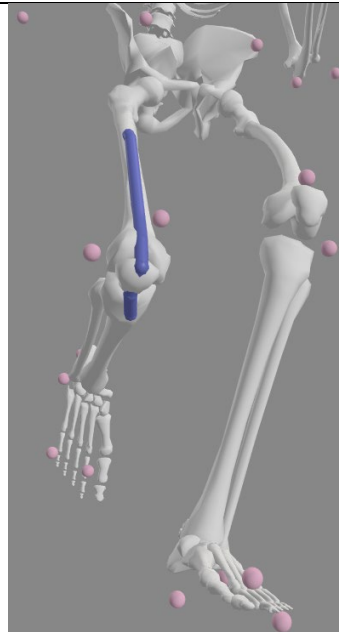
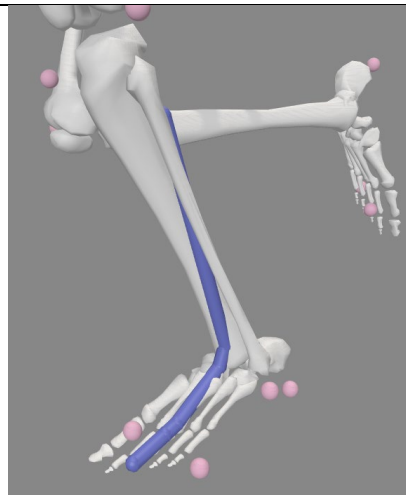
Deep Muscle (Right)	Figures
Adductor magnus ischial	
Sartorius	

Table 3.4: (Continue)

Semitendinosus**Vastus intermedius****Extensor digitorum longus**

3.5.2 Computed Muscle Control & Static Optimization

In the aspect of muscle driven simulation in OpenSim, there are three techniques that can be used to perform it, which are CMC, SO and MocoInverse. CMC is to calculate muscle activations and forces that drive a musculoskeletal model based on tracking the kinematics data (Hicks, 2024a). This method uses a feedback control strategy where muscle activations are adjusted iteratively to minimize the error between the simulated movement and the experimental applied external forces data and is particularly useful for analyzing complex, dynamic tasks because it accounts for muscle dynamics and the inertia of body segments.

CMC uses Proportional-Derivative (PD) Control Law and the spring-mass damping system to compute the desired acceleration under the governed by the velocity and position feedback gains. In most cases, k_v would be 20 and k_p would be 100 to make the running motion system to be in critical damp. The desired acceleration would be used to compute the actuator controls, x via the cost function J .

$$\ddot{\mathbf{q}}\mathbb{E}^*(t+T) = \ddot{\mathbf{q}}_{exp}(t+T) + \mathbf{k}_v[\dot{\mathbf{q}}_{exp}(t) - \dot{\mathbf{q}}(t)] + \mathbf{k}_p[\mathbf{q}_{exp}(t) - \mathbf{q}(t)] \quad (3.6)$$

$$\mathbf{k}_v = 2\sqrt{\mathbf{k}_p} \quad (3.7)$$

$$\text{Minimize } J = \sum_{i=1}^{n_x} x_i^2 \quad (3.8)$$

$$C_j = \ddot{q}_j^* - \ddot{q}_j \quad \forall j \quad (3.9)$$

Where

$\ddot{\mathbf{q}}\mathbb{E}^*$ is the desired acceleration,

T is a futuristic time and it should be as small as about 0.001 seconds to allow the muscle force to change,

C_j is the equality constraints and $C_j = 0$.

Static Optimization, on the other hand, is an extension to inverse dynamics that further resolves the net joint moments into individual muscle forces at each instant in time. The muscle forces are resolved by minimizing the objective function while satisfying equilibrium and physiological

constraints. It has the tendency in finding the minimum muscle activation state for a given force movement. SO uses the given motion to solve the equation of motion for the unknown singular muscular generalized forces (Hicks, 2018b).

$$\sum_{m=1}^n (a_m F_m^0) r_{mj} = \tau_j \quad (3.10)$$

$$\text{Minimize } J = \sum_{m=1}^n (a_m)^p \quad (3.11)$$

where

J is the cost function that focus on minimizing the sum of squared muscle activations,

a_m is the activation level of the particular muscle,

F_m^0 is the maximum isometric force,

r_{mj} is the moment arm about the j th joint axis,

p is the defined constant (Hicks, 2018c).

Both CMC and SO can generate the results that can be used to proceed with the muscle mechanical estimation and analysis.

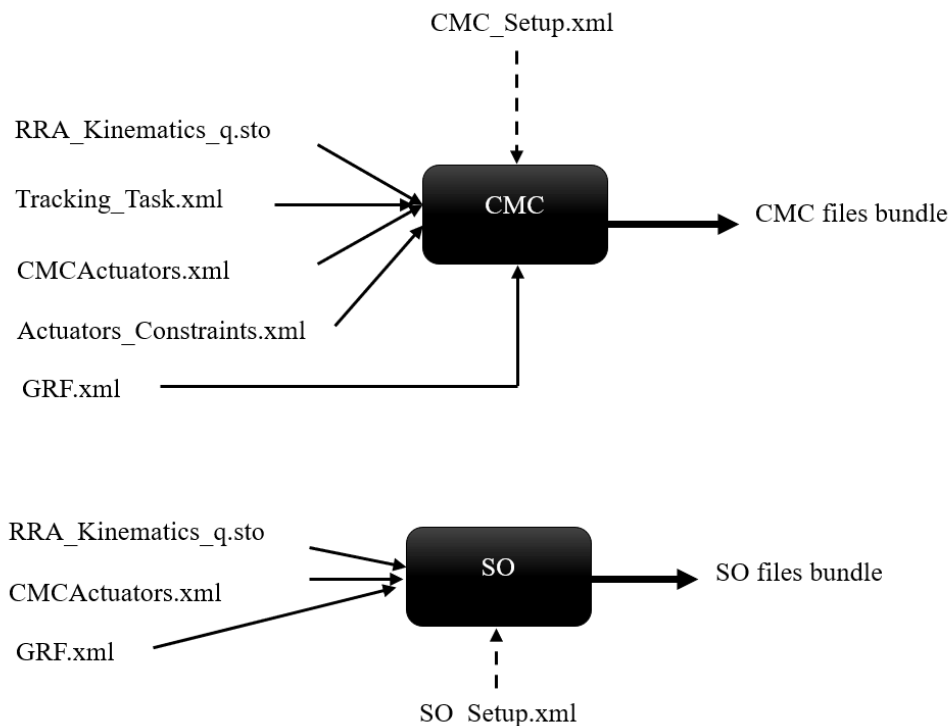


Figure 3.14: The Files Requirements of Running the CMC and SO

3.6 OpenSim Moco

Moco is a software under the framework of OpenSim designed to solve optimal control problems in biomechanics. Moco allows goal to be customized, such as aiming for minimizing movement effort for a specific motion, tracking virtual markers with experimental setup, and minimizing joint loading. Moco leverages direct collocation, a numerical method that transcribes continuous optimal control problems into a finite-dimensional nonlinear programming problem. Direct collocation allows trajectory path to be tracked by using piecewise polynomial function. This enables efficient and accurate simulations of complex musculoskeletal dynamics, providing insights into movement mechanics, muscle coordination, and rehabilitation outcomes. The direct collocation approach used in Moco discretizes the time-dependent variables, such as states and controls, into a series of time points, enabling simultaneous optimization of both the movement trajectory and control signals.

The Moco framework operates within an Anaconda Python environment, which does not provide an interactive skeleton or graphical user interface (GUI) for direct manipulation. All Moco-related simulations must be executed via Python coding and command-line instructions, limiting

interaction to script-based workflows rather than visual interfaces. Moco is only recommended to be used for advanced users comfortable with coding and it also requires more technical proficiency for simulation control and analysis.

3.6.1 MocoTrack

This tool performs simulation by tracing marker trajectory data while solving the model kinematics and actuator controls optimization problem. It serves to produce kinematics data by tracking the VGRF reference data and the marker positions under direct collocation optimal control problem.

$$\min \int_0^T \|x(t) - x_{exp}(t)\|^2 dt \quad (3.12)$$

subject to:

$$\dot{x}(t) = f(x(t), u(t)) \quad (3.13)$$

$$x(0) = x_0 \quad (3.14)$$

$$g(x(t), u(t)) \leq 0 \quad (3.15)$$

Where:

$x(t)$ is the system state,

$u(t)$ is the control input,

$f(x(t), u(t))$ represents the system dynamics,

$x_{exp}(t)$ is the experimental data,

T is the time duration of the simulation (Lin and Pandy, 2017).

MocoTrack solves an optimal control problem where the objective is to minimize the error between the model's predicted motion $x(t)$ and the experimental data $x_{exp}(t)$, subject to the system dynamics $\dot{x}(t)$ and other constraints $g(x(t), u(t))$.

Figure 3.15 presents the schematic diagram for executing MocoTrack. To successfully run MocoTrack, the most essential Python functions include `opensim.Model`, `opensim.ModOpAddExternalLoads`, and `opensim.MocoTrack.setMarkersReferenceFromTRC`, which are responsible for importing the necessary files into the Moco simulation. On the other hand, Figure 3.16 shows the skeleton running result that was visualized

by Moco under Python environment when the simulation process have been completed.

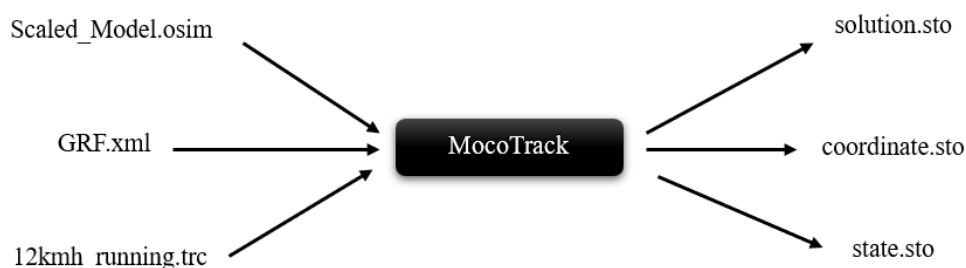


Figure 3.15: The Schematic Diagram for Mocotrack File Requirements

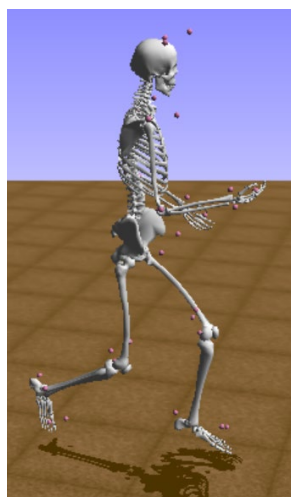


Figure 3.16: OpenSim MocoTrack Result Visualization

3.6.2 MocoInverse

MocoInverse is used to perform inverse simulations, where the objective is to estimate joint moments (torques) or generalized forces needed to reproduce an experimentally observed motion. It calculates the generalized forces necessary to match the recorded kinematics while adhering to the dynamic equations of the model.

$$\min \int_0^T \|\tau(t)\|^2 dt \quad (3.16)$$

subject to:

$$M(x(t))\ddot{x}(t) + C(x(t), \dot{x}(t)) + G(x(t)) = 0 \quad (3.17)$$

$$x(t) = x_{exp}(t) \quad (3.18)$$

Where:

$M(x(t))$ is the mass matrix of the system,

$C(x(t), \dot{x}(t))$ represents Coriolis and centrifugal forces,

$G(x(t))$ represents gravitational forces,

$\tau(t)$ is the vector of generalized forces (De Groote et al., 2016).

In MocoInverse, the task is to solve for joint moments $\tau(t)$ that produce the observed motion $x_{exp}(t)$, subject to the musculoskeletal model's dynamics.

Figure 3.17 illustrates the schematic diagram for executing MocoInverse. `opensim.Model`, `opensim.ModOpAddExternalLoads`, and `osim.MocoInverse.setKinematics` are the most important Python functions required to assure successfully simulation.

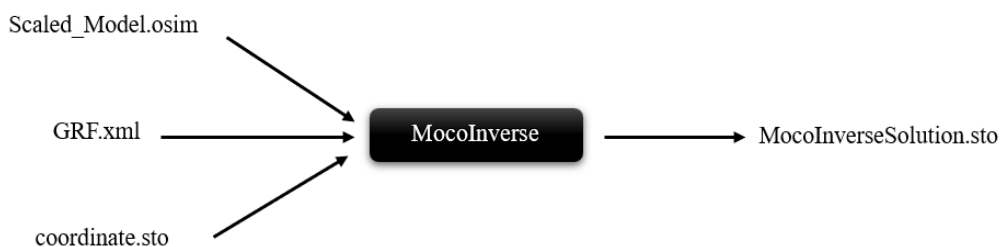


Figure 3.17: The Schematic Diagram for MocoInverse File Requirements

3.7 Data Analysis with MATLAB

MATLAB was used to process simulation results for a clearer, informative and interpretable stance-swing running analysis. Data indices for one running gait were identified based on right hip rotation. Isolated indices were used to extract interested biomechanics parameters, followed by averaging, standard deviation calculation, and visualization. The resulting averaged running moment gait was compared to other OpenSim inverse kinematics techniques

using root mean square error (RMSE), correlation (r), and computational time, presented in bar graphs.

On the other hand, MATLAB was used for data processing, including filtering EMG data (6 Hz 4th Butterworth lowpass filter), rectified, and normalized by MVC before validation. Based on the validation results, only one muscle-driven optimization technique was selected for further muscular force estimation. After that, only five deep muscles as shown in Table 3.4, were selected as the target of analysis. Those muscle are adductor magnus ischial, sartorius, semitendinosus, vastus intermedius and extensor digitorum longus.

CHAPTER 4

RESULTS AND DISCUSSION

4.1 Introduction

The simulation files for all 10 subjects were successfully extracted and read by OpenSim, as illustrated in Figure 4.1 and Figure 4.2. For each subject's data, there are four subfolders corresponding to the accumulated running distances, and the OpenSim-related files are organized within these subfolders based on the respective running distances.

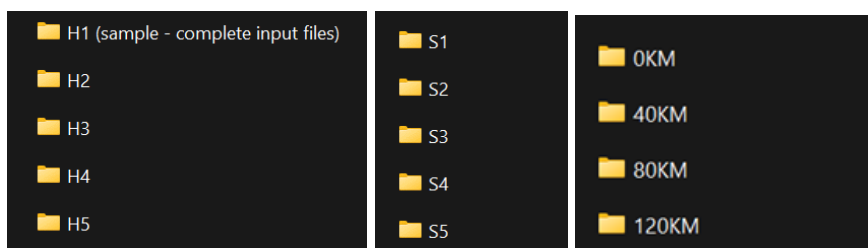


Figure 4.1: The Simulation Files for 5 Hard Shoe Cushioning and 5 Soft Cushioning

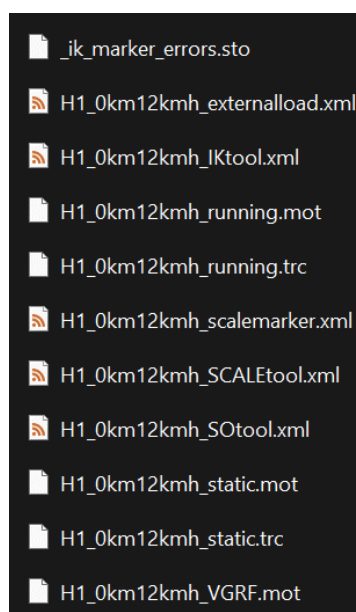


Figure 4.2: The Simulation Files That Contain the Static and Running Trajectory Marker Files and VGRF File That are Acquired from the Subject Experimentally

4.2 Scaling for Musculoskeletal Models

According to the OpenSim official documentation, the RMS error for scaling should be less than 1 cm. As shown in Table 4.1, the scaling results for all randomly selected subjects meet this standard, with RMS errors falling below the specified threshold (Hicks, 2019).

Table 4.1: The RMS of the Scaling Results for Randomly Picked Subjects

Hard Cushioning	RMS (cm)	Soft Cushioning	RMS (cm)
H1 (0km)	0.475	S1 (0km)	0.333
H1 (40km)	0.453	S1 (40km)	0.500
H1 (80km)	0.625	S1 (80km)	0.499
H1 (120km)	0.544	S1 (120km)	0.569
H4 (0km)	0.392	S2 (0km)	0.379
H4 (40km)	0.554	S2 (40km)	0.771
H4 (80km)	0.556	S2 (80km)	0.223
H4 (120km)	0.556	S2 (120km)	0.599

4.3 OpenSim's Knee and Ankle Moments Kinetics Validation

4.3.1 Gait Analysis

Wearing a shoe would have a huge impact on the moment gait, which means that $\mathbf{F} \neq \mathbf{ma}$. As a result, inconsistency of dynamically kinematic and kinetic parameters was distinguished. This inconsistency leads to different tools in OpenSim treating the data differently. RRA can reduce the residual force and report on the inconsistency, but it cannot eliminate it entirely. Table 4.2 presents the results of the RRA, showing the average residual force. Notably, F_y , the vertical force, is influenced by shoe cushioning in this study.

Table 4.2: Average Residuals Forces After RRA for Two Randomly Picked Subjects Wearing Hard Cushioning and Soft Cushioning Respectively

Shoe Cushioning	Average Residual	Force, N
Hard	F_x	-1.47503
	F_y	16.2115
	F_z	-1.79812
Soft	F_x	-3.50227
	F_y	-4.04652
	F_z	-2.72094

Figure 4.3 and Figure 4.4 show the knee moment gait for hard and soft running shoe cushioning, respectively, of a randomly selected subject, while Figure 4.5 and Figure 4.6 show the ankle moment gait under hard and soft, of a randomly selected subject.

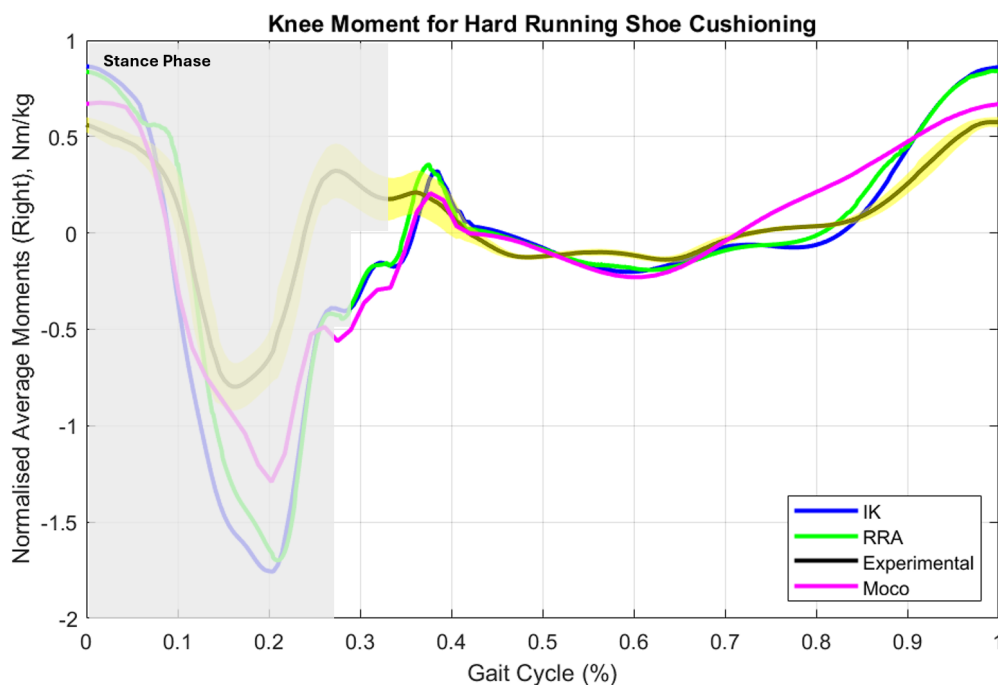


Figure 4.3: Knee Moment Gait for Hard Running Shoe Cushioning



Figure 4.4: Knee Moment Gait for Soft Running Shoe Cushioning

Both Figure 4.3 and Figure 4.4 show that different tools treat the impact force due to the shoe cushioning differently. In the stance phase, MocoTrack is more closely approximated to the experimental data, when comparing with the others two. In the hard shoe cushioning, as shown in Figure 4.3, MocoTrack overestimated the knee moment on the stance phase, while in the soft shoe cushioning (Figure 4.4), it underestimated the knee moment. Thus, it is believed that stance phase is the stage where the RMSE is accumulating, and correlation, r , behaves differently. However, in the swing phase, all tools simulated quite accurate to the experimental data, regardless of the type of the cushioning. It is mainly because during swing phase, the feet were not in contact with the ground, force accumulation does not involve. Swing phase is an energy releasing stage, where the movement is purely based on the kinematic driven. Thus, the effect of the cushioning is minimal during this phase.

However, as shown in Figure 4.5 and Figure 4.6, all tools perform well, and the results are closely approximated to the experimental data. It is because compared to the knee, the ankle is a less moveable part of the body segment. As the ankle is also closer to the force plate, causing the kinematic

parameters to be more dynamically consistent with the kinetic parameters, especially during the swing phase, where there is almost no performance difference for all tools. Nevertheless, if viewed closely, minor performance differences still exist among all tools in the stance phase, especially MocoTrack, which underestimates the ankle moment when compared to RRA and IK. Such underestimation is due to the tracking algorithm where MocoTrack performs tracking that is based on the VGRF and the trajectory markers information, and this tracking will harmonize the effect between these two mechanics parameters. On the other hand, IK is simulated more closely to the experimental data when compared with RRA and MocoTrack. In the meanwhile, RRA saw the VGRF information as the comparator to eliminate the residual force, attempting to minimize the dynamics gap in between kinematics and kinetics data.

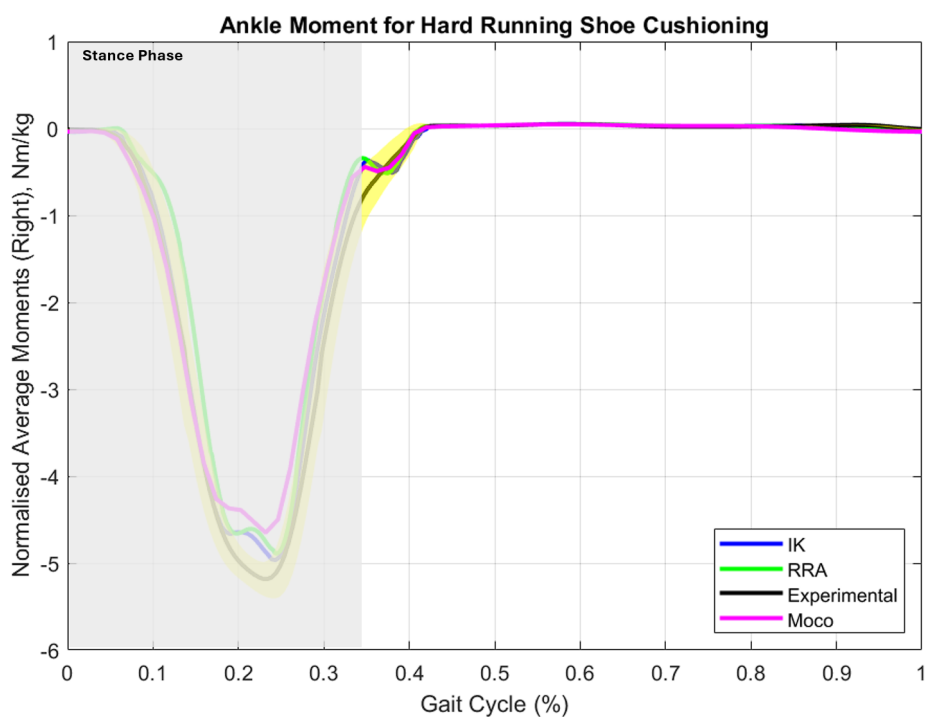


Figure 4.5: Ankle Moment Gait for Hard Running Shoe Cushioning

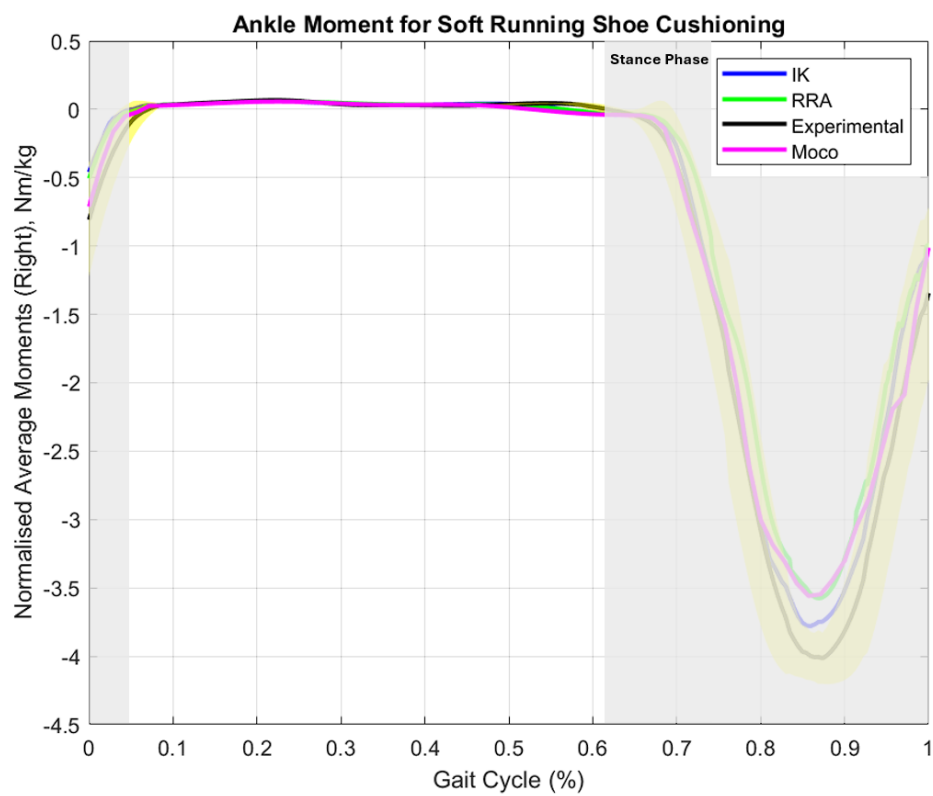


Figure 4.6: Ankle Moment Gait for Soft Running Shoe Cushioning

4.3.2 RMSE, Correlation and Computational Time

Figure 4.7 to Figure 4.10 show the performance comparison of IK, RRA, and MocoTrack in terms of RMSE, correlation (r), and computational time. The simulation computational time is based on the specifications of the devices, which were AMD Ryzen7 6,800HS, Nvidia RTX 3070 Ti, and 24 GB RAM. Higher computing specifications can significantly reduce computational time, particularly in OpenSim Moco, where the computational cost is notably higher compared to other tools. Indeed, more advanced computing devices enable the execution of more precise simulations within shorter timeframes, thereby improving the validation performance of virtual marker trajectory tracking-based inverse kinematics tools. RMSE was tabulated to compare the difference between the experimental data and the simulation result, and correlation (r) examine how closely the simulated data relates to the experimental data.

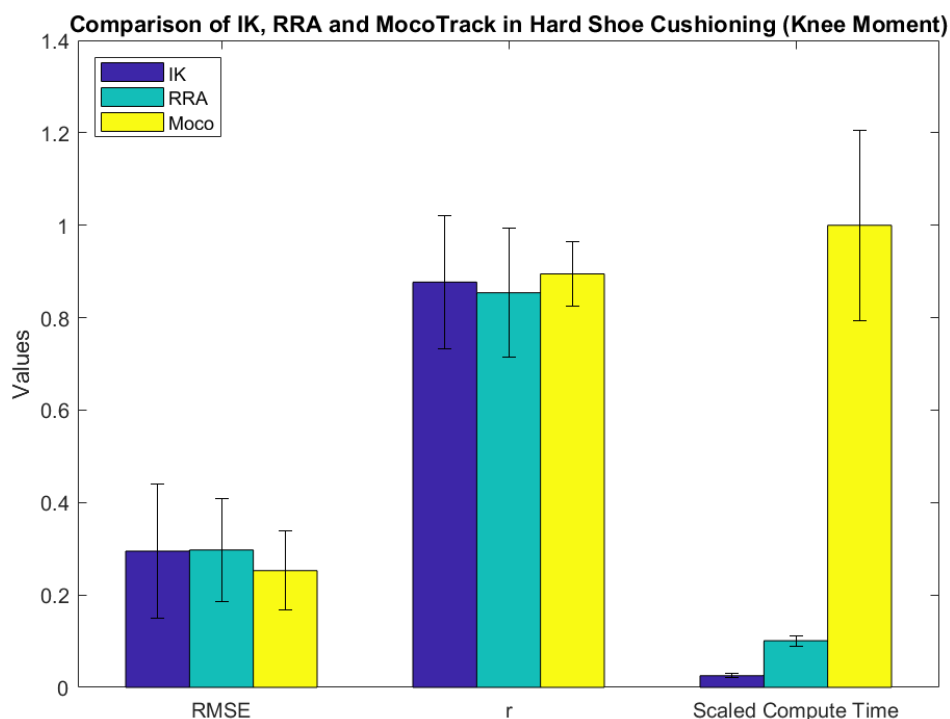


Figure 4.7: Comparison Of IK, RRA, and Mocotrack for Knee Moment Running Gait under Hard Shoe Cushioning

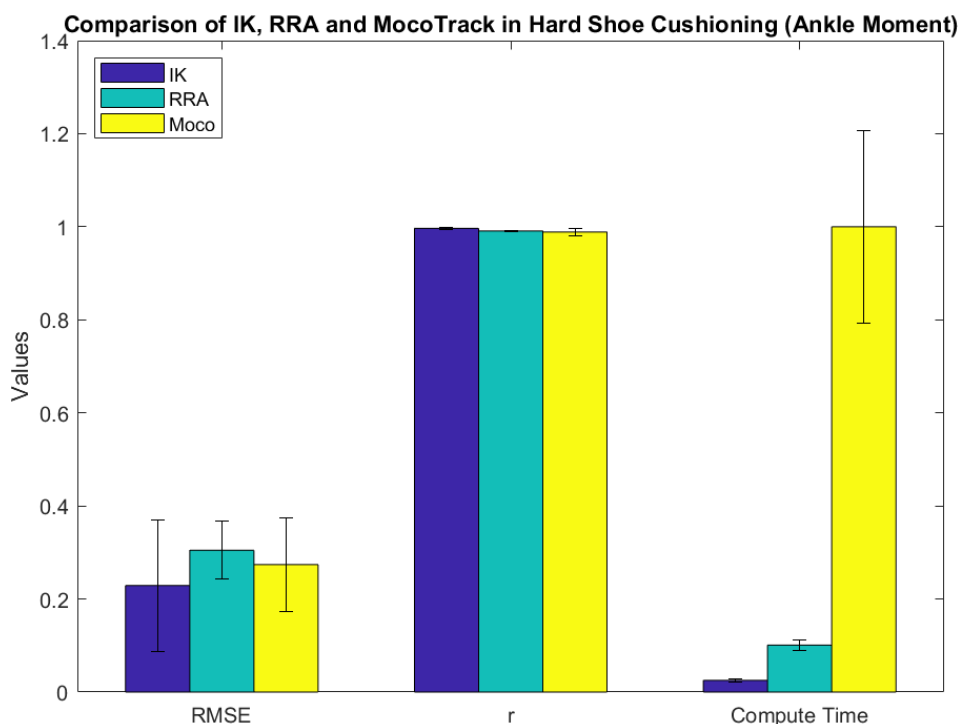


Figure 4.8: Comparison of IK, RRA, and Mocotrack for Ankle Moment Running Gait under Hard Shoe Cushioning

Table 4.3: Quantitative View of RMSE, r, and the Computational Time for IK, RRA and MocoTrack in Hard Running Shoe Cushioning

Body Segment	OpenSim Tools	Analysis Parameters	Average Value
Knee	IK	RMSE (Nm/kg)	0.295 ± 0.146
		r	0.877 ± 0.145
		Compute Time (s)	436.8 ± 70.92
	RRA	RMSE (Nm/kg)	0.297 ± 0.112
		r	0.854 ± 0.139
		Compute Time (s)	1479 ± 195.6
	MocoTrack	RMSE (Nm/kg)	0.253 ± 0.0852
		r	0.895 ± 0.0688
		Compute Time (s)	17313 ± 3572

Table 4.3: (Continue)

Ankle	IK	RMSE (Nm/kg)	0.229 ± 0.141
		r	0.997 ± 0.0028
	RRA	RMSE (Nm/kg)	0.305 ± 0.0624
		r	0.991 ± 0.00157
	MocoTrack	RMSE (Nm/kg)	0.274 ± 0.10
		r	0.989 ± 0.0076

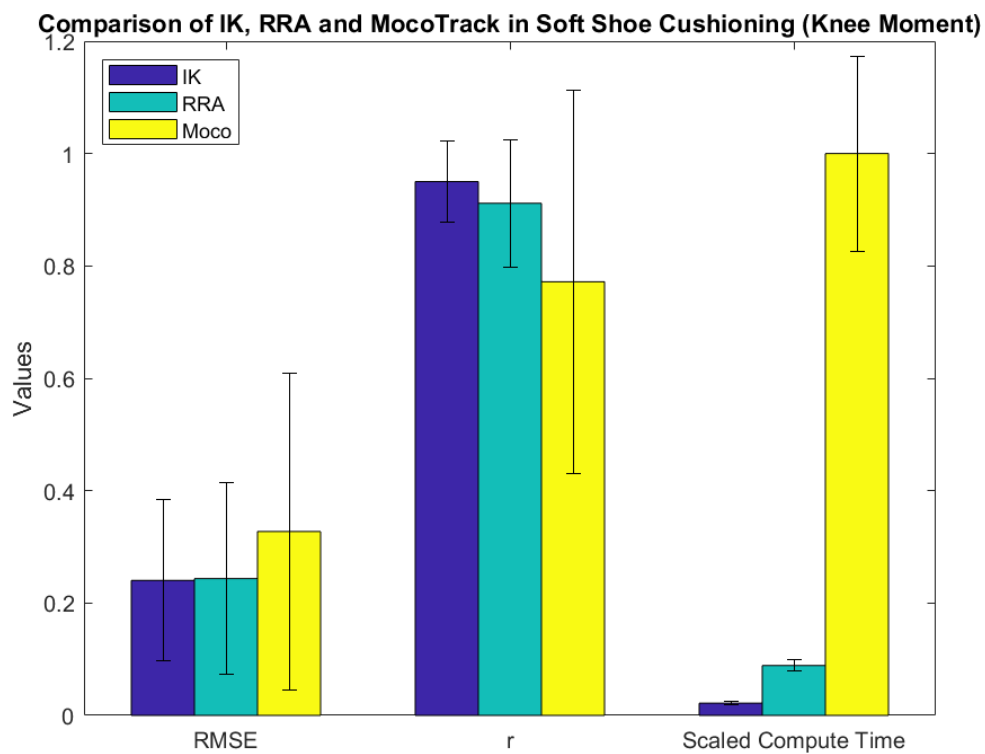


Figure 4.9: Comparison of IK, RRA, and Mocotrack for Knee Moment Running Gait under Soft Shoe Cushioning

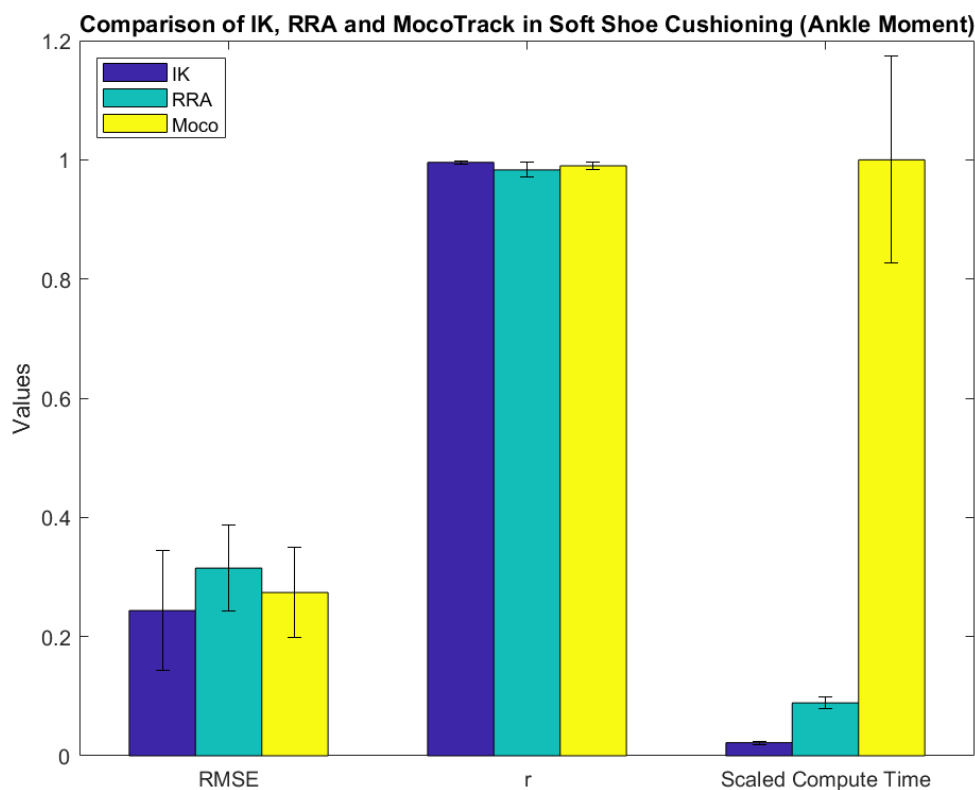


Figure 4.10: Comparison of IK, RRA, and Mocotrack for Ankle Moment
Running Gait under Soft Shoe Cushioning

Assessing closer in terms of RMSE, in running shoes with hard cushioning, MocoTrack performed the best compared to IK and RRA, and was also most highly correlated to the experimental data for knee moment (Table 4.3). The additional impulsive force exerted onto the body is obvious, thus it becomes the reason for the outstanding performance where MocoTrack uses direct collocation and optimal control problems to ensure the dynamic consistency between kinematic and kinetic parameters of running.

However, with the same type of cushioning, ankle moment is not the case. IK becomes the outstanding tool for tracking running motion. Compared to knee moment, ankle moment is a less movable body segment, and the additional impulse due to the hard cushioning may cause the moment to deviate. Despite this, the correlation shows that all tools generated moment gait that is very highly related to the experimental data.

In soft running shoe cushioning, the performance of MocoTrack is dropping in tracking running motion especially for knee moment (Table 4.4). Soft shoe cushioning indeed absorbs some extent of additional reaction force, which can

be shown in Table 4.2. The force is minor and ignorable, but it may cause MocoTrack, which is a tool that carefully considers dynamic consistency, to incorrectly interpret this minor force. It may incorrectly enlarge the force, causing overestimation and deviating from the true result. Its correlation also proves this deviation.

Table 4.4: Quantitative View of RMSE, r , and the Computational Time for IK, RRA and Mocotrack in Soft Running Shoe Cushioning

Body Segment	OpenSim Tools	Analysis Parameters	Average Value
Knee	IK	RMSE (Nm/kg)	0.240 ± 0.144
		r	0.950 ± 0.0717
		Compute Time (s)	419.25 ± 58.83
	RRA	RMSE (Nm/kg)	0.244 ± 0.170
		r	0.912 ± 0.113
		Compute Time (s)	1695 ± 194.07
	MocoTrack	RMSE (Nm/kg)	0.327 ± 0.282
		r	0.772 ± 0.341
		Compute Time (s)	19112 ± 3314
Ankle	IK	RMSE (Nm/kg)	0.244 ± 0.10
		r	0.996 ± 0.00279
	RRA	RMSE (Nm/kg)	0.315 ± 0.0718
		r	0.983 ± 0.0124
	MocoTrack	RMSE (Nm/kg)	0.274 ± 0.0755
		r	0.989 ± 0.00649

Soft shoe cushioning absorbs minor reaction force to the body but is negligible. Thus, IK and RRA performed equally well. IK and RRA are the tools that do not prioritize dynamic consistency, focusing on tracking the experimental kinematic trajectory data. In this case, they performed with a lower error than MocoTrack. In knee moment, the performance of both is

nearly identical in terms of RMSE and r . While in ankle moment, RRA is slightly better than IK, due to the properties of RRA as being an inverse kinematics optimization tool, allowing the data to be free from residual force which is then more accurate to the experimental value.

4.3.3 Performance Evaluation

Strictly speaking, all three OpenSim tools performed well in tracking the running kinematic motion. This is evident in their low RMSE, which was around 0.3 Nm/kg, and high correlation, with most of them providing the R-value greater than 95%. IK, RRA, and MocoTrack are profound, trustworthy, and reliable tools for performing biomechanical simulations of running with shoe cushioning. Although their results for RMSE and correlation differed from each other, the extent of these differences was not significant. In this scenario, computational time was the key factor for evaluating their performance, where some degree of accuracy could be sacrificed. Specifically, while MocoTrack generated lower RMSE in some cases, its computational cost was much heavier than IK and RRA. Therefore, IK has the best performance, followed by RRA, and lastly is MocoTrack. Additionally, in the case where the muscle-driven simulation is not required, IK definitely is the tools that is suffice enough to perform the marker trajectory inverse kinematics-based analysis.

4.4 Assessing Muscle Driven Optimization Techniques

4.4.1 EMG Validation

As shown Table 4.5, the lateral gastrocnemius (Gaslat)'s EMG validation identified CMC as having the lowest root mean square error (RMSE) and the highest correlation (R-value). However, CMC also had the longest computation time, followed by MocoInverse and SO. MocoInverse showed a lower RMSE than SO and a slightly higher average correlation than SO. Figure 4.11 and Figure 4.12 showed the lateral gastrocnemius muscle activation of experimental, CMC, SO and MocoInverse simulations for 40km and 80km accumulated running distance respectively. Theoretically, CMC uses PD control law and spring-mass damping system to solve the muscle-driven simulation problem, while SO is the further resolve of the inverse

dynamics problem by assuming that the system's dynamics are completely driven by the kinematics (positions, velocities, and accelerations) provided as input. CMC modelling muscle as Hill-type muscle, equipping springs, damping system, active force and passive force. CMC also modelling tendon with limited elasticity and Young Modulus. These are the key points making CMC results more realistic to the real-world scenario. However, CMC is very susceptible to the dynamics consistency, where any unmatched in between kinematics and kinetics information would lead to CMC system being collapsed, probing error to halt the simulation process. Whereas in SO, its further resolve algorithm restricts it only accounting for net force for a particular muscle that can generate, which is the force that direct contributing to the overall movement. Under this algorithm, SO would not consider muscle to have any passive force and assuming tendon is not a force transmission media, rigid and inextensible. More direct way to view this phenomenon is the muscle would be completely deactivated when the muscle does not move. Whereas MocoInverse implicitly handles multibody dynamics by solving for accelerations and generalized forces as variables in the optimal control problem, The solver in MocoInverse treats the accelerations as unknowns, optimizing them in a way that satisfies the equations of motion. This helps in achieving more accurate muscle force predictions. It can minimize the effect due to the residual force, but the effect of the shoe cushioning would be eliminated from the system simulation.

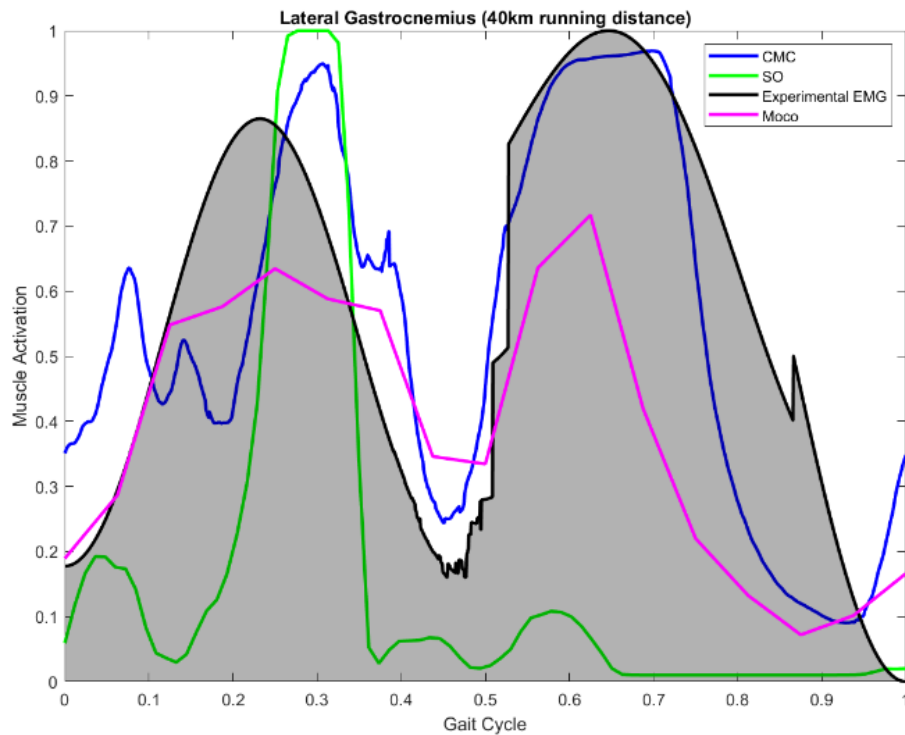


Figure 4.11: The EMG Validation Graph for 40 km Accumulated Running Distance

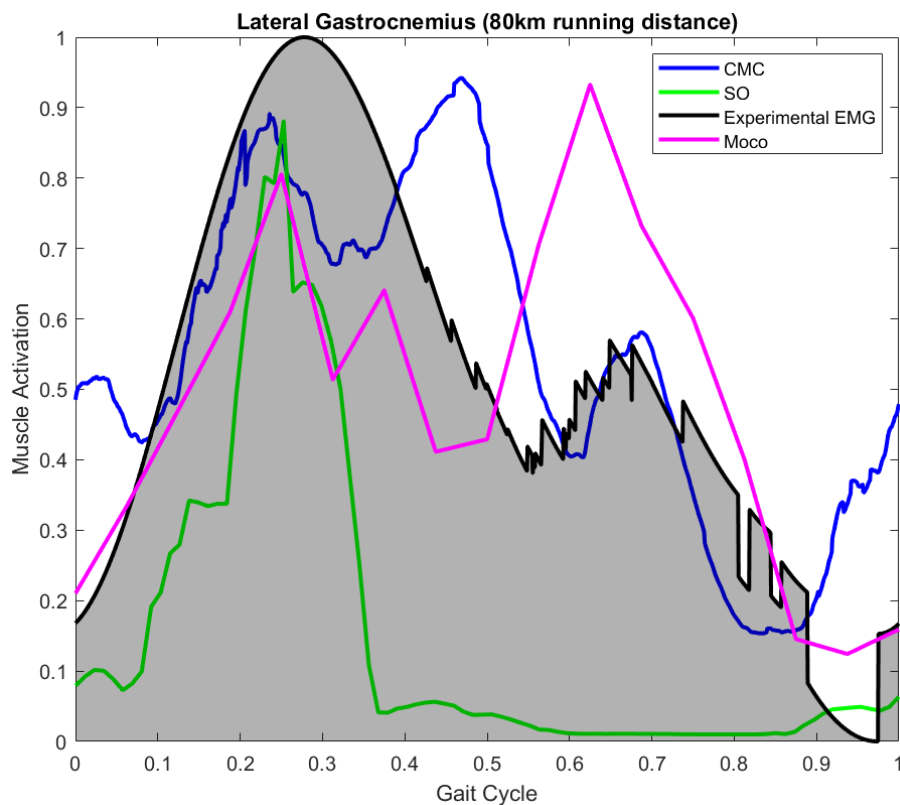


Figure 4.12: The EMG Validation Graph for 80 km Accumulated Running Distance

Table 4.5: The rmse, R-Value and the Computational Time for CMC, SO and MocoInverse Gaslat Validation

Running Distance	Optimization Techniques	RMSE	r	Compute time (hours)
40km	CMC	0.2042	0.7596	16.41
	SO	0.541	0.2329	7.68
	MocoInverse	0.2875	0.6308	10.51
80km	CMC	0.1934	0.7376	16.91
	SO	0.4068	0.7185	7.27
	MocoInverse	0.2119	0.6621	11.40

Based on the validation results, CMC can be concluded as the most effective muscle-driven optimization technique in OpenSim when compared to MocoInverse and SO. Consequently, the subsequent predictions will focus exclusively on the muscular forces of five deep muscles— adductor magnus ischial, sartorius, semitendinosus, vastus intermedius, and extensor digitorum longus—generated using CMC. The simulations were conducted on a computer equipped with an AMD Ryzen 7 6800HS, Nvidia RTX 3070 Ti, and 24 GB of RAM. Higher computer specifications would reduce computational time and allow for finer simulation settings, potentially leading to significant improvements in validation results.

4.4.2 CMC Muscular Force Estimation

The muscular estimation results generated via OpenSim CMC showed significant changes or turning points at 80 km of accumulated running distance. This indicates that the body adapts to such a long-accumulated running distance. Starting with the hip portion, as shown in Figure 4.13 dash line, the adductor magnus ischial muscle shows opposite trends at the 80 km accumulated running distance. It uses less force in the stance phase but more force in the swing phase. Unlike other running distances, force exertion increases as the accumulated running distance increases from 0 km to 120 km. When the subject reached 80 km, the muscle's adaptability was unable to keep

up, leading to fatigue in other hip muscles. By reducing the load on the adductor magnus ischial during the stance phase and increasing its role during the swing phase, the body might be trying to balance muscle workload and reduce the risk of overuse injuries. After adapting to the long running distance workload, the trend restored to what it was at 0 km and 40 km.

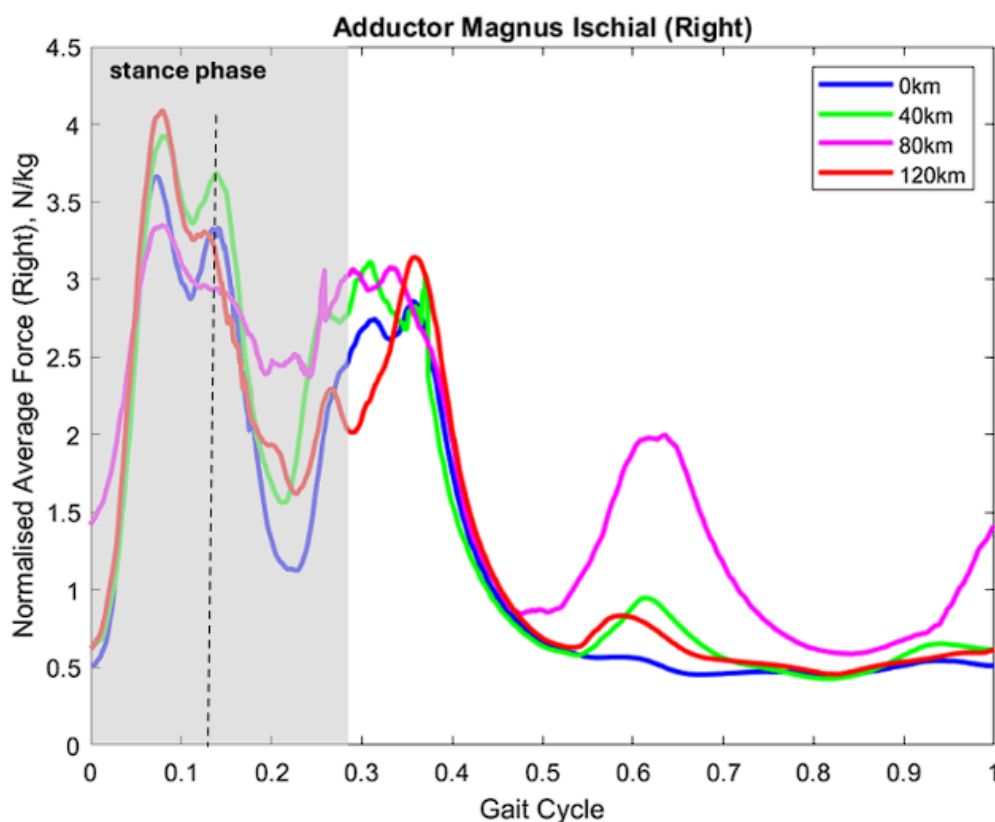


Figure 4.13: The Muscular Force Estimation for the Adductor Magnus Ischial across Different Accumulated Running Distance

Figure 4.14 shows the sartorius muscle force during one average gait cycle of running across different accumulated running distances. As shown on the dash lines of analysis, the force decreases in both stance and swing phases but increases at 120 km of accumulated running distance. Anatomically, the sartorius muscle plays a complex role in hip flexion, abduction, and knee flexion. Its long, thin structure spans both the hip and knee joints. As running distances increase, the efficiency of this muscle in performing these functions may decrease, especially if other hip muscles begin to fatigue. The increase in

force at 120 km could indicate a compensatory mechanism where the sartorius takes on a greater role to maintain joint stability and proper movement patterns.

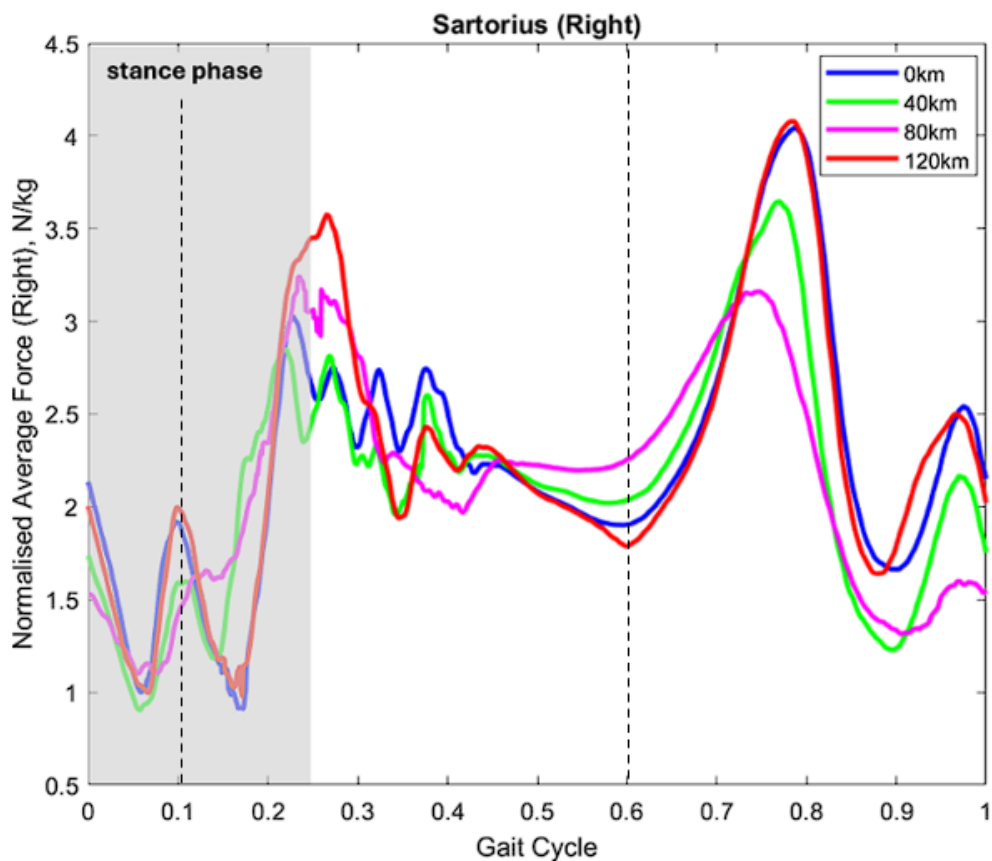


Figure 4.14: The Muscular Force Estimation for the Sartorius across Different Accumulated Running Distance

The dash lines of analysis in Figure 4.15 shows that the semitendinosus muscle force increases in the stance phase but decreases at 120 km, continuing this trend until the end of toe-off. At mid-swing, the force rises but starts to decrease at 80 km of accumulated running distance. However, at terminal swing, the trend restores to match the stance phase.

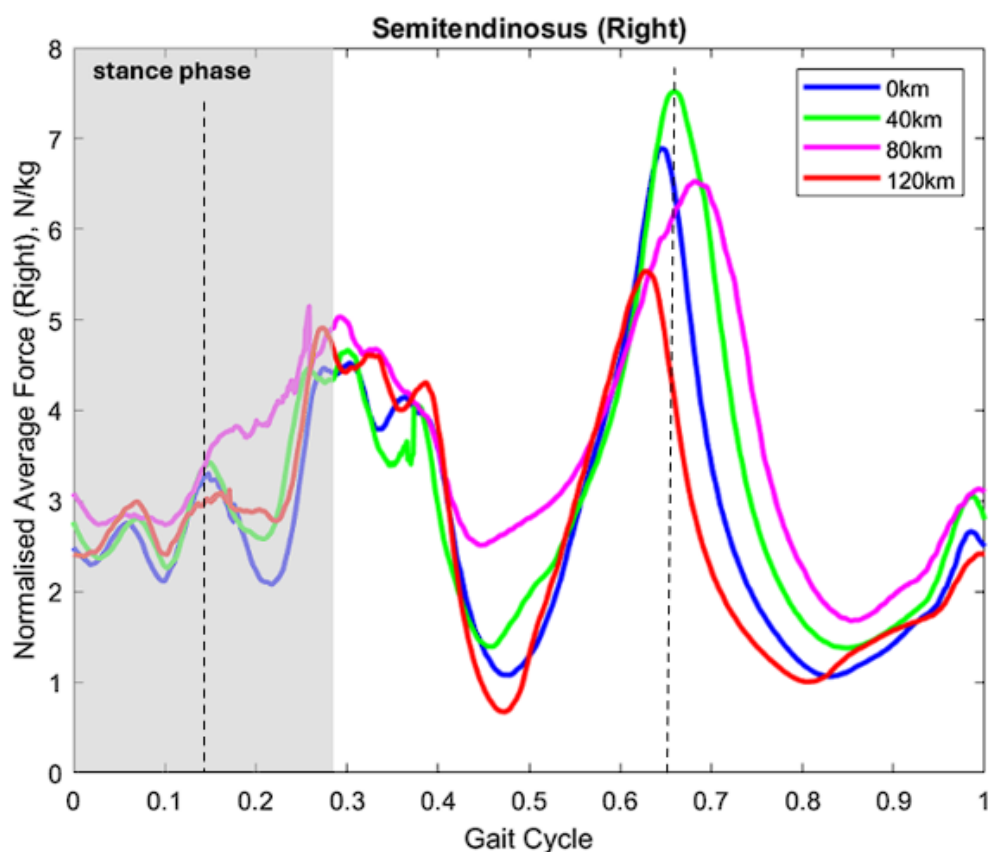


Figure 4.15: The Muscular Force Estimation for the Semitendinosus across Different Accumulated Running Distance

During the swing phase, which involves the transition from toe-off to terminal swing, the semitendinosus controls leg movement. The initial increase in force from 0 km to 40 km at mid-swing could be the body's attempt to maintain proper leg acceleration and deceleration for smooth forward motion. As the distance accumulates, the muscle may fatigue, leading to decreased force generation from 80 km to 120 km. The return to a similar trend as the stance phase during terminal swing suggests that the muscle's function as a decelerator and stabilizer at the knee becomes increasingly compromised due to fatigue.

For the knee extensor muscle, the stance phase of the dash line of analysis for the vastus intermedius shows a decrease in force at 0 km, followed by an increase at 120 km. At mid-swing, the force generally decreases from 0 km to 120 km. At terminal swing, the force rises from 0 km to 80 km but decreases again at 120 km of accumulated running distance. As shown in Figure 4.16, the vastus intermedius muscle demonstrates how the body adapts

to running distance. At 120 km of accumulated running distance during the stance phase, the body might be compensating for fatigue in other muscles, requiring more contribution from the vastus intermedius to maintain stability and propulsion. Energy optimization is observed at mid-swing, where the muscle force generally decreases. At terminal swing, force generation efficiency is compromised due to the need for precise control and leg stabilization before the next ground contact, making the muscle prone to fatigue.

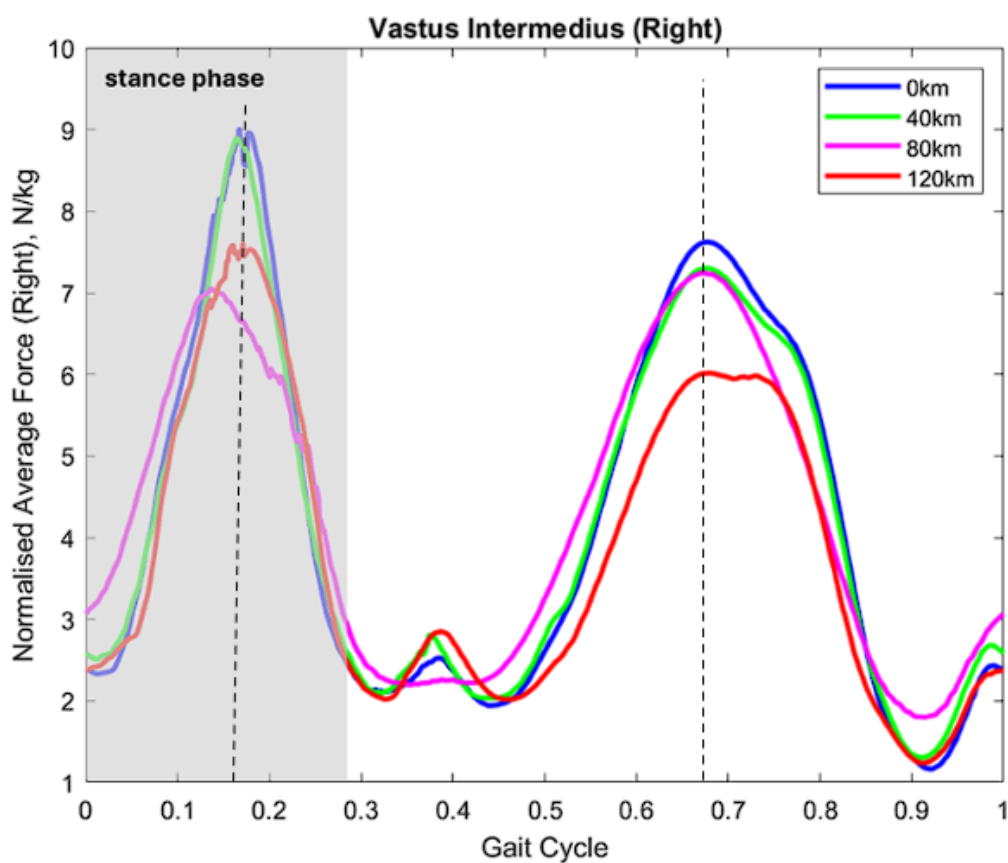


Figure 4.16: The Muscular Force Estimation for the Vastus Intermedius across Different Accumulated Running Distance

For the ankle, the extensor digitorum longus (EDL) muscle force increases from 0 km to 80 km but starts to decrease at 120 km, as shown in Figure 4.17. However, starting at mid-swing, the force increases until 40 km, drops to its lowest point at 80 km, and then begins to rise again at 120 km.

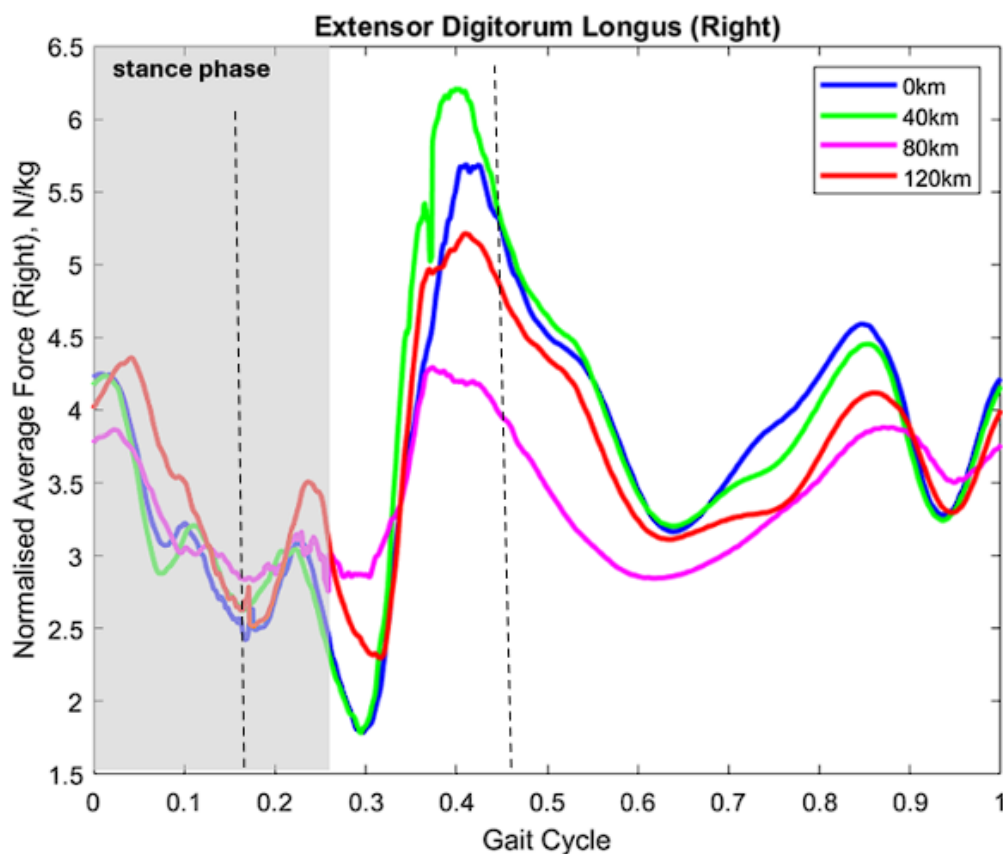


Figure 4.17: The Muscular Force Estimation for the EDL across Different Accumulated Running Distance

In the stance phase, the increase in force generation from 0 km to 80 km suggests that the body might be compensating for other muscle fatigue by relying more heavily on the EDL. The decrease at 120 km could indicate a shift in biomechanics, where other muscles or tendons might take over some of the EDL's role, or the running form itself changes to reduce reliance on the EDL.

4.5 Muscle Length and Muscle Velocity Relationship

The analysis of muscle length across the gait cycle provides deeper insights into how shoe cushioning affects muscle force, length, and overall energy expenditure ($E = Fd$). When examining a randomly selected subject with accumulation 40 km running distance, the semitendinosus (Semiten) muscle length trends during running were found to be similar to the results reported by Arnold et al. (2013). Showing the muscle length simulation results were valid and trustable, as shown in Figure 4.18, where the works can be extended to

plotting 3D graphs showing the relationship between muscle length or muscle velocity, muscle force and the gait cycle.

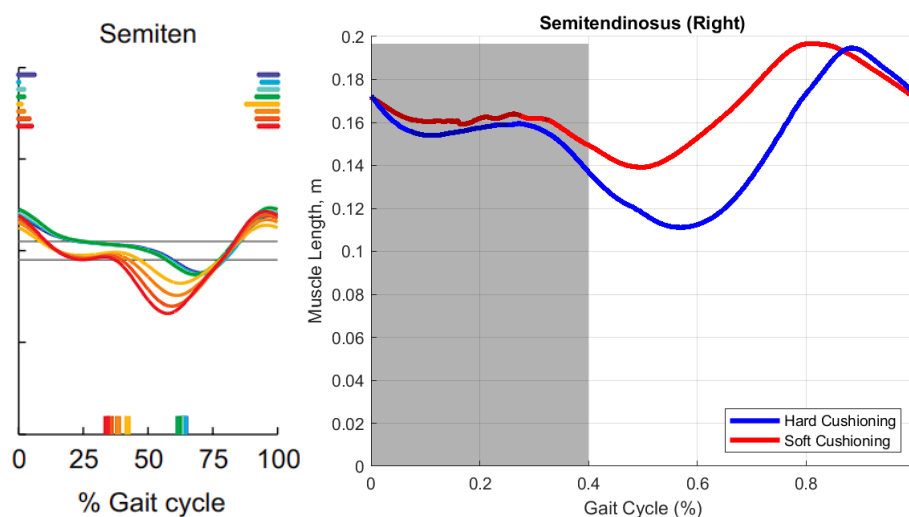


Figure 4.18: Semiten Muscle Length Graph Reported by Arnold et al. (2013) vs the Simulation Result

The adductor magnus ischial muscle demonstrated more stable force output during the stance phase with hard shoe cushioning compared to soft cushioning, as observed in the shaded region of Figure 4.19. In the toe-off stage, muscle length began to increase in soft cushioning, which marked the initiation of energy release from the muscle. Notably, the force output in soft cushioning decreased more sharply during the swing phase compared to hard cushioning, indicating less efficient energy release. Despite similar muscle lengths during the swing phase in both conditions, hard shoe cushioning enables greater force exertion, suggesting better energy return and muscular performance in adductor magnus ischial. This difference in force dynamics indicated that hard cushioning provided more effective shock absorption and force generation in adductor magnus ischial, particularly during load bearing and propulsion stages.

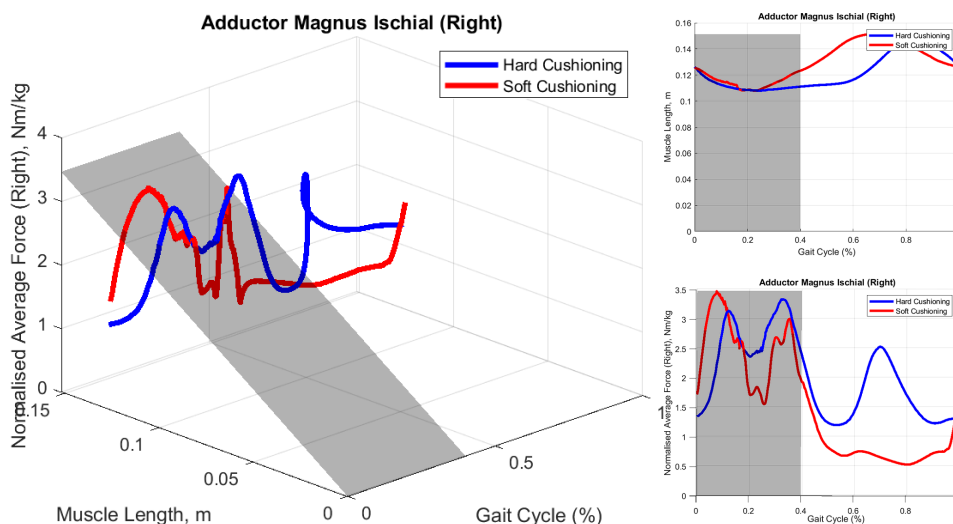


Figure 4.19: The Muscle Length-Force-Gait 3D Curve for Adductor Magnus Ischial

Anatomically, the adductor magnus ischial plays a critical role in thigh adduction and stabilizing the pelvis during running. With hard cushioning, the muscle’s ability to generate consistent force during the stance phase reflects its increased engagement in maintaining pelvic stability and controlling leg movement. The more intense force drop with soft cushioning during the swing phase may indicate reduced activation, potentially causing less effective stabilization and energy transfer. The anatomical demands on the muscle are therefore heightened with hard cushioning, which might lead to greater muscular effort but improved efficiency in force transmission and stabilization during the gait cycle.

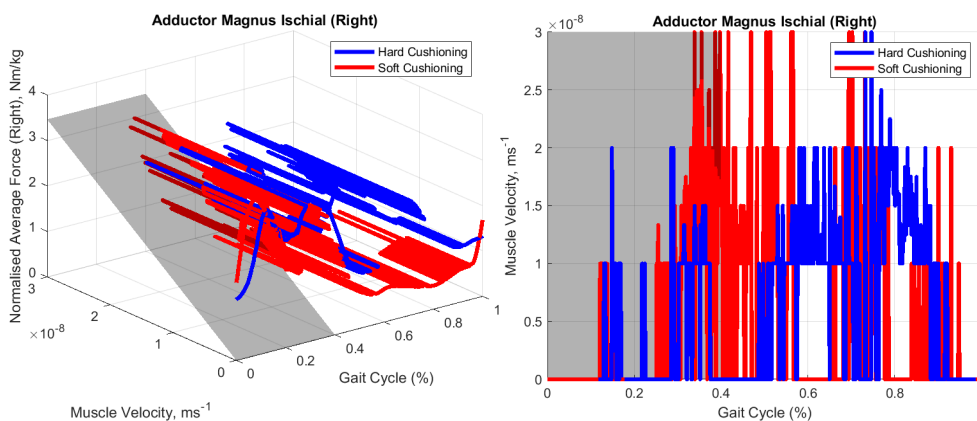


Figure 4.20: The Muscle Velocity-Force-Gait 3D Curve for Adductor Magnus Ischial

As depicted in Figure 4.21, the Sartorius muscle exhibited greater force exertion during the stance phase with soft cushioning compared to hard cushioning. However, during the swing phase, the force generated with soft cushioning gradually declined, whereas hard cushioning maintained more stable and consistent force output. It is important to note that the muscle length remained nearly identical for both types of cushioning throughout the entire running gait cycle.

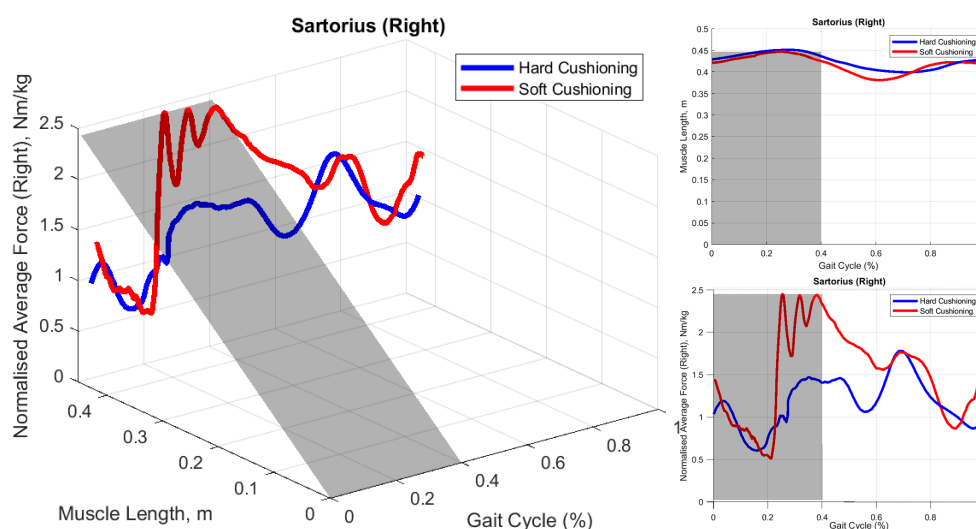


Figure 4.21: The Muscle Length-Force-Gait 3D Curve for Sartorius

The Sartorius muscle shows higher force exertion in the stance phase with soft cushioning, which may suggest a greater involvement in shock absorption and propulsion during this phase. However, the force decline during the swing phase with soft cushioning, in contrast to the more consistent force output observed with hard cushioning, indicates that hard cushioning supports better energy retention and return. The similarity in muscle length across both cushioning types throughout the gait cycle suggests that the differences in force generation are likely due to variations in cushioning properties affecting the muscle's energy utilization and efficiency, particularly in force transmission during running.

Anatomically, the sartorius muscle is a key player in hip and knee flexion, contributing significantly to leg movement and stabilization. With soft cushioning, the increased force during the stance phase may reflect a heightened engagement in stabilizing the leg during ground contact and

propulsion. However, the decline in force during the swing phase under soft cushioning may indicate reduced muscle activation or inefficient energy transfer. In contrast, the more stable force with hard cushioning during the swing phase suggests that the Sartorius is better able to contribute to leg positioning and control when the cushioning provides more consistent support.

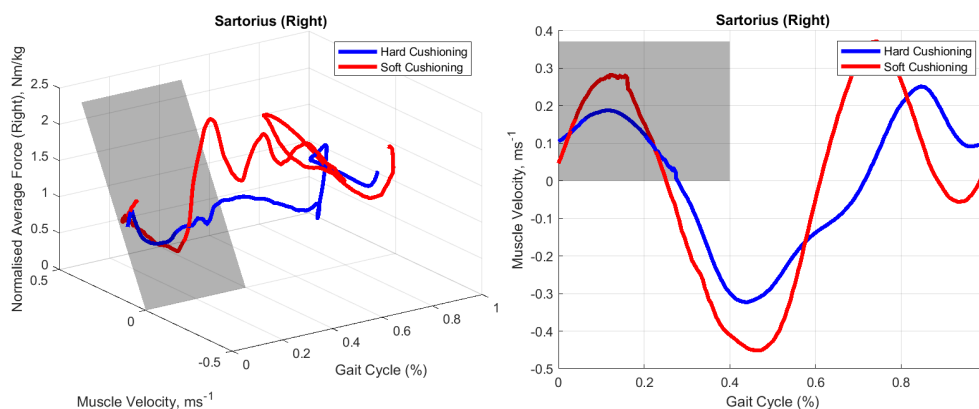


Figure 4.22: The Muscle Velocity-Force-Gait 3D Curve for Sartorius

In Figure 4.22, the soft cushioning exhibited slightly more extreme velocity variations compared to hard cushioning. Specifically, the velocity was higher during the stance phase and mid-swing with soft cushioning but lower during the initial and terminal swing phases when compared to hard cushioning. In terms of velocity, the Sartorius demonstrates higher speeds during the stance phase and mid-swing with soft cushioning, reflecting faster muscle contraction and movement. However, the lower velocities observed in the initial and terminal swing phases indicate that soft cushioning may lead to less efficient muscle performance during the non-weight-bearing phases, which is the phases where no weight is supported by the limb. The more moderate and stable velocity profile with hard cushioning suggests better energy efficiency and consistent power generation. This implies that hard cushioning supports a more balanced distribution of muscular effort, contributing to sustained power output throughout the gait cycle.

As shown in Figure 4.23, the semitendinosus muscle exhibited trends opposite to those of the Sartorius. In the swing phase, hard cushioning resulted in shorter muscle length but generated higher force. Additionally, although the muscle lengths were nearly identical in both types of cushioning during the

stance phase, the force exerted was notably higher with hard cushioning compared to soft cushioning.

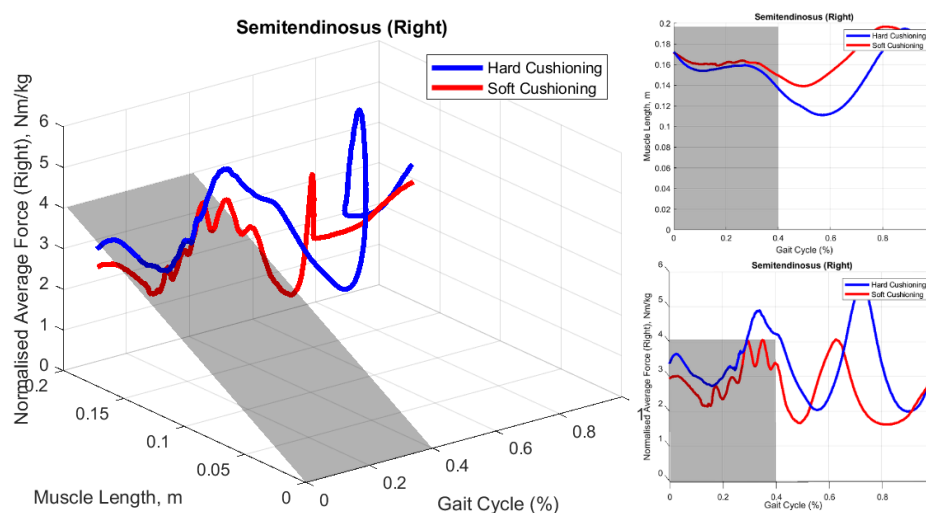


Figure 4.23: The Muscle Length-Force-Gait 3D Curve for Semitendinosus

The semitendinosus muscle performed differently under hard and soft cushioning conditions. During the swing phase, hard cushioning resulted in a shorter muscle length yet enabled the muscle to produce higher force, suggesting better energy efficiency in force transmission. In the stance phase, where muscle lengths were comparable between both cushioning types, the higher force exertion with hard cushioning indicates enhanced muscular engagement in stabilizing and propelling the body. This suggests that hard cushioning may optimize the force-length relationship of the semitendinosus, allowing it to generate more effective force throughout the gait cycle.

The semitendinosus, part of the hamstring group, plays a crucial role in hip extension and knee flexion during running. The higher force observed with hard cushioning during both stance and swing phases implies that this cushioning type provides better support for the muscle's function in extending the hip and decelerating the leg during the swing phase. The shorter muscle length during the swing phase with hard cushioning suggests that the muscle may be more efficient at controlling leg retraction, potentially reducing strain and improving overall energy conservation during running.

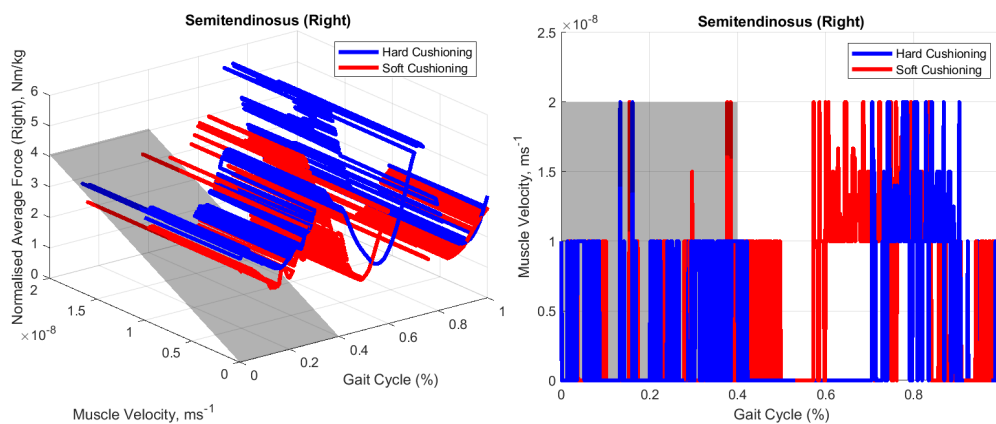


Figure 4.24: The Muscle Velocity-Force-Gait 3D Curve for Semitendinosus

As shown in Figure 4.24, the velocity profiles of the semitendinosus were relatively similar for both types of shoe cushioning. However, the velocity values remained consistently low, within the order of magnitude of only 10^{-8} . This consistent velocity pattern suggests that while the muscle is not generating high-speed contractions, it was still contributing to stability and power generation in a controlled manner.

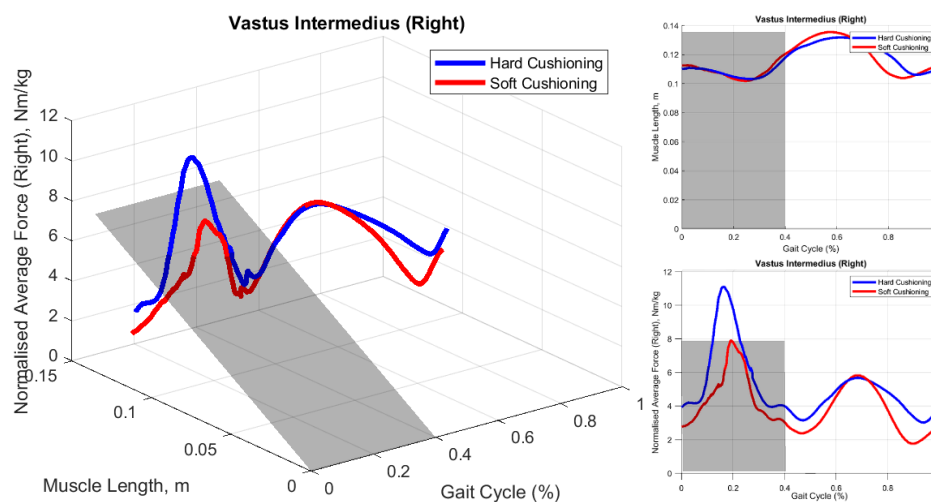


Figure 4.25: The Muscle Length-Force-Gait 3D Curve for Vastus Intermedius

In Figure 4.25, although the vastus intermedius demonstrated similar muscle length patterns across both hard and soft cushioning conditions, the force generated was substantially higher with hard cushioning during the stance phase. In the swing phase, while the force exerted with hard cushioning remained higher than with soft cushioning, the difference was minor and not statistically significant.

From a biomechanical perspective, the vastus intermedius exhibited consistent muscle length trends during the gait cycle, irrespective of cushioning type. However, the force production during the stance phase was significantly greater with hard cushioning, indicating a more effective engagement of the quadriceps group, particularly in stabilizing the knee and supporting the body during weight-bearing, which is another term describing phases in which the legs support the body's weight. The increased force output under hard cushioning suggests improved energy transfer, aiding in greater propulsion and control throughout the gait cycle. During the swing phase, while the force remained slightly higher with hard cushioning, the minimal difference implies that the muscle's energy release and contraction efficiency were not substantially impacted during this phase.

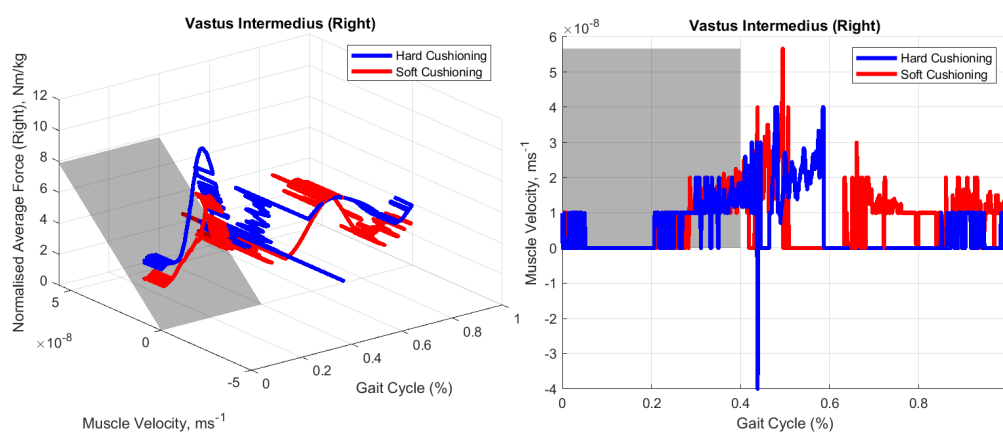


Figure 4.26: The Muscle Velocity-Force-Gait 3D Curve for Vastus Intermedius

Anatomically, the vastus intermedius, part of the quadriceps group, is primarily responsible for knee extension. The enhanced force production observed with hard cushioning during the stance phase indicates that this type of cushioning may better support the muscle's function in maintaining knee stability and controlling leg extension, essential for absorbing impact and generating forward momentum. The relatively minor force difference during the swing phase suggests that the muscle's role in non-weight-bearing movement, such as leg recovery and knee flexion, is less affected by cushioning type, though hard cushioning may provide a slight advantage in stabilizing the knee for subsequent ground contact.

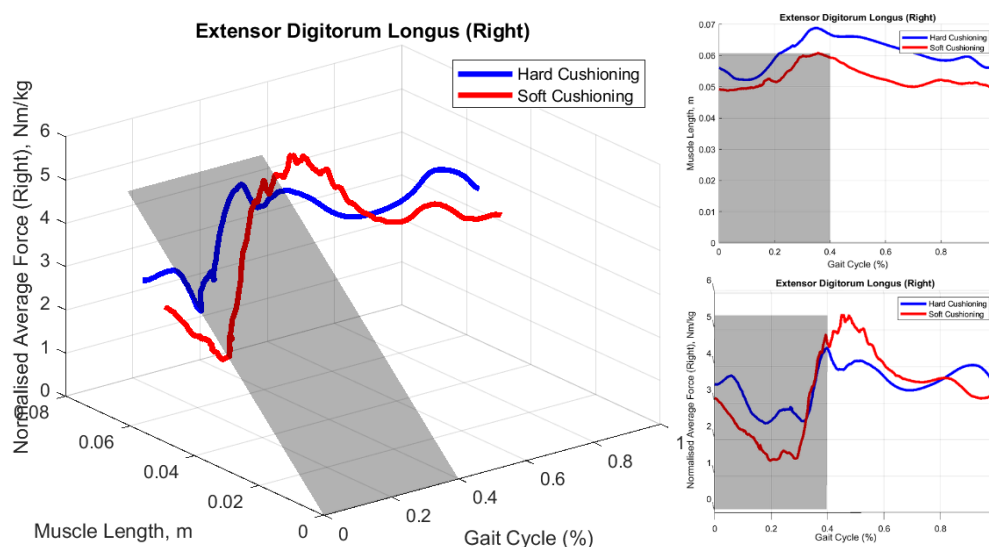


Figure 4.27: The Muscle Length-Force-Gait 3D Curve for Extensor Digitorum Longus

Interestingly, during the stance phase, hard cushioning resulted in a greater muscle length for the extensor digitorum longus compared to soft cushioning, with a corresponding higher force output in hard cushioning. In contrast, while the muscle length remained consistent during the swing phase, the force exerted in soft cushioning exceeded that of hard cushioning.

The vastus intermedius demonstrated similar muscle length dynamics across both cushioning types throughout the gait cycle. However, the muscle's force production was notably higher in hard cushioning during the stance phase, which aligns with the muscle's role in knee extension and ground impact absorption. This indicates that hard cushioning may promote more efficient force generation and energy transfer during weight-bearing activities, contributing to greater stability and propulsion. In the swing phase, while hard cushioning still maintained a slightly higher force, the differences were less pronounced, suggesting that the cushioning type has a more substantial impact during weight-bearing than during the non-weight-bearing portion of the gait cycle.

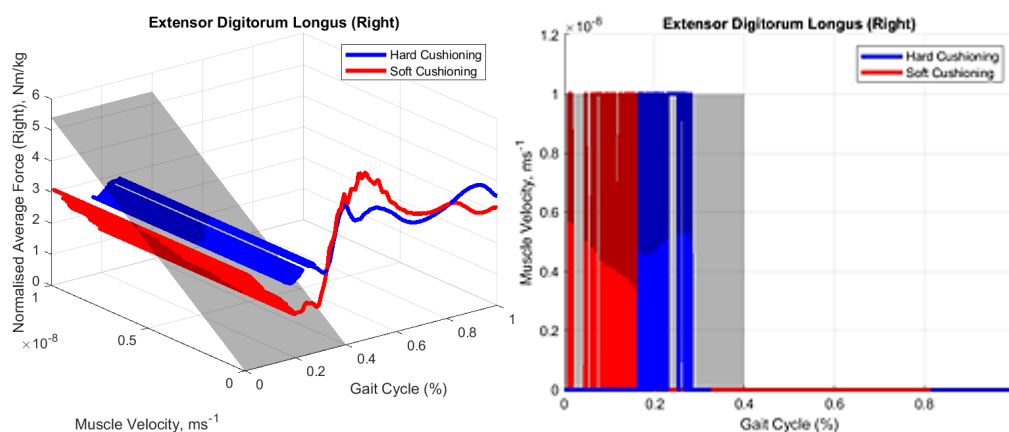


Figure 4.28: The Muscle Velocity-Force-Gait 3D Curve for Extensor Digitorum Longus

The vastus intermedius plays a critical role in knee extension and stabilization, particularly during the stance phase of running. The increased force exertion observed in hard cushioning suggests that this type of footwear better supports the muscle's function in managing the mechanical demands of running, particularly in maintaining knee stability and enabling efficient force transmission to the ground. In the swing phase, where the muscle is less involved in force generation and more focused on leg recovery, the differences in force output between the two cushioning types were minimal, indicating that both types allow for adequate muscle function in non-weight-bearing conditions.

CHAPTER 5

CONCLUSIONS AND RECOMMENDATIONS

5.1 Conclusions

This study successfully modelled the musculoskeletal dynamics of amateur runners and analysed the impact of running distances and shoe cushioning on muscle activation. By using techniques such as CMC, SO, and MocoInverse, it was possible to estimate muscle forces accurately and understand the biomechanical patterns involved in running.

On the other hand, after evaluating RMSE, correlation, and computational time for knee and ankle joint simulations under various shoe cushioning conditions, it can be concluded that IK is the most recommended tool for tracking virtual marker trajectories in inverse kinematics, particularly when accounting for the added impulsive force during the stance phase of running, and this is particularly true if the further muscle-driven simulation is not required to proceed. This is because in among all these tools, IK has the shortest computational time, under the scenario that IK, RRA and MocoTrack provided almost identical values of RMSE and correlation. Despite this, increasing the sample data could provide more robust and reliable results, while also minimizing the impact of subject-specific outliers caused by loose markers, unnatural running postures, or incorrect experimental setups.

The comparison of CMC, SO, and MocoInverse revealed that CMC provided the best muscle-driven simulation results, particularly for the lateral gastrocnemius (Gaslat) and knee moments, offering superior accuracy in muscle force prediction. SO and MocoInverse followed in performance, each with distinct strengths in computational efficiency and dynamic consistency.

The analysis highlighted that shoe cushioning plays a significant role in altering the kinematic and kinetic parameters, especially during the stance phase. Hard shoe cushioning tends to increase impact forces, requiring muscles like the adductor magnus and sartorius to adapt over longer running distances.

Accumulated running distance was shown to influence muscle activation, with noticeable fatigue in deep muscles like the vastus intermedius and extensor digitorum longus at longer distances. This provides insight into how muscle endurance can be managed to prevent injuries in amateur runners.

The study identified the limitations of the simulations, such as the difficulty in fully replicating the complex biomechanics of human running in silico. However, the results offer a foundation for further research and practical applications in improving amateur runner training programs.

Overall, this research contributes to a deeper understanding of running biomechanics and demonstrates the utility of musculoskeletal simulations in providing insights that can lead to injury prevention and enhanced running performance.

5.2 Recommendations for Future Work

Future studies should explore forward dynamics using single shooting methods via SCONE and reinforcement learning via osim-rl, as shown in Figure 5.1. This will allow for more detailed simulations of neuromuscular control during running and provide greater insights into dynamic adaptations.

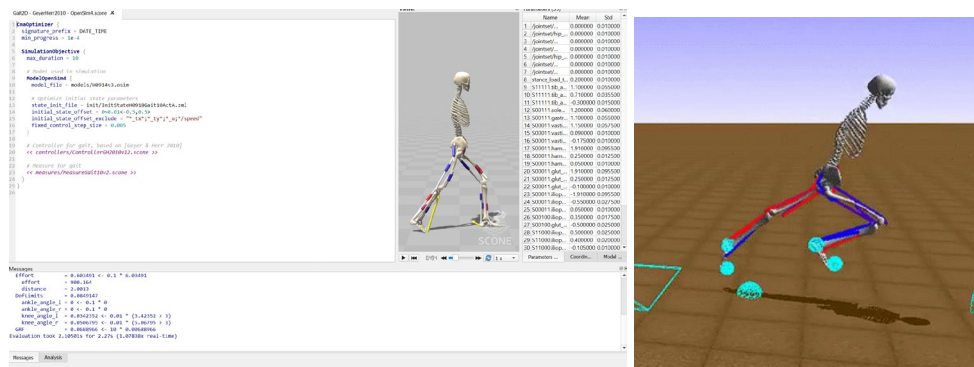


Figure 5.1: SCONE's Interface (Left) and osim-rl Training Interface (Right)

As illustrated in Figure 5.2, the osim-rl environment failed to run properly, halting without displaying any error message. Troubleshooting is required to identify the cause of this issue, which may stem from insufficient computer RAM, poor maintenance or lack of updates in the osim-rl platform,

or the need for modifications to the source code of the Python training packages.

```

Administrator: Anaconda Pro
(opensim-rl) C:\Users\yewwe>cd D:\Documents\OpenSimRL_Learn
(opensim-rl) C:\Users\yewwe>D:
(opensim-rl) D:\Documents\OpenSimRL_Learn>python BasicUsage.py
C:\ProgramData\anaconda3\envs\opensim-rl\lib\site-packages\gym\core.py:27: UserWarning: WARN: Gym minimally supports python 3.6 as the python foundation not longer supports the version, please update your version to 3.7+
  "Gym minimally supports python 3.6 as the python foundation not longer supports the version, please update your version to 3.7+"
Traceback (most recent call last):
  File "BasicUsage.py", line 6, in <module>
    observation, reward, done, info = env.step(my_controller(observation))
NameError: name 'env' is not defined
(opensim-rl) D:\Documents\OpenSimRL_Learn>cd osim-rl/examples
(opensim-rl) D:\Documents\OpenSimRL_Learn\osim-rl\examples>python sim_L2M2019_randomrun
python: can't open file 'sim_L2M2019_randomrun': [Errno 2] No such file or directory
(opensim-rl) D:\Documents\OpenSimRL_Learn\osim-rl\examples>python sim_L2M2019_randomrun.py
C:\ProgramData\anaconda3\envs\opensim-rl\lib\site-packages\gym\core.py:27: UserWarning: WARN: Gym minimally supports python 3.6 as the python foundation not longer supports the version, please update your version to 3.7+
  "Gym minimally supports python 3.6 as the python foundation not longer supports the version, please update your version to 3.7+"
Updating Model file from 30000 to latest format...
Loaded model gait14dof22musc from file C:\ProgramData\anaconda3\envs\opensim-rl\lib\site-packages\osim\env\..\models\gait14dof22musc_20170320.osim
(opensim-rl) D:\Documents\OpenSimRL_Learn\osim-rl\examples>

```

Figure 5.2: osim-rl Python Package Stops Without Prompting Any Coding Error

Recruiting more subjects, especially female participants, and expanding age coverage will increase the generalizability of the results. A more diverse subject pool could reveal variations in biomechanical performance across different demographics, helping to refine training recommendations.

Improving the precision of the simulation settings, such as reducing the mesh interval to 0.01 or increasing the decimal precision to 20 places during CMC, will enhance the accuracy of musculoskeletal models, leading to more reliable predictions results of muscle forces and joint moments.

Open-loop forward dynamics can be attempted for simulating running motion given the neural command-based muscle control. However, this approach will require significantly more computational resources and precise simulation settings, given the complexity of accurately modelling these dynamics.

REFERENCES

- Arnold, E.M., Hamner, S.R., Seth, A., Millard, M. and Delp, S.L., 2013. How muscle fiber lengths and velocities affect muscle force generation as humans walk and run at different speeds. *Journal of Experimental Biology*, 216(11), pp.2150–2160. <https://doi.org/10.1242/JEB.075697/>
- Boon, R.W.K., 2023. *OpenSim Gait Model: Exploring the impact of shoe cushioning hardness and accumulated running distance on musculoskeletal dynamics in amateur runners*. Master Dissertation, Universiti Tunku Abdul Rahman.
- Boon, R.W.K., Chong, Y.Z., Tan, Y.Q., Sundar, V., Selva, Y. and Chan, S.C., 2022. *Effect of Running Shoe Cushioning on Muscle Activation using OpenSim*. 2022 IEEE-EMBS Conference on Biomedical Engineering and Sciences (IECBES), Kuala Lumpur, Malaysia, 2022, pp. 228-233, <https://doi.org/10.1109/IECBES54088.2022.10079302>.
- Brooks, L., Weyand, P. and Clark, K., 2020. *UPPER EXTREMITY MOTION AND SPRINT RUNNING: A FAREWELL TO ARMS?* ISBS Proceedings Archive, 38(1), <https://commons.nmu.edu/isbs/vol38/iss1/39>.
- de Araujo, M.K., Baeza, R.M., Zalada, S.R.B., Alves, P.B.R. and de Mattos, C.A., 2015. Injuries among amateur runners. *Revista Brasileira de Ortopedia (English Edition)*, 50(5), pp.537–540. <https://doi.org/10.1016/J.RBOE.2015.08.012>.
- De Groote, F., Kinney, A.L., Rao, A. V. and Fregly, B.J., 2016. Evaluation of Direct Collocation Optimal Control Problem Formulations for Solving the Muscle Redundancy Problem. *Annals of Biomedical Engineering*, 44(10), pp.2922–2936. <https://doi.org/10.1007/S10439-016-1591-9>.
- Dembia, C.L., Bianco, N.A., Falisse, A., Hicks, J.L. and Delp, S.L., 2020. OpenSim Moco: Musculoskeletal optimal control. *PLOS Computational Biology*, 16(12), p.e1008493. <https://doi.org/10.1371/JOURNAL.PCBI.1008493>.
- Fischer, F., Bachinski, M., Klar, M., Fleig, A. and Müller, J., 2021. Reinforcement learning control of a biomechanical model of the upper extremity. *Scientific Reports 2021*, 11(1), pp.1–15. <https://doi.org/10.1038/s41598-021-93760-1>.
- Geijtenbeek, T., 2019. SCONE: Open Source Software for Predictive Simulation of Biological Motion. *Journal of Open Source Software*, 4(38), p.1421. <https://doi.org/10.21105/JOSS.01421>.

Hicks, J., 2018. *How inverse Kinematics Works*. [online] OpenSim Documentation. Available at:
<<https://opensimconfluence.atlassian.net/wiki/spaces/OpenSim/pages/53090047/How+Inverse+Kinematics+Works>> [Accessed 6 October 2024].

Hicks, J., 2018b. *How RRA Works*. [online] OpenSim Documentation. Available at:
<<https://opensimconfluence.atlassian.net/wiki/spaces/OpenSim/pages/53089688/How+RRA+Works>> [Accessed 6 October 2024].

Hicks, J., 2018c. *How Static Optimization Works*. [online] OpenSim Documentation. Available at:
<<https://opensimconfluence.atlassian.net/wiki/spaces/OpenSim/pages/53089619/How+Static+Optimization+Works>> [Accessed 6 October 2024].

Hicks, J., 2019. *Getting Started with Scaling*. [online] OpenSim Documentation. Available at:
<<https://opensimconfluence.atlassian.net/wiki/spaces/OpenSim/pages/53089123/Getting+Started+with+Scaling>> [Accessed 6 October 2024].

Hicks, J., 2024a. *Getting Started with CMC*. [online] OpenSim Documentation. Available at:
<<https://opensimconfluence.atlassian.net/wiki/spaces/OpenSim/pages/53089712/Getting+Started+with+CMC>> [Accessed 6 October 2024].

Hicks, J., 2024b. *Getting started with inverse dynamics*. [online] OpenSim Documentation. Available at:
<<https://opensimconfluence.atlassian.net/wiki/spaces/OpenSim/pages/53090063/Getting+Started+with+Inverse+Dynamics>> [Accessed 6 October 2024].

Hislop, H.J. and Montgomery, J., 2007. *Muscle Testing Technique of Manual Examination*. 8th ed. St. Louis, Mo.: Saunders.

Jarmey, Chris., 2018. *The concise book of muscles*. 4th ed. California: North Atlantic Books.

Jung, Y., Jung, M., Ryu, J., Yoon, S., Park, S.K. and Koo, S., 2016. Dynamically adjustable foot-ground contact model to estimate ground reaction force during walking and running. *Gait & Posture*, 45, pp.62–68.
<https://doi.org/10.1016/J.GAITPOST.2016.01.005>.

Kakouris, N., Yener, N. and Fong, D.T.P., 2021. A systematic review of running-related musculoskeletal injuries in runners. *Journal of Sport and Health Science*, 10(5), pp.513–522.
<https://doi.org/10.1016/J.JSHS.2021.04.001>.

- Kim, Y., Jung, Y., Choi, W., Lee, K. and Koo, S., 2018. Similarities and differences between musculoskeletal simulations of OpenSim and AnyBody modeling system. *Journal of Mechanical Science and Technology*, 32(12), pp.6037–6044. <https://doi.org/10.1007/S12206-018-1154-0>.
- Lin, Y.C. and Pandy, M.G., 2017. Three-dimensional data-tracking dynamic optimization simulations of human locomotion generated by direct collocation. *Journal of Biomechanics*, 59, pp.1–8. <https://doi.org/10.1016/J.JBIOMECH.2017.04.038>.
- Lin, Y.C., Dorn, T.W., Schache, A.G. and Pandy, M.G., 2011. Comparison of different methods for estimating muscle forces in human movement, *Proceedings of the Institution of Mechanical Engineers, Part H: Journal of Engineering in Medicine*. 2012, 226(2), pp.103–112. <https://doi.org/10.1177/0954411911429401>.
- McCully, K., 2004. Running for health: how much running for how much health? *Clinical Science*, 107(6), pp.559–560. <https://doi.org/10.1042/CS20040273>.
- Millard, E., 2021. *Almost half of recreational runners get injured, according to new research*. [online] Runner's World. Available at: <<https://www.runnersworld.com/news/a36201575/injury-risk-in-recreational-runners-study>> [Accessed 6 October 2024].
- Oswald, F., Campbell, J., Williamson, C., Richards, J. and Kelly, P., 2020. A Scoping Review of the Relationship between Running and Mental Health. *International Journal of Environmental Research and Public Health* 2020, 17(21), p.8059. <https://doi.org/10.3390/IJERPH17218059>.
- Parson, S.H., 2009. Clinically Oriented Anatomy, 6th edn. *Journal of Anatomy*, 215(4), p.474. <https://doi.org/10.1111/J.1469-7580.2009.01136.X>.
- Platzer, W. and Kahle, W., 2003. *Color Atlas and Textbook of Human Anatomy: Locomotor system*. Leipzig: Thieme.
- Quan, W., Gao, L., Xu, D., Zhou, H., Korim, T., Shao, S., Baker, J.S. and Gu, Y., 2023. Simulation of Lower Limb Muscle Activation Using Running Shoes with Different Heel-to-Toe Drops Using Opensim. *Healthcare* 2023, 11(9), p.1243. <https://doi.org/10.3390/HEALTHCARE11091243>.
- Rajagopal, A., Dembia, C.L., DeMers, M.S., Delp, D.D., Hicks, J.L. and Delp, S.L., 2016. Full-Body Musculoskeletal Model for Muscle-Driven Simulation of Human Gait. *IEEE Transactions on Biomedical Engineering*, 63(10), pp.2068–2079. <https://doi.org/10.1109/TBME.2016.2586891>.

Seth, A., Sherman, M., Reinbolt, J.A. and Delp, S.L., 2011. OpenSim: a musculoskeletal modeling and simulation framework for in silico investigations and exchange. *Procedia IUTAM*, 2, pp.212–232. <https://doi.org/10.1016/J.PIUTAM.2011.04.021>.

Song, S. et al., 2020, *Reinforcement learning with musculoskeletal models* [Online]. Available at: <http://osim-rl.kidzinski.com/docs/home>. [Accessed 6 October 2024].

Song, S., Kidziński, Ł., Peng, X. Bin, Ong, C., Hicks, J., Levine, S., Atkeson, C.G. and Delp, S.L., 2021. Deep reinforcement learning for modeling human locomotion control in neuromechanical simulation. *Journal of NeuroEngineering and Rehabilitation* 2021, 18(1), pp.1–17. <https://doi.org/10.1186/S12984-021-00919-Y>.

Stetter, B.J., Krafft, F.C., Ringhof, S., Stein, T. and Sell, S., 2020. A Machine Learning and Wearable Sensor Based Approach to Estimate External Knee Flexion and Adduction Moments During Various Locomotion Tasks. *Frontiers in Bioengineering and Biotechnology*, 8(9), p.508120. <https://doi.org/10.3389/FBIOE.2020.00009>.

Su, B. and Gutierrez-Farewik, E.M., 2023. Simulating human walking: a model-based reinforcement learning approach with musculoskeletal modeling. *Frontiers in Neurorobotics*, 17, p.1244417. <https://doi.org/10.3389/FNBOT.2023.1244417>.

Thompson, M.A., 2017. Physiological and Biomechanical Mechanisms of Distance Specific Human Running Performance. *Integrative and Comparative Biology*, 57(2), pp.293–300. <https://doi.org/10.1093/ICB/ICX069>.

Trinler, U., Schwameder, H., Baker, R. and Alexander, N., 2019. Muscle force estimation in clinical gait analysis using AnyBody and OpenSim. *Journal of Biomechanics*, 86, pp.55–63. <https://doi.org/10.1016/J.JBIOMECH.2019.01.045>.

Tsuji, K., Ishida, H., Oba, K., Ueki, T. and Fujihashi, Y., 2015. Activity of lower limb muscles during treadmill running at different velocities. *Journal of Physical Therapy Science*, 27(2), pp.353–356. <https://doi.org/10.1589/JPTS.27.353>.

Uchida, T.K., Delp, Scott. and Delp, David., 2020. *Biomechanics of movement: the science of sports, robotics, and rehabilitation*. Cambridge: The MIT Press

Wang, S., Wang, Y., Pai, Y.C., Wang, E. and Bhatt, T., 2020. Effects of Optimization Technique on Simulated Muscle Activations and Forces. *Journal of Applied Biomechanics*, 36(4), pp.259–278.
<https://doi.org/10.1123/JAB.2018-0332>.

Zhao, K., Shan, C. and Luximon, Y., 2022. Contributions of individual muscle forces to hip, knee, and ankle contact forces during the stance phase of running: a model-based study. *Health Information Science and Systems*, 10(1), pp.1–13.
<https://doi.org/10.1007/S13755-022-00177-9/METRICS>.

Zong, C., Ma, -Hao, Li, Z., He, C., Tang, H., Pan, J., Munkasy, B., Duffy, K. and Li, L., 2022. Comparison of Lower Extremity Joint Moment and Power Estimated by Markerless and Marker-Based Systems during Treadmill Running. *Bioengineering 2022*, 9(10), p.574.
<https://doi.org/10.3390/BIOENGINEERING9100574>.

APPENDICES

Appendix A: Simulation Result with MocoInverse Mesh Interval 0.08

```

total | 107.79ks (107.79ks) 107.79ks (107.79ks) 1

Breakdown of objective (including weights):
  excitation_effort: 1.7457e+06
[info] Set log level to Info.
[info] -----
[info] Elapsed real time: 107867 second(s) (29 hour(s), 57 minute(s),
[info] Thu Sep 12 20:46:19 2024
[info] MocoCasADiSolver succeeded!
[info] =====
Solution written successfully.
PS D:\Documents\Pyosim_Learn>

```

The screenshot shows a code editor with an XML file named `H1_0km_CMCActuators.xml`. The XML defines a `PointActuator` named "FX" applied to the `pelvis` body. The actuator parameters include a point `(-0.073, -0.02525, 0)`, a direction `(1, -0, -0)`, and a maximum force of `1`. The terminal window at the bottom displays the following simulation results:

Iteration	excitation_effort	inf_pr	inf_du	lg(mu)	d	lg(rg)	alpha_du	alpha_pr	ls
1348	1.7456897e+06	4.66e-04	1.56e+00	-3.7	3.56e-02	-7.22e-01	5.77e-01	1	1
1349	1.7456897e+06	4.52e-04	1.41e+00	-3.7	2.01e-02	-6.15e-01	3.12e-02	6	6
1350	1.7456898e+06	9.85e-05	4.84e-01	-3.7	1.01e-02	-1.00e+00	1.00e+00	1	1
1351	1.7456898e+06	1.82e-05	6.44e-01	-3.7	4.25e-03	-1.00e+00	1.00e+00	1	1
1352	1.7456897e+06	3.17e-05	1.10e+00	-3.7	8.29e-03	-1.00e+00	1.00e+00	1	1
1353	1.7456898e+06	8.75e-06	2.77e+00	-3.7	2.70e-02	-5.61e-01	1.00e+00	1	1
1354	1.7456897e+06	3.88e-04	1.04e+00	-3.7	2.73e-02	-1.00e+00	1.00e+00	1	1
1355	1.7456897e+06	6.37e-05	7.76e-01	-3.7	8.70e-03	-7.30e-01	1.00e+00	1	1
1356	1.7456898e+06	6.42e-07	1.33e+00	-3.7	9.31e-03	-1.00e+00	1.00e+00	1	1
1357	1.7456898e+06	2.72e-06	1.06e+00	-3.7	3.54e-02	-1.00e+00	9.84e-02	4	4

Appendix B: IECBES 2024 Conference Paper Submission

My pending, active and accepted papers
 Only papers for upcoming and recently-concluded conferences and journal issues are shown.

Conference	Paper title (details)	Status	Edit	Add and delete authors	Withdraw or unwithdraw	Registration	Review Manuscript
IECBES 2024	Performance Evaluation on OpenSim's Virtual Markers Trajectory System for Running Simulation	Active (has manuscript)					
IECBES 2024	Assessing Muscle Driven Optimization Techniques in OpenSim for Long Distance Running and Deep Muscle Adaptations	Active (has manuscript)					

Recent email messages

Search:

Date	Conference	Message
Sep 2, 2024 02:09 UTC	IECBES 2024	[IECBES 2024] Information about paper #1571070405 (Assessing Muscle Driven Optimization Techniques in OpenSim for Long Distance Running and Deep Muscle Adaptations) has been changed
Sep 2, 2024 02:09 UTC	IECBES 2024	[IECBES 2024] Information about paper #1571070405 (Assessing Muscle Driven Optimization Techniques in OpenSim for Long Distance Running and Deep Muscle Adaptations) has been changed
Sep 2, 2024 02:09 UTC	IECBES 2024	[IECBES 2024] Information about paper #1571070405 (Assessing Muscle Driven Optimization Techniques in OpenSim for Long Distance Running and Deep Muscle Adaptations) has been changed
Sep 2, 2024 02:07 UTC	IECBES 2024	[IECBES 2024] Information about paper #1571070405 (Assessing Muscle Driven Optimization Techniques in OpenSim for Long Distance Running and Deep Muscle Adaptations) has been changed
Sep 2, 2024 02:07 UTC	IECBES 2024	[IECBES 2024] Information about paper #1571070405 (Assessing Muscle Driven Optimization Techniques in OpenSim for Long Distance Running and Deep Muscle Adaptations) has been changed

Appendix C: IECBES 2024 1st Paper Submission Content: Performance Evaluation on OpenSim's Virtual Markers Trajectory System for Running Simulation

Performance Evaluation on OpenSim's Virtual Markers Trajectory System for Running Simulation

Siow Cheng Chan
Department of Mechatronics and
Biomedical Engineering
Universiti Tunku Abdul Rahman
Selangor, Malaysia
chansc@utar.edu.my

Yin Qing Tan
Department of Mechatronics and
Biomedical Engineering
Universiti Tunku Abdul Rahman
Selangor, Malaysia
tanyq@utar.edu.my

Yew Wei Teh
Department of Mechatronics and
Biomedical Engineering
Universiti Tunku Abdul Rahman
Selangor, Malaysia
yewwei9909@utar.my

Yu Zheng Chong
Department of Mechatronics and
Biomedical Engineering
Universiti Tunku Abdul Rahman
Selangor, Malaysia
chongyz@utar.my

Yallini Selva
Department of Sports Biomechanics
National Sports Institute of Malaysia,
Bukit Jalil
Selangor, Malaysia
yalliniselva89@gmail.com

Viswanath Sundar
Visva-Bharati Central University,
India
viswabdu@gmail.com

Abstract — Running is a locomotion ability that human equipped to move from one place to another in faster pace compared to walking. Shoe cushioning alters the running gait in some extent. Depending on the hardness of the shoe cushioning, some may cause increase in the ground reaction force. Thus, this paper investigated on the moment gait between hard and soft shoe cushioning under running, and evaluating the performance via the OpenSim virtual marker trajectory tracking based on inverse kinematics tools, which include inverse kinematics (IK), Reduce Residual Algorithm (RRA) and MocoTrack. The results show that in knee moment with hard shoe cushioning, MocoTrack performed the best, and vice-versa in soft shoe cushioning. RRA was found to be most effective in the determination of ankle moment. Statistically, the Root Mean Square Error (RMSE), correlation (r), in knee and ankle moments, under different types of shoe cushioning, no significant differences were found, with 0.3 kg/Nm of RMSE and approximately 95% of correlation in comparison with the experimental data. Thus, in this case, the computational time does become the key factor in evaluating them. In conclusion, IK was the best performed in simulating the knee and ankle joint moments in running motion under different types of hardness shoe cushioning, then followed by RRA and MocoTrack, which had the longest computational time respectively.

Keywords — OpenSim, Inverse Kinematics, Reduce Residual Algorithm, MocoTrack, Markers Trajectory System

I. INTRODUCTION

Running is a widely practiced physical activity that promote a healthier life free from cardiovascular diseases and psychological diseases [1], yet it is associated with a notably high incidence of muscle-related and overuse injuries of the lower extremities among amateur runners. Studies indicated that between 27% and 70% of runners experienced these injuries annually, which not only affects their health and performance but also discourages continued participation in the activity [2, 3]. Shoe cushioning can be attributed to inadequate shock absorption during foot strike and inefficient motion patterns [4, 5]. Computational models that incorporate detailed anatomical data can potentially offer personalized insights into the biomechanical and anatomical interactions that is able to prevent potential risk of amateur runners to injuries [6-8].

Biomechanically, computing inverse kinematics is an essential step in analyzing the marker trajectory of a motion. Through inverse kinematics, the generalized motion coordinates and angles can be calculated, allowing for further inverse-based

simulations. With only trajectory marker data available, OpenSim currently offers several approaches for kinematics analysis namely, Inverse Kinematics (IK), Reduce Residual Algorithm (RRA), and MocoTrack. IK uses the Weighted Least Squares Equation to estimate the generalized coordinates and marker position during a subject's motion, while RRA is a kinematics optimization technique that ensures reaction forces and acceleration are dynamically consistent with the model's kinematics [9, 10]. MocoTrack, a newer OpenSim technique, tracks and infers trajectory markers using the direct collocation method, claiming to provide fast, accurate results and customization options for analysis goals [11, 12].

Studies conducted based on data from ten (10) male participants running at three different speeds, MocoTrack outperformed RRA by producing lower residual forces and moments [13, 14]. Such deduction reflects that MocoTrack can perform motion tracking where the kinematics information is the more dynamically consistent to the running virtual ground reaction forces.

However, running is typically studied with running shoes and different shoe cushioning will affect performance. Shoes cushioning have been reported to affected the range of motion and hard cushioning creates higher impact forces during the stance phase, while soft cushioning absorbs shock [15, 16]. This cushioning impact can alter the consistencies in kinematics and dynamics parameters.

Therefore, this paper aims to evaluate the performance of IK, RRA, and MocoTrack under different shoe cushioning conditions, focusing on their effects on the joint moments of knee and ankle. Moments of body segments are the overall mechanical result of musculoskeletal system interactions, influenced by muscle attachments and bone geometry [17].

II. METHODS

A. Participants and Experimental Data

The experimental testing comprising of eight (8) male participants aged 29.67 ± 3.44 years, with a height of 170.32 ± 3.36 cm and body mass of 68.23 ± 4.90 kg [15]. Randomly, half of the participants wore hard cushioning running shoes, while the other half wore soft cushioning shoes during the study, as illustrated in Fig. 1. Table I outlines the "Hard" and "Soft" cushioning categories based on the Shore A hardness scale. Ethical approval, study protocol, and informed consent were obtained from the relevant committee and participants, respectively.



Fig. 1: Shoes of hard cushioning (left) and soft cushioning (right)

TABLE I. HARDNESS OF THE RUNNING SHOE CUSHIOING

Cushioning	Hardness Scale
Soft	32A
Hard	42A

Data acquisition took place at the Sports Performance Laboratory, National Sport Institute of Malaysia (Institut Sukan Negara, ISN), using an 11-camera motion capture system (Qualisys Track Manager, QTM 2022, 300 Hz) to record running motion trajectory and a 3-Dimensional instrumented treadmill with force plates (Bertec Instrumented Treadmill, 1500 Hz) to obtain virtual ground reaction force (VGRF) data. Participants wore the specified shoes for an accumulative 40 km of recreational running before treadmill data acquisition. Data was collected at a running speed of 12 km/h (3.33 m/s) for 30 seconds, with motion capture data saved in .c3d format, viewable and editable in Mokka software, and convertible to OpenSim readable .trc marker file format.

Thirty-five (35) optical markers were placed on participants according to Qualisys marker sets as shown in Fig. 2 [18].

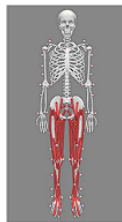


Fig. 2: Marker Placement on OpenSim generic model. [18]

B. Scaling

The study employed a full-body musculoskeletal model where generic virtual markers on the model were adjusted to match the experimental marker placement. This scaling process was iterated until the root mean square (RMS) location error for each marker was below 1.5 cm.

C. Inverse Kinematics (IK)

IK was performed using the scaled model and running trajectory file. To enhance lower limb marker tracking and minimize errors, the weighting of all lower limb markers was increased to 20 compared to upper limb markers. The output, representing the inverse kinematics of the running motion, was saved in mot motion file format.

D. Residual Reduction Algorithm (RRA)

RRA required the scaled model .osim file, inverse kinematics .mot file, and VGRF .xml file specifying force and torque application to the musculoskeletal model. Residual and reserve actuators for each body segment were defined in the .xml

file, with actuator values set to 5,000 to avoid restricting running kinematics and allow adjustments based solely on VGRF.

E. MocoTrack

MocoTrack was implemented in the Python programming environment using installed OpenSim packages in the Anaconda virtual environment. The analysis required the scaled model, running trajectory file, and running VGRF. Similar to RRA and IK, reserve was set to 5,000 and lower limb weightage to 20. The direct collocation solver mesh interval, set to 0.02. Generally, lower interval enables generating better results, but consuming more computational cost as the trade-off. As shown in Fig. 3, visualization of solver results occurred in a separate Python OpenSim Moco window, differing from the standard OpenSim interface.



Fig. 3: OpenSim MocoTrack result visualization

F. Inverse Dynamics (ID)

To obtain generalized force and moment data for running, inverse kinematics results from IK, RRA, and MocoTrack were further processed through OpenSim's Inverse Dynamics tool, together with subject VGRF information as input. Subsequently, only ankle and knee moments were extracted for further data analysis.

G. Data Analysis with MATLAB

MATLAB was used to process simulation results for a clearer, informative and interpretable stance-swing running analysis. Data indices for one running gait were identified based on right hip rotation. Isolated indices were used to extract knee and ankle running moments, followed by averaging, standard deviation calculation, and visualization. The resulting averaged running moment gait was compared to other OpenSim inverse kinematics techniques using the Root Mean Square Error (RMSE), correlation (r), and computational time, presented in bar graphs.

III. RESULTS AND DISCUSSION

A. Gait Analysis

Wearing a shoe would have a huge impact on the moment gait, which means that $F \neq ma$. As a result, inconsistency of dynamically kinematic and kinetic parameters was distinguished. This inconsistency leads to different tools in OpenSim treating the data differently. RRA can reduce the residual force and report on the inconsistency, but it cannot eliminate it entirely. Table II presents the results of the RRA, showing the average residual force. Notably, F_y , the vertical force, is influenced by shoe cushioning in this study.

TABLE II. AVERAGE RESIDUALS FORCES AFTER RRA FOR TWO RANDOMLY PICKED SUBJECTS WEARING HARD CUSHIONING AND SOFT CUSHIONING RESPECTIVELY

Shoe Cushioning	Average Residuals	Force, N
Hard	F_x	-1.47503
	F_y	16.2115
	F_z	-1.79812
Soft	F_x	-3.50227
	F_y	-4.04652
	F_z	-2.72094

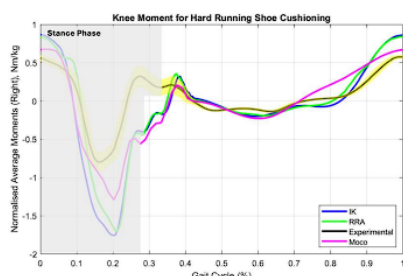


Fig. 4: Knee Moment Gait for Hard Running Shoe Cushioning

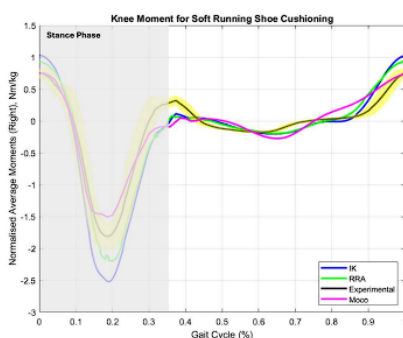


Fig. 5: Knee Moment Gait for Soft Running Shoe Cushioning

Fig. 4 and Fig. 5 show the knee moment gait for hard and soft running shoe cushioning, respectively, of a randomly selected subject, while Fig. 6 and Fig. 7 show the ankle moment gait under hard and soft, of a randomly selected subject.

Both Fig. 4 and Fig. 5 show that different tools treat the impact force due to the shoe cushioning differently. In the stance phase, MocoTrack is more closely approximated to the experimental data, when comparing with the others two. In the hard shoe cushioning, as shown in Fig. 4, MocoTrack overestimated the knee moment on the stance phase, while in the soft shoe cushioning (Fig. 5), it underestimated the knee moment. Thus, it is believed that stance phase is the stage where the RMSE is accumulating, and correlation, r , behaves differently. However, in the swing phase, all tools simulated quite accurate to the experimental data, regardless of the type of the cushioning. It is

mainly because during swing phase, the feet were not in contact with the ground, force accumulation does not involve. Swing phase is an energy releasing stage, where the movement is purely based on the kinematic driven. Thus, the effect of the cushioning is minimal during this phase.

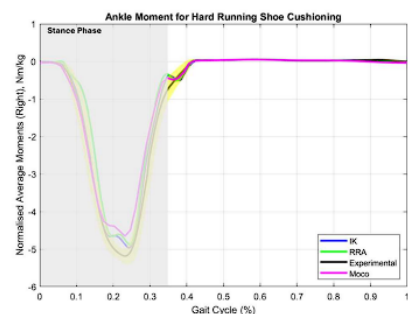


Fig. 6: Ankle Moment Gait for Hard Running Shoe Cushioning

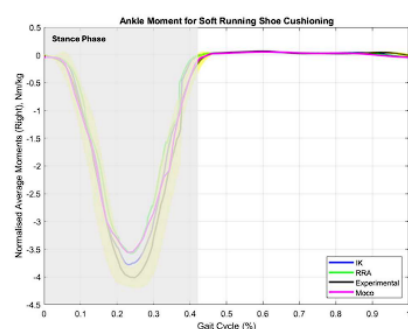


Fig. 7: Ankle Moment Gait for Soft Running Shoe Cushioning

However, as shown in Fig. 6 and Fig. 7, all tools perform well, and the results are closely approximated to the experimental data. It is because compared to the knee, the ankle is a less moveable part of the body segment. As the ankle is also closer to the force plate, causing the kinematic parameters to be more dynamically consistent with the kinetic parameters, especially during the swing phase, where there is almost no performance difference for all tools. Nevertheless, if viewed closely, minor performance differences still exist among all tools in the stance phase, especially MocoTrack, which underestimates the ankle moment when compared to RRA and IK. Such underestimation is due to the tracking algorithm where MocoTrack performs tracking that is based on the VGRF and the trajectory markers information, and this tracking will harmonize the effect between these two mechanics parameters. On the other hand, IK is simulated more closely to the experimental data when compared with RRA and MocoTrack.

B. RMSE, Correlation and Computational Time

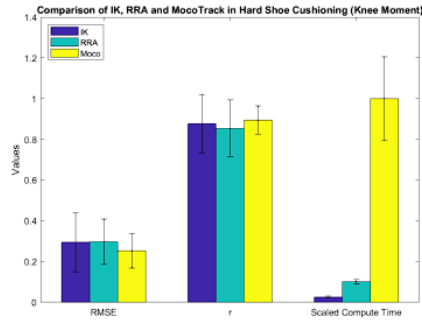


Fig. 8: Comparison of IK, RRA, and MocoTrack for knee moment running gait under hard shoe cushioning

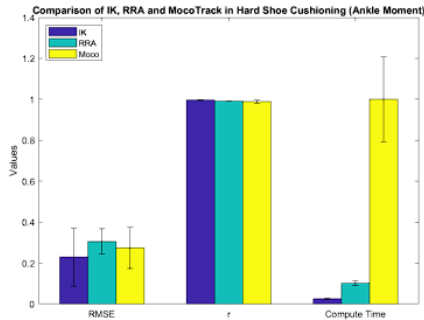


Fig. 9: Comparison of IK, RRA, and MocoTrack for ankle moment running gait under hard shoe cushioning

TABLE III. RMSE, r VALUE AND THE COMPUTATIONAL TIME IN HARD SHOE CUSHIOING

Body Segment	OpenSim Tools	Analysis Parameters	Average Value
Knee	IK	RMSE (Nm/kg)	0.295 ± 0.146
		r	0.877 ± 0.145
		Compute Time (s)	436.8 ± 70.92
	RRA	RMSE (Nm/kg)	0.297 ± 0.112
		r	0.854 ± 0.139
		Compute Time (s)	1479 ± 195.6
MocoTrack	RMSE (Nm/kg)	0.253 ± 0.0852	
	r	0.895 ± 0.0688	
	Compute Time (s)	17313 ± 3572	
Ankle	IK	RMSE (Nm/kg)	0.229 ± 0.141
		r	0.997 ± 0.0028
		RMSE (Nm/kg)	0.305 ± 0.0624
	RRA	r	0.991 ± 0.00157
		RMSE (Nm/kg)	0.274 ± 0.10
		r	0.989 ± 0.0076

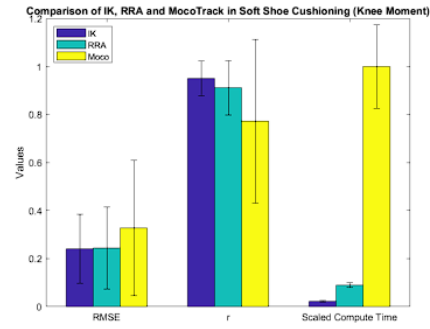


Fig. 10: Comparison of IK, RRA, and MocoTrack for knee moment running gait under soft shoe cushioning

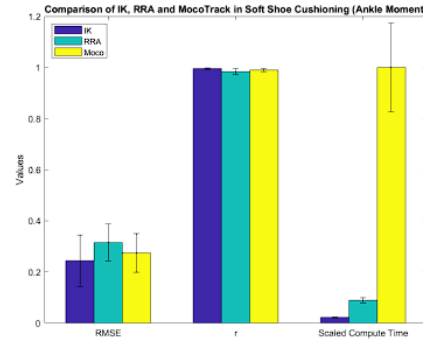


Fig. 11: Comparison of IK, RRA, and MocoTrack for ankle moment running gait under soft shoe cushioning

TABLE IV. RMSE, r-VALUE AND THE COMPUTATIONAL TIME IN SOFT SHOE CUSHIOING

Body Segment	OpenSim Tools	Analysis Parameters	Average Value
Knee	IK	RMSE (Nm/kg)	0.240 ± 0.144
		r	0.950 ± 0.0717
		Compute Time (s)	419.25 ± 58.83
	RRA	RMSE (Nm/kg)	0.244 ± 0.170
		r	0.912 ± 0.113
		Compute Time (s)	1695 ± 194.07
MocoTrack	RMSE (Nm/kg)	0.327 ± 0.282	
	r	0.772 ± 0.341	
	Compute Time (s)	19112 ± 3314	
Ankle	IK	RMSE (Nm/kg)	0.244 ± 0.10
		r	0.996 ± 0.00279
		RMSE (Nm/kg)	0.315 ± 0.0718
	RRA	r	0.983 ± 0.0124
		RMSE (Nm/kg)	0.274 ± 0.0755
		r	0.989 ± 0.00649

Fig. 8 to Fig. 11 show the performance comparison of IK, RRA, and MocoTrack in terms of RMSE, correlation (r), and computational time. The simulation computational time is based on the specifications of the devices, which are AMD Ryzen7 6,800HS, Nvidia RTX 3070 Ti, and 24 GB RAM. Higher specifications allow the computational time to be shortened, especially in OpenSim Moco, where its computational cost is much heavier than the other tools. RMSE was tabulated to compare the difference between the experimental data and the simulation result, and correlation (r) examine how closely the simulated data relates to the experimental data.

Assessing closer in terms of RMSE, in running shoes with hard cushioning, MocoTrack performed the best compared to IK and RRA, and was also most highly correlated to the experimental data for knee moment (Table III). The additional impulsive force exerted onto the body is obvious, thus it becomes the reason for the outstanding performance where MocoTrack uses direct collocation and optimal control problems to ensure the dynamic consistency between kinematic and kinetic parameters of running.

However, with the same type of cushioning, ankle moment is not the case. IK becomes the outstanding tool for tracking running motion. Compared to knee moment, ankle moment is a less movable body segment, and the additional impulse due to the hard cushioning may cause the moment to deviate. Despite this, the correlation shows that all tools generated moment gait that is very highly related to the experimental data.

In soft running shoe cushioning, the performance of MocoTrack is dropping in tracking running motion especially for knee moment (Table IV). Soft shoe cushioning indeed absorbs some extent of additional reaction force, which can be shown in Table II. The force is minor and ignorable, but it may cause MocoTrack, which is a tool that carefully considers dynamic consistency, to incorrectly interpret this minor force. It may incorrectly enlarge the force, causing it to deviate from the true result. Its correlation also proves this deviation.

Soft shoe cushioning absorbs minor reaction force to the body but is negligible. Thus, IK and RRA performed equally well. IK and RRA are the tools that do not prioritize dynamic consistency, focusing on tracking the experimental kinematic trajectory data. In this case, they performed with a lower error than MocoTrack. In knee moment, the performance of both is nearly identical in terms of RMSE and r . While in ankle moment, RRA is slightly better than IK, due to the properties of RRA as being an inverse kinematics optimization tool, allowing the data to be free from residual force which is then more accurate to the experimental value.

C. Performance Evaluation

Strictly speaking, all three OpenSim tools performed well in tracking the running kinematic motion. This is evident in their low RMSE, which was around 0.3 Nm/kg, and high correlation, with most of them providing an r value greater than 95%. IK, RRA, and MocoTrack are profound, trustworthy, and reliable tools for performing biomechanical simulations of running with shoe cushioning. Although their results for RMSE and correlation differed from each other, the extent of these differences was not significant. In this scenario, computational time was the key factor for evaluating their performance, where some degree of accuracy could be sacrificed. Specifically, while MocoTrack generated lower RMSE in some cases, its computational cost was much larger than IK and RRA. Therefore, IK has the best performance, followed by RRA, and lastly is MocoTrack. Additionally, in the case where the muscle-driven simulation is

not required, IK definitely is the tools that suffice enough to perform the marker trajectory inverse kinematics-based analysis.

IV. CONCLUSION

After evaluating RMSE, correlation, and computational time for knee and ankle joint simulations under various shoe cushioning conditions, it can be concluded that IK is the most recommended tool for tracking virtual marker trajectories in inverse kinematics, particularly when accounting for the added impulsive force during the stance phase of running, and this is particularly true if the further muscle-driven simulation is not required to proceed. This is because in among all these tools, IK has the shortest computational time, under the scenario that IK, RRA and MocoTrack provided almost identical values of RMSE and correlation. Despite this, increasing the sample data could provide more robust and reliable results, while also minimizing the impact of subject-specific outliers caused by loose markers, unnatural running postures, or incorrect experimental setups.

V. ACKNOWLEDGMENT

This study was supported by Universiti Tunku Abdul Rahman under grant number IPSR/ UTARRF RMC/ 2020-C2/C01 and Centre of Healthcare Science and Technology (CHST) fund.

REFERENCES

- [1] F. Oswald, J. Campbell, C. Williamson, J. Richards, P. J. I. j. o. e. r. Kelly, and p. health, "A scoping review of the relationship between running and mental health," vol. 17, no. 21, p. 8059, 2020.
- [2] M. K. d. Araujo, R. M. Baeza, S. R. B. Zalada, P. B. R. Alves, and C. A. d. J. R. b. d. o. Mattos, "Injuries among amateur runners," vol. 50, pp. 537-540, 2015.
- [3] N. Kakouris, N. Yener, D. T. J. J. o. s. Fong, and h. science, "A systematic review of running-related musculoskeletal injuries in runners," vol. 10, no. 5, pp. 513-522, 2021.
- [4] L. Malisoux, N. Delattre, A. Urhausen, and D. J. T. A. j. o. s. m. Theisen, "Shoe cushioning influences the running injury risk according to body mass: a randomized controlled trial involving 848 recreational runners," vol. 48, no. 2, pp. 473-480, 2020.
- [5] X. Jiang *et al.*, "Ground reaction force differences between bionic shoes and neutral running shoes in recreational male runners before and after a 5 km run," vol. 18, no. 18, p. 9787, 2021.
- [6] W. Quan *et al.*, "Simulation of lower limb muscle activation using running shoes with different heel-to-toe drops using opensim," in *Healthcare*, 2023, vol. 11, no. 9, p. 1243: MDPI.
- [7] K. Zhao, C. Shan, Y. J. H. I. S. Luximon, and Systems, "Contributions of individual muscle forces to hip, knee, and ankle contact forces during the stance phase of running: a model-based study," vol. 10, no. 1, p. 11, 2022.
- [8] R. W. K. Boon, Y. Z. Chong, Y. Q. Tan, V. Sundar, Y. Selva, and S. C. Chan, "Effect of Running Shoe Cushioning on Muscle Activation using OpenSim," in *2022 IEEE-EMBS Conference on Biomedical Engineering and Sciences (IECBES)*, 2022, pp. 228-233: IEEE.
- [9] J. T. Sturdy, A. K. Silverman, and N. T. J. J. o. B. Pickle, "Automated optimization of residual reduction algorithm parameters in OpenSim," vol. 137, p. 111087, 2022.
- [10] J. Lavikainen, P. Vartiainen, L. Stenroth, and P. A. J. P. Karjalainen, "Open-source software library for real-time inertial measurement unit data-based inverse kinematics using OpenSim," vol. 11, p. e15097, 2023.
- [11] C. L. Dembia, N. A. Bianco, A. Falisse, J. L. Hicks, and S. L. J. P. C. B. Delp, "Opensim moco: Musculoskeletal optimal control," vol. 16, no. 12, p. e1008493, 2020.
- [12] F. De Groot, A. L. Kinney, A. V. Rao, and B. J. J. A. o. b. e. Fregly, "Evaluation of direct collocation optimal control

- problem formulations for solving the muscle redundancy problem," vol. 44, pp. 2922-2936, 2016.
- [13] A. S. J. R. S. O. S. Fox, "The quest for dynamic consistency: a comparison of OpenSim tools for residual reduction in simulations of human running," vol. 11, no. 5, p. 231909, 2024.
- [14] S. R. Hamner and S. L. J. J. o. b. Delp, "Muscle contributions to fore-aft and vertical body mass center accelerations over a range of running speeds," vol. 46, no. 4, pp. 780-787, 2013.
- [15] H. X. Lim, Y. Z. Chong, Y. Q. Tan, V. Sundar, Y. Selva, and S. C. Chan, "Effect Of Shoe Cushioning Hardness to Running Biomechanics," in *2022 IEEE-EMBS Conference on Biomedical Engineering and Sciences (IECBES)*, 2022, pp. 131-136: IEEE.
- [16] L. Malisoux, N. Delattre, P. Gette, A. Urhausen, and D. J. F. S. Theisen, "The effect of shoe cushioning on injury risk, landing impact forces and spatiotemporal parameters during running: results from a randomised trial including 800+ recreational runners," vol. 13, no. sup1, pp. S55-S56, 2021.
- [17] T. K. Uchida and S. L. Delp, *Biomechanics of movement: the science of sports, robotics, and rehabilitation*. Mit Press, 2021.
- [18] A. Rajagopal, C. L. Dembia, M. S. DeMers, D. D. Delp, J. L. Hicks, and S. L. J. I. t. o. b. e. Delp, "Full-body musculoskeletal model for muscle-driven simulation of human gait," vol. 63, no. 10, pp. 2068-2079, 2016.

Appendix D: IECBES 2024 2nd Paper Submission Content: Assessing Muscle Driven Optimization Techniques in OpenSim for Long Distance Running and Deep Muscle Adaptations

Assessing Muscle Driven Optimization Techniques in OpenSim for Long Distance Running and Deep Muscle Adaptations

Siow Cheng Chan
Department of Mechatronics and
Biomedical Engineering
Universiti Tunku Abdul Rahman
Selangor, Malaysia
chance@utar.edu.my

Yin Qing Tan
Department of Mechatronics and
Biomedical Engineering
Universiti Tunku Abdul Rahman
Selangor, Malaysia
tanyq@utar.edu.my

Yew Wei Teh
Department of Mechatronics and
Biomedical Engineering
Universiti Tunku Abdul Rahman
Selangor, Malaysia
yewwei9909@utar.my

Yu Zheng Chong
Department of Mechatronics and
Biomedical Engineering
Universiti Tunku Abdul Rahman
Selangor, Malaysia
chongyz@utar.my

Yallini Selva
Department of Sports Biomechanics
National Sports Institute of Malaysia,
Bukit Jalil
Kuala Lumpur, Malaysia
yallinselva89@gmail.com

Viswanath Sundar
Department of Physical Education and
Sports Science,
Visva-Bharati Central University,
India
viswabdu@gmail.com

Abstract— Understanding how deep muscles contribute to running performance and adapt to accumulated distance remains underexplored in biomechanics. This study addresses this gap by validating muscle-driven optimization techniques in OpenSim, focusing on the behavior of five deep muscles—adductor magnus ischial, sartorius, semitendinosus, vastus intermedius, and extensor digitorum longus—during long-distance running. Biomechanical data were collected for run distances of 0 km, 40 km, 80 km, and 120 km through motion capture, vertical ground reaction force (VGRF) measurement, and electromyogram (EMG) analysis. Muscle-driven simulations were conducted using Static Optimization (SO), Computed Muscle Control (CMC), and MocoInverse techniques in OpenSim, with validation against experimental EMG data. The results demonstrated that CMC provided the most accurate muscle force estimations, exhibiting the lowest root mean square error (RMSE) and highest correlation, though at the cost of increased computational time. Analysis revealed significant changes in muscle force generation at 80 km, indicating the body's adaptation to accumulated running distance. Muscles like the sartorius and semitendinosus exhibited compensatory force generation, while the adductor magnus ischial showed adaptive shifts between stance and swing phases. In conclusion, CMC was identified as the most reliable optimization technique for muscle-driven simulations in OpenSim. The study highlights the biomechanical adjustments during long-distance running and the role of deep muscles in maintaining running efficiency as the body adapts to prolonged activity.

Keywords— *OpenSim, Computed Muscle Control, Static Optimization, MocoInverse, Muscle-Driven Optimization Techniques*

I. INTRODUCTION

Simulation and modeling of neuromusculoskeletal systems allow us to examine, analyze, and understand muscle behavior during specific movements. This process is known as muscle-driven simulation. In OpenSim, various techniques are used to calculate and model these simulations: Computed Muscle Control (CMC), Static Optimization (SO), and

MocoInverse [1-3]. CMC uses a PD control law with a spring-mass-damper system for muscle-driven simulation [4, 5]. SO resolves inverse dynamics from body segments to individual muscles, assuming that tendons are rigid, and no passive forces are present [6, 7]. MocoInverse, on the other hand, uses an optimal control problem solver within a direct collocation framework to prescribe running kinematics and is believed to effectively address the muscle redundancy problem [8, 9].

It is well known that running patterns change with accumulated distance. During ultramarathons (50 km to 100 km), the body adapts by increasing stride frequency, reducing maximum vertical ground reaction forces (GRFs), and decreasing vertical impulse during heel strikes [10]. Beyond these surface-level changes, biomechanically, there is interest in understanding the behavior of individual muscles during long-distance running. Such studies allow for a detailed analysis of how specific muscles contribute to agonist-antagonist interactions, balance, and coordination [11, 12].

Deep muscles, located beneath superficial muscles and closer to the bones, play a crucial role in stabilizing joints, maintaining posture, and controlling fine movements. For instance, the adductor magnus muscle, located at the hip, plays a significant role in extending the hip joint and assisting in thigh adduction [13]. The sartorius muscle flexes the knee and laterally rotates the hip joint [14]. At the knee, the semitendinosus muscle helps with knee flexion and hip extension [15, 16]. The vastus intermedius, found deep to the rectus femoris in the anterior thigh, contributes to knee extension during running. The extensor digitorum longus, an ankle dorsiflexor muscle, extends the toes by pulling them upwards during running [17].

Comparisons of the performance between SO and CMC have been conducted. Six subject models were validated using experimental muscle activation and joint torque data [3]. The study found that knee extension torque error was greater with CMC than with SO, and that muscle forces, activations, and co-contraction indices were generally lower with SO. The study concluded that to choose the best optimization technique

for muscle-driven simulation in OpenSim, validation with experimental activation data is essential.

Since there are limited detailed studies on the role of deep muscles in overall running performance and their relationship to muscle behavior over accumulated running distance, this research aims to validate the muscle-driven optimization technique available in OpenSim. The lateral gastrocnemius, an electromyogram (EMG)-measurable muscle, will be used for validation. Our goal is to identify a more accurate and reliable technique for studying force estimation in the adductor magnus ischial, sartorius, semitendinosus, vastus intermedius, and extensor digitorum longus muscles..

II. METHODS

A. Experimental Data Collection

Ethical approval and study protocol were obtained from the relevant committee, and informed consent was received from the participant. A male participant, aged 29 years, with a height of 170.32 cm and a body mass of 68.03 kg, was recruited to perform overground running, accumulating distances of 0 km (before starting), 40 km, 80 km, and 120 km [18]. The participant was required to run an average distance of 12.83 ± 4.14 km per week, monitored through individual health apps and watches. The running activities were conducted wearing a running shoe with soft cushioning, measuring 32A on the Shore A hardness scale, as shown in Fig. 1.



Fig. 1: The 32A soft cushioning running shoe

After the participant reached each specified distance milestone, follow-up data collection was conducted at the Sports Performance Laboratory, National Sport Institute of Malaysia (Institut Sukan Negara, ISN). Trajectory data was captured using an 11-camera motion capture system (Qualisys Track Manager, QTM 2022, 300 Hz) to record the running motion, and a 3-dimensional instrumented treadmill with force plates (Bertec Instrumented Treadmill, 1500 Hz) was used to obtain virtual ground reaction force (VGRF) data. During the session, the participant performed maximum voluntary contraction (MVC) exercises to collect experimental EMG data for the lateral gastrocnemius. Running data was then collected with a running speed of 12 km/h (3.33 m/s) for 30 seconds. EMG data during running was wirelessly recorded using the Noraxon system (Noraxon MyoMuscle 1500 Hz DTS Desktop Receiver System, Noraxon, Scottsdale, USA).

Motion capture data was saved in .c3d format, which is convertible to OpenSim-readable .trc marker file. Thirty-five optical markers were placed on the participant according to the Qualisys marker set, as shown in Fig. 2.



Fig. 2: Markers placement based on Qualisys's guidelines

B. Scaling of Generic Model

Subsequent simulation and modeling began with scaling the full-body musculoskeletal model to match the participant's size [19]. Iterative scaling was performed, allowing the program to automatically adjust the virtual markers to match the experimental marker placements until the root mean square (RMS) error for each marker was below 1.5 cm.

C. Inverse Kinematics (IK)

Using the scaled musculoskeletal model and experimental trajectory marker data, the subject's running kinematics were reconstructed and saved in a .mot motion file. To enhance lower limb marker tracking and minimize errors, the weighting of all lower limb markers was set higher than that of the upper limb markers.

D. Residual Reduction Algorithm (RRA)

The IK file was filtered to ensure the kinematic data was free from noise, improving the consistency of running dynamics. The .mot file, scaled model, and VGRF file were then processed using the RRA.

E. Static Optimization (SO)

The cleaned kinematic data was used for SO, along with the residual and reserve actuators appended to the model. The step interval was set to 10 steps. At the end of the simulation, muscle activation and force during running were generated and stored in .sto files.

F. Computed Muscle Control (CMC)

Using the kinematic data, tracking tasks, actuator constraints, residual and reserve actuators, and VGRF files, CMC was performed with the settings of "slow targeting" and an interior point optimizer (IPOPT) convergence tolerance of 0.1. Due to the soft shoe cushioning causing dynamic inconsistency, fast targeting CMC simulation could not digest the running inverse kinematics and VGRF data.

G. MocoTrack

OpenSim Moco-based simulation was run in the Python programming environment. The simulation was set with a reserve actuator of 5000, lower limb tracking weights of 20,

and a direct collocation mesh interval of 0.02. The solver results were visualized in a separate Python OpenSim Moco window, as shown in Fig. 3.



Fig. 3: OpenSim MocoTrack result visualization



H. MocoInverse

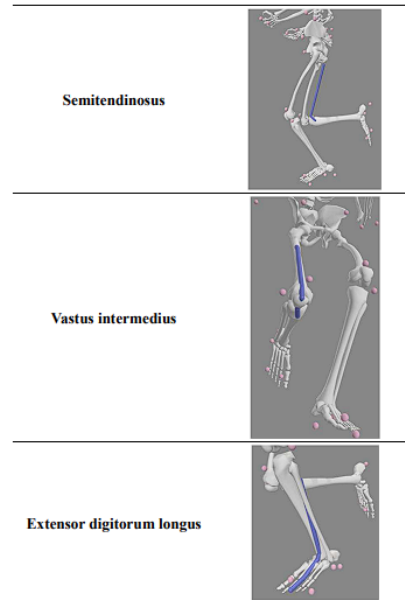
The coordinate results from MocoTrack were used in MocoInverse for prescribed kinematics analysis, also in a Python environment. The reserve actuator was set to 5.0, with a mesh interval of 0.1 and a MocoCasADiSolver convergence tolerance of 0.1. All Moco-based simulation results were saved in .sto files.

I. Data Validation and Analysis with MATLAB

MATLAB was used for data processing, including filtering, averaging, and graph visualization. EMG data was filtered (6 Hz 4th Butterworth lowpass filter), rectified, and normalized by MVC before validation. Based on the validation results, only one muscle-driven optimization technique was selected for further muscular force estimation. After that, only five deep muscles as shown in Table I, were selected as the target of analysis. Those muscle are adductor magnus ischial, sartorius, semitendinosus, vastus intermedius and extensor digitorum longus.

TABLE I. DEEP MUSCLES SELECTION FOR MUSCULAR FORCE PREDICTION ANALYSIS

Deep Muscle (Right)	Figures
Adductor magnus ischial	
Sartorius	



Semitendinosus

Vastus intermedius

Extensor digitorum longus

III. RESULTS AND DISCUSSION

A. EMG Validation

As shown Table II, the lateral gastrocnemius (Gaslat)'s EMG validation identified CMC as having the lowest root mean square error (RMSE) and the highest correlation (r-value). However, CMC also had the longest computation time, followed by MocoInverse and SO. MocoInverse showed a lower RMSE than SO and a slightly higher average correlation than SO. Fig. 4 and 5 showed the lateral gastrocnemius muscle activation of experimental, CMC, SO and MocoInverse simulations for 40km and 80km accumulated running distance respectively.

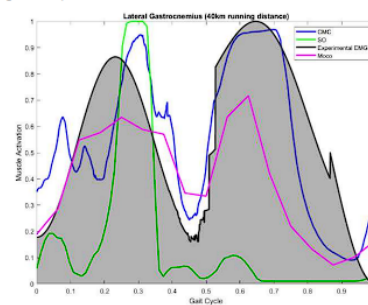


Fig. 4: The EMG validation graph for 40 km accumulated running distance

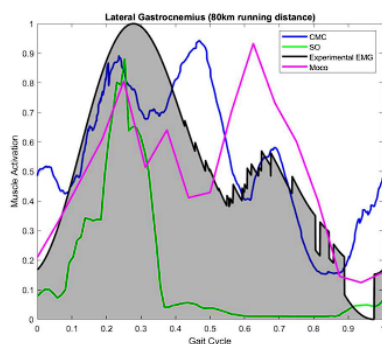


Fig. 5: The EMG validation graph for 80 km accumulated running distance

TABLE II. THE RMSE, R-VALUE AND THE COMPUTATIONAL TIME FOR CMC, SO AND MOCOINVERSE GASLAT VALIDATION

Running Distance	Optimization Techniques	RMSE	r	Compute time (hours)
40km	CMC	0.2042	0.7596	16.41
	SO	0.541	0.2329	7.68
	MocoInverse	0.2875	0.6308	10.51
80km	CMC	0.1934	0.7376	16.91
	SO	0.4068	0.7185	7.27
	MocoInverse	0.2119	0.6621	11.40

Based on the validation results, CMC can be concluded as the most effective muscle-driven optimization technique in OpenSim when compared to MocoInverse and SO. Consequently, the subsequent predictions will focus exclusively on the muscular forces of five deep muscles—adductor magnus ischial, sartorius, semitendinosus, vastus intermedius, and extensor digitorum longus—generated using CMC. The simulations were conducted on a computer equipped with an AMD Ryzen 7 6800HS, Nvidia RTX 3070 Ti, and 24 GB of RAM. Higher computer specifications would reduce computational time and allow for finer simulation settings, potentially leading to significant improvements in validation results.

B. CMC Muscular Force Estimation

The muscular estimation results generated via OpenSim CMC showed significant changes or turning points at 80 km of accumulated running distance. This indicates that the body adapts to such a long-accumulated running distance.

Starting with the hip portion, as shown in Fig. 6, the adductor magnus ischial muscle shows opposite trends at the 80 km accumulated running distance. It uses less force in the stance phase but more force in the swing phase. Unlike other running distances, force exertion increases as the accumulated running distance increases from 0 km to 120 km. When the subject reached 80 km, the muscle's adaptability was unable to keep up, leading to fatigue in other hip muscles. By reducing the load on the adductor magnus ischial during the stance phase and increasing its role during the swing phase, the body might be trying to balance muscle workload and reduce the risk of overuse injuries. After adapting to the

long running distance workload, the trend restored to what it was at 0 km and 40 km.

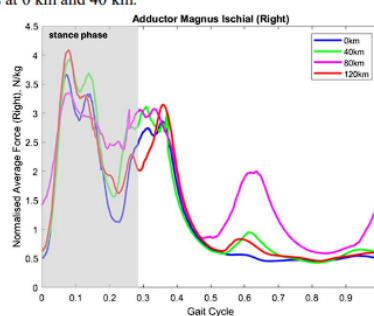


Fig. 6: The muscular force estimation for the adductor magnus ischial across different accumulated running distance

Fig. 7 shows the sartorius muscle force during one average gait cycle of running across different accumulated running distances. The force decreases in both stance and swing phases but increases at 120 km of accumulated running distance. Anatomically, the sartorius muscle plays a complex role in hip flexion, abduction, and knee flexion. Its long, thin structure spans both the hip and knee joints. As running distances increase, the efficiency of this muscle in performing these functions may decrease, especially if other hip muscles begin to fatigue. The increase in force at 120 km could indicate a compensatory mechanism where the sartorius takes on a greater role to maintain joint stability and proper movement patterns.

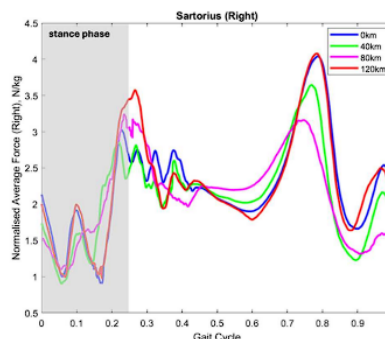


Fig. 7: The muscular force estimation for the sartorius across different accumulated running distance

Fig. 8 shows that the semitendinosus muscle force increases in the stance phase but decreases at 120 km, continuing this trend until the end of toe-off. At mid-swing, the force rises but starts to decrease at 80 km of accumulated running distance. However, at terminal swing, the trend restores to match the stance phase.

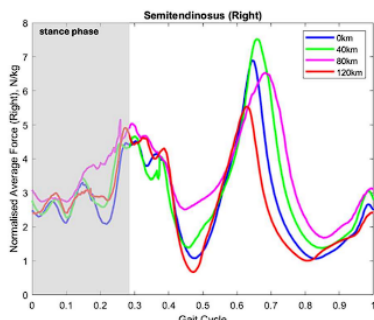


Fig. 8: The muscular force estimation for the semitendinosus across different accumulated running distance

During the swing phase, which involves the transition from toe-off to terminal swing, the semitendinosus controls leg movement. The initial increase in force from 0 km to 40 km at mid-swing could be the body's attempt to maintain proper leg acceleration and deceleration for smooth forward motion. As the distance accumulates, the muscle may fatigue, leading to decreased force generation from 80 km to 120 km. The return to a similar trend as the stance phase during terminal swing suggests that the muscle's function as a decelerator and stabilizer at the knee becomes increasingly compromised due to fatigue.

For the knee extensor muscle, the vastus intermedius shows a decrease in force at 0 km, followed by an increase at 120 km. At mid-swing, the force generally decreases from 0 km to 120 km. At terminal swing, the force rises from 0 km to 80 km but decreases again at 120 km of accumulated running distance. As shown in Fig. 9, the vastus intermedius muscle demonstrates how the body adapts to running distance. At 120 km of accumulated running distance during the stance phase, the body might be compensating for fatigue in other muscles, requiring more contribution from the vastus intermedius to maintain stability and propulsion. Energy optimization is observed at mid-swing, where the muscle force generally decreases. At terminal swing, force generation efficiency is compromised due to the need for precise control and leg stabilization before the next ground contact, making the muscle prone to fatigue.

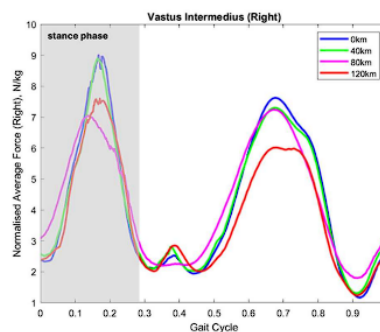


Fig. 9: The muscular force estimation for the vastus intermedius across different accumulated running distance

For the ankle, the extensor digitorum longus (EDL) muscle force increases from 0 km to 80 km but starts to decrease at 120 km, as shown in Fig. 10. However, starting at mid-swing, the force increases until 40 km, drops to its lowest point at 80 km, and then begins to rise again at 120 km.

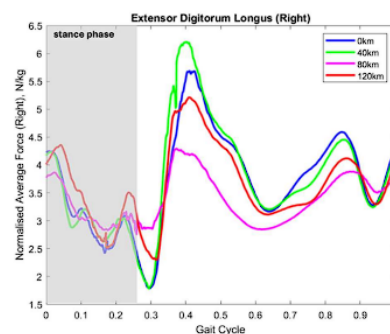


Fig. 10: The muscular force estimation for the EDL across different accumulated running distance

In the stance phase, the increase in force generation from 0 km to 80 km suggests that the body might be compensating for other muscle fatigue by relying more heavily on the EDL. The decrease at 120 km could indicate a shift in biomechanics, where other muscles or tendons might take over some of the EDL's role, or the running form itself changes to reduce reliance on the EDL.

IV. CONCLUSION

Based on the validation RMSE and r-value result, CMC was the best optimization techniques compared to SO and MocoInverse. However, lowering the convergence tolerance of the IPOPT and MocoCasADiSolver, and the mesh interval of the direct collocation were firmly believed that the validation result could be much more accurate, but the

computational time and cost would be the tradeoff factors needed to consider.

The analysis of the five deep muscles (adductor magnus ischial, sartorius, semitendinosus, vastus intermedius, and extensor digitorum longus) across accumulated running distances reveals a complex interplay of compensatory mechanisms. During the stance phase, muscles such as the semitendinosus and vastus intermedius exhibit initial decreases in force. As these muscles reduce their force output, other muscles, like the extensor digitorum longus and sartorius, increase their force generation to maintain stability and propulsion. However, by 120 km, these compensatory adjustments seem to reach their limit, leading to a noticeable decrease in force generation across several muscles. This indicates that as the body adapts to prolonged running, it redistributes the workload among these deep muscles, but beyond a certain threshold, the effectiveness of these adaptations diminishes, resulting in overall reduced muscle performance. The adductor magnus ischial's shifting role between the stance and swing phases further illustrates the body's strategy to balance muscle workload, reduce the risk of overuse injuries, and maintain running efficiency. To enhance the validity of these findings, future studies should recruit a larger number of participants.

ACKNOWLEDGMENT

This study was supported by Universiti Tunku Abdul Rahman under grant number IPSR/ UTARRF RMC/ /2020-C2/C01 and Centre of Healthcare Science and Technology (CHST) fund.

REFERENCES

- [1] C. L. Dembia, *Simulating Assistive Technology: Insights, Tools, and Open Science*. Stanford University, 2020.
- [2] R. W. K. Boon, Y. Z. Chong, Y. Q. Tan, V. Sundar, Y. Selva, and S. C. Chan, "Effect of Running Shoe Cushioning on Muscle Activation using OpenSim," in *2022 IEEE-EMBS Conference on Biomedical Engineering and Sciences (IECBES)*, 2022, pp. 228-233: IEEE.
- [3] S. A. Roelker, E. J. Caruthers, R. K. Hall, N. C. Pelz, A. M. Chaudhari, and R. A. J. J. o. A. B. Siston, "Effects of optimization technique on simulated muscle activations and forces," vol. 36, no. 4, pp. 259-278, 2020.
- [4] M. T. Karimi *et al.*, "Determination of the correlation between muscle forces obtained from OpenSim and muscle activities obtained from electromyography in the elderly," vol. 44, pp. 243-251, 2021.
- [5] P. Liu, J. Hua, L. Wang, and Y. Zhao, "Opensim-Based Dynamics Simulation of Upper Limb," in *Proceedings of the 2023 3rd International Conference on Robotics and Control Engineering*, 2023, pp. 38-43.
- [6] J. M. Kaneda, K. A. Seegers, S. D. Uhlrich, J. A. Kolesar, K. A. Thomas, and S. L. J. J. o. b. Delp, "Can static optimization detect changes in peak medial knee contact forces induced by gait modifications?," vol. 152, p. 111569, 2023.
- [7] B. Michaud, M. J. C. M. i. B. Begon, and B. Engineering, "Two efficient static optimization algorithms that account for muscle-tendon equilibrium: approaching the constraint Jacobian via a constant or a cubic spline function," vol. 23, no. 11, pp. 703-709, 2020.
- [8] F. De Groot, A. L. Kinney, A. V. Rao, and B. J. J. A. o. b. e. Fregly, "Evaluation of direct collocation optimal control problem formulations for solving the muscle redundancy problem," vol. 44, pp. 2922-2936, 2016.
- [9] C. L. Dembia, N. A. Bianco, A. Falisse, J. L. Hicks, and S. L. J. P. C. B. Delp, "OpenSim moco: Musculoskeletal optimal control," vol. 16, no. 12, p. e1008493, 2020.
- [10] M. J. L. Thompson and e. biology, "Physiological and biomechanical mechanisms of distance specific human running performance," vol. 57, no. 2, pp. 293-300, 2017.
- [11] M. Rubega *et al.*, "Muscular and cortical activation during dynamic and static balance in the elderly: A scoping review," vol. 1, p. 100013, 2021.
- [12] G. Garcia, L. Vieira, V. Seibel, M. Razuk, and N. J. B. J. o. M. B. Rinaldi, "Agonist/Antagonist Ratio for ankle joint is similar between active and inactive older adults compared to hip and knee joints," vol. 14, no. 1, pp. 4-13, 2020.
- [13] D. Corcoran, T. McNamara, J. Feehan, and N. J. L. J. o. O. M. Tripodi, "Adductor magnus: Extending the knowledge—A short review of structure and function," vol. 49, p. 100671, 2023.
- [14] A. Khan and A. Arain, "Anatomy, Bony Pelvis and Lower Limb: Anterior Thigh Muscles," in *StatPearls [Internet]*: StatPearls Publishing, 2023.
- [15] K. L. Moore and A. F. Dalley, *Clinically oriented anatomy*. Wolters kluwer india Pvt Ltd, 2018.
- [16] R. W. J. I. Bohannon and E. Science, "Reliability of manual muscle testing: A systematic review," vol. 26, no. 4, pp. 245-252, 2018.
- [17] C. Jarmey, *The concise book of muscles*. North atlantic books, 2018.
- [18] H. X. Lim, Y. Z. Chong, Y. Q. Tan, V. Sundar, Y. Selva, and S. C. Chan, "Effect Of Shoe Cushioning Hardness to Running Biomechanics," in *2022 IEEE-EMBS Conference on Biomedical Engineering and Sciences (IECBES)*, 2022, pp. 131-136: IEEE.
- [19] A. Rajagopal, C. L. Dembia, M. S. DeMers, D. D. Delp, J. L. Hicks, and S. L. J. I. t. o. b. e. Delp, "Full-body musculoskeletal model for muscle-driven simulation of human gait," vol. 63, no. 10, pp. 2068-2079, 2016.

Appendix E: Open Access to Image Rights

[< Back to orders](#)

Order Number: MP1054419-1		Print order	
Order Date: 11 Oct 2024			
Payment Information			
Yew Wei Teh yewwei9909@1utar.my Payment method: Credit Card		Billing Address: Mr. Yew Wei Teh Jalan Sungai Long Bandar Sungai Long Kajang, Selangor 43000 Malaysia +60 103405261 yewwei9909@1utar.my	Customer Location: Mr. Yew Wei Teh Jalan Sungai Long Bandar Sungai Long Kajang, Selangor 43000 Malaysia
Order Details			
1. Biomechanics of Movement : The Science of Sports, Robotics, and Rehabilitation			Billing Status: Open
Order License ID	MP1054419-1-1	Type of Use	Post in electronic reserves
Order detail status	Completed	Publisher	The MIT Press
Project Name	Final Year Project Thesis	Portion	Page
ISBN-13	978-0-262-04420-2		
			3.75 USD
Hide Details			Digital Course Materials Permission
LICENSED CONTENT			
Publication Title	Biomechanics of Movement ...	Rightsholder	MIT Press - Books
Date	01/01/2020	Publication Type	Book
PERMISSION DETAILS			
Page Range(s)	47	Publication Year of Title Being Used	2024
Total Number of Pages	1	Number of Students/Copies	1
REQUESTED CONTENT DETAILS			
Article/Chapter	1	Author/Editor	Uchida, Thomas K.; Delp, Sc...
COURSE DETAILS			
University/Institution	Universiti Tunku Abdul Rah...	Course Name	Project
Start of Term	2024-10-11		
Total Items: 1		Subtotal:	3.75 USD
		Order Total:	3.75 USD